CREATION RESEARCH SOCIETY

QUARTERLY

Volume 57 Winter 2021 Number 3

- *A YOUNG-EARTH ICE SHEET MODEL TO ESTIMATE ANNUAL LAYER THICKNESSES*
- *SUPERNOVA LIGHT CURVES AND ACCELERATED DECAY*
- *BARAMINIC CLASSIFICATION OF THE TUATARA*
- *A DAM BREACH UNLIKELY FOR THE ORIGIN OF GRAND CANYON*
- *A CATASTROPHIC PLATE TECTONICS EXPLANATION FOR LOW-SHEAR-VELOCITY PROVINCES*
- *THE tôlĕdôt STRUCTURE OF GENESIS*
- *MINUTES OF THE 2020 CRS BOARD MEETING*

Creation Research Society Quarterly

Volume 57
Number 3
Winter 2021

Articles

Departments

Haec Credimus

For in six days the Lord made heaven and earth, the sea, and all that in them is, and rested on the seventh.—Exodus 20:11

Creation Research Society Quarterly

Volume 57
Number 3
Winter 2021

Cover by Michael E. Erkel, Afton, Virginia

Design services by Cindy Blandon, cblandon@aol.com

The *Creation Research Society Quarterly* is published by the Creation Research Society, 1 W. Firestorm Way #145, Glendale, AZ 85306, and it is indexed in the *Christian Periodical Index* and the *Zoological Record.*

Send papers on all subjects to the Editor:
CRSQeditor@creationresearch.org or to
Tim Clarey, 1806 Royal Lane, Dallas, TX 75229.

Send book reviews to the Book Review Editor:
Don B. DeYoung, 200 Seminary Dr.,
Winona Lake, IN 46590, dbdeyoung@grace.edu.

ISSN 0092-9166

Printed in the United States of America

A Catastrophic Plate Tectonics Explanation for Earth's Large Low Shear Velocity Provinces (Also Known as Superplumes)

Evan Arthur Navarro*

Abstract

This paper provides a hypothesis to account for the two Large Low-Shear-Velocity Provinces (LLSVPs) and discusses evidence supporting this hypothesis. These features are located in the lower mantle just above the core-mantle boundary and display strikingly low seismic-shear wave speed relative to adjacent rock. They are nearly antipodal to each other, with one lying roughly beneath Africa and the other beneath the central Pacific Ocean. While secular literature does not have an explanation for how these structures arose or even why they display such low seismic speeds, we postulate that LLSVPs are a direct consequence of catastrophic plate tectonic activity during the Genesis Flood. This paper posits that LLSVPs correspond to hot lower-mantle rock that was forcibly shoved aside by subducted lithospheric slab material as it reached the core-mantle boundary during the Flood. The large contrast in seismic speed between the LLSVP material and the surrounding rock is due primarily to the large difference in temperature. The apparent paradox of why these two LLSVPs, if their low seismic speed is due to high temperature and reduced density, did not rise to the surface millions of years ago is resolved by the realities that the Flood occurred only a few thousand years ago and that mean mantle viscosity returned quickly to its present value at the end of the cataclysm. Numerical simulations with the mantle dynamics code, terra, support this scenario.

Introduction

Seismic tomography has revealed the existence of two provinces of anomalously slow seismic-wave propagation in the lowermost regions of Earth's mantle (McNamara, 2019). These provinces are nearly antipodal to each other, with one beneath the central Pacific Ocean and the other roughly below the African continent. These zones, which exhibit such a striking reduction in seismic wave speed, are generally referred to as Large Low-Shear-Velocity Provinces (LLSVPs), but sometimes as thermochemical piles (Deschamps et al., 2012). In the 1990's they were widely referred to as "super-

* Evan Arthur Navarro, Lynchburg, Virginia, en8hb@virginia.edu
Accepted for publication January 23, 2021

plumes" (Kellogg et al., 1999). Recently, the African LLSVP has been designated Tuzo (**T**he **U**nmoved **Z**one **O**f Earth's deep mantle) and the Pacific LLSVP as Jason (**J**ust **A**s **S**table **On** the opposite meridian), in honor, respectively, of Tuzo Wilson and Jason Morgan, both of plate tectonics fame (Niu, 2018). Each LLSVP consists of hot material of unknown chemical/physical composition (McNamara, 2019) surrounded by colder silicate rock. Secular scientists have only been able to speculate as to the origin of LLSVPs and are still without a strong explanation (McNamara, 2019). However, it is speculated that LLSVPs may be composed of material enriched by iron and magnesium, and thus may be of a primitive origin (Maruyama et al., 2007; Deschamps et al., 2012). The secular community requires that LLSVPs have a chemical composition different from the bulk mantle to offset the positive buoyancy caused by their high temperature in order for these features to be neutrally buoyant and gravitationally stable.

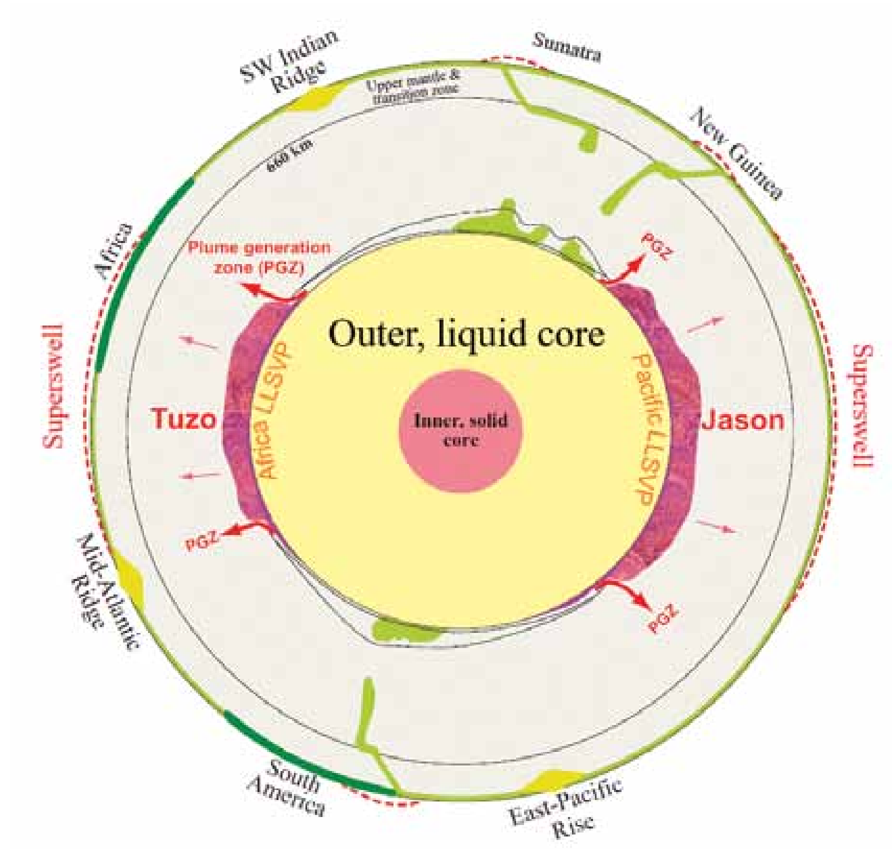

Figure 1. Cartoon cross-section of the Earth as viewed from the South Pole, modified and adapted from Torsvik et al. (2014). Two large low-shear-wave velocity provinces (LLSVPs) are present at Earth's lower mantle: one beneath Africa (Tuzo) and one beneath the central Pacific (Jason). Plume generation zones (PGZs) along the LLSVP margins are the principal source regions for Earth's large igneous provinces. Elevated regions in Earth's gravitational potential field (or geoid) are marked by red dashed lines. The broad regions of elevated geoid above the LLSVPs have been called "superswells."

As previously mentioned, the name for these structures most widely accepted by the scientific community has undergone a significant evolution since their initial discovery in the latter 1980's. Initially nothing was known about these structures save for their low seismic-wave speed. The natural interpretation of this low seismic-wave speed was initially that of elevated temperatures and, therefore, reduced density. Reduced density implies that these structures are buoyant relative to the surrounding mantle and therefore ought to be rising like plumes towards the Earth's surface. Given their large size, it is not surprising that the popular name for these features within the Earth science community was that of "superplume" (Fukao et al., 1994). It was eventually realized, however, that such an interpretation presented a severe problem for uniformitarian thinking and deep-time considerations. A density difference of the magnitude inferred between these superplumes and the surrounding mantle ought to result in strong instability and a rapid rise of the structures to the Earth's surface in a time span far shorter than the hundreds of millions of years the secular paradigm requires. This realization prompted that community to propose that the chemical composition of the rock within these structures must be different from that of the surrounding mantle to make their intrinsic density higher and compensate for their higher temperature (Kellogg et al., 1999). This chemical difference could make the "superplumes" neutrally buoyant and gravitationally stable, thus able to persist in place over spans of hundreds of millions of years. This prompted the general change in nomenclature from "superplume" to Large Low-Shear-Velocity Province (LLSVP), a name agnostic relative to their buoyancy and stability. The name "superplume" is still used, but is representative of the more traditional view for these phenomena.

Closely akin to LLSVP research, the later 20th century also saw research into superswell phenomena. Geophysicists such as Marcia McNutt published several papers on what are termed "superswells," namely regions of uplifted seafloor dotted with countless underwater volcanoes (McNutt, 1998). The volcanic nature of these geoid anomalies can be accounted for by a higher concentration of melt in the shallow ocean floor as compared with the surrounding lithosphere. It was typically posited that these volcanoes were being fed by sub-surface plumes. However, McNutt contradicted this theory with a seismically-defended assertion that a hot layer of mantle above the transition zone at the base of the upper mantle fed this volcanic activity (McNutt, 1998). Figure 1 displays a cartoon of the relationship between a superplume and a superswell, and identifies several other key aspects of the surrounding geology.

As seen in Figure 1, LLSVPs are flanked by the aptly termed plume generation zones (PGZs), which are conventionally regions of approximately 1% slow shear velocity located at the intersections of the outer core, mantle, and LLSVPs (Burke et al., 2008). The steep temperature gradient between the LLSVP margin at the mantle and the interior of the plume is critical in the plume generation that takes place at the zones. The PGZs and superswells consequently all feed the visible Large Igneous Provinces (LIPs), shown at the top of the figure. The LIPs represent massive eruptions of basalt on the Earth's surface (Wignall, 2001).

In a survey of the latest publications, it is clear that there are still more questions than answers as to the nature of the LLSVPs, especially concerning possible chemical differences relative to the bulk mantle. Beyond the issues relating to spatial resolution of their structure are the following more important questions:

- What were the processes responsible for their formation?
- When did they first appear?
- Are they stationary or buoyant and mobile?

The answer to each of these questions has profound impact on a correct understanding of mantle dynamics and Earth history in general. We will address these questions in the remainder of this paper.

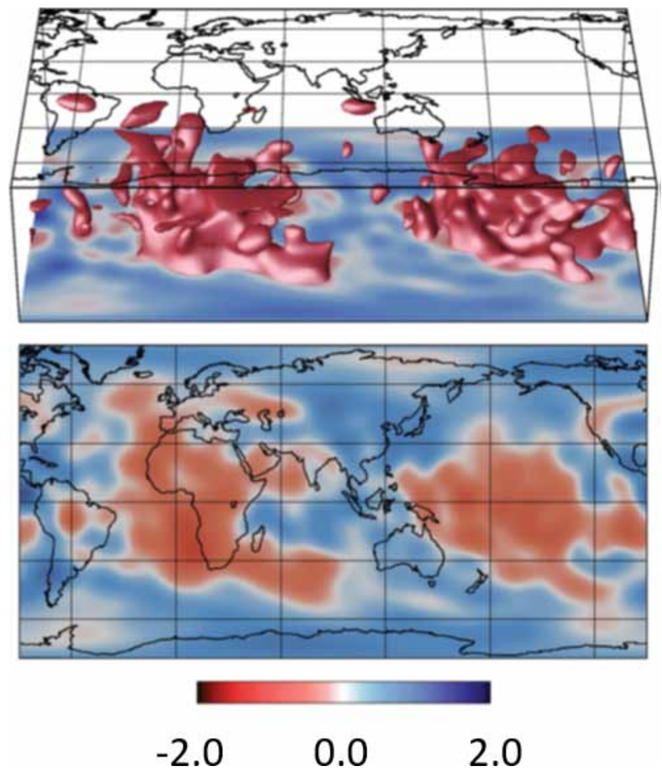

Figure 2. Maps of Large Low-Shear-Velocity Provinces, with 3D iso-surface depiction in top panel and 2D average across the lowermost mantle at 2750 km depth in the bottom panel. Colors represent the percentage of shear wave deviation from the mean value. Figure modified from (Ritsema et al., 2011).

A Brief History

Over the past thirty years, several differing approaches have been taken to understand and explain the LLSVP anomalies. Early in that history, it was found that shear-wave tomography provided the clearest definition and resolution of these features. Figure 2 displays a relatively recent map of the variation of seismic shear-wave speed in the lowermost mantle and includes 3-dimensional iso-surfaces for the LLSVPs (Ritsema et al., 2011). However, the features also appear in compressional wave tomography. Figure 3 displays the results of several joint shear and compressional wave seismic tomography models, with regions of low shear-wave speed distinguished by color from regions of low compressional-wave speed. Notice the gradient in wave speed that so famously prompted the recognition of these phenomena.

Has anyone in the secular scientific community provided a plausible explanation for the formation of LLSVPs? The short answer is no. Not only is there

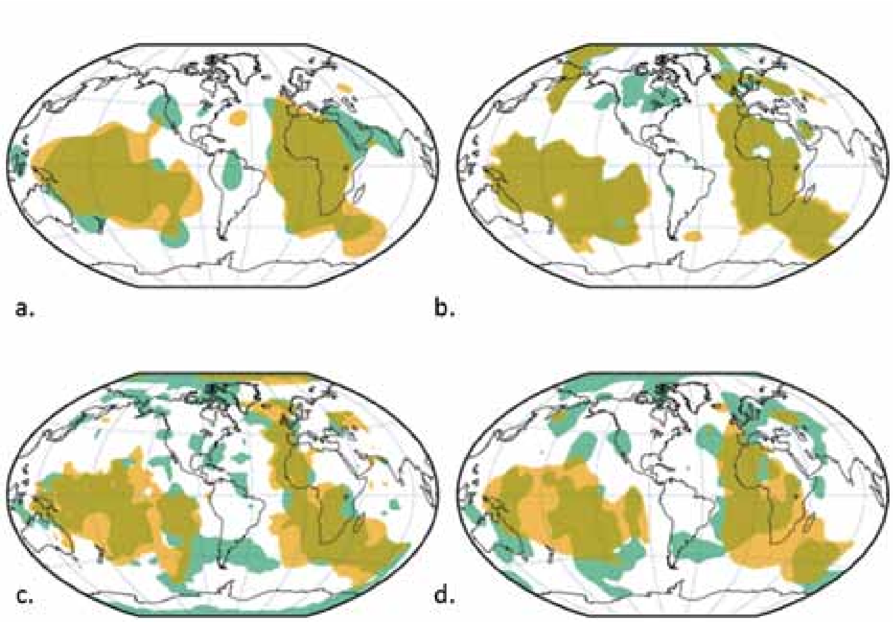

Figure 3. Joint shear- (S-wave) and compressional- (P-wave) tomography models. Yellow denotes regions with low S-wave speed, while green denotes regions of low P-wave speed, within the lowest portion of the mantle. a. SP12RTS model (Koelemeijer et al., 2016); b. GyPsum model (Simmons et al., 2010); c. HMSL model (Houser et al., 2008); d. An average of earlier models (Becker and Boschi, 2002). Plots modified from Garnero et al. (2016).

a lack of agreement among the proposed explanations, but there is a general perception that no solution to date is anywhere close to a satisfying one. Let us survey briefly several of the more recent attempts to account for the LLSVPs.

In its explanation of LLSVP formation, a paper published in 2007 hypothesized that a partial melting of recycled Mid-Oceanic-Ridge Basalt (MORB) caused a phase change at the core-mantle boundary (CMB), raising its temperature and causing the residual solid MORB to rise and leave behind anti-crust. The repetition of this process over millions of years slowly formed the LLSVPs (Maruyama et al., 2007). The issue of LLSVP stability, although briefly mentioned, is not adequately considered and is largely avoided.

In a 2018 paper, Niu valiantly posited that the LLSVPs are composed of subducted oceanic crust that has somehow separated from the remainder of the subducted slab due to its density difference (Niu, 2018). Niu's scenario consists of the subduction of oceanic plates to the CMB where they then separate into subducted oceanic crust (SOC) and slab mantle lithosphere (SML) (Niu, 2018). This separation is far more easily said than done, as it is not easy to imagine how the thin SOC layer might separate from the SML as they fold together at the CMB.

Mulyukova also discusses the formation of LLSVPs from SOC accumulation at the CMB in her 2015 paper (Mulyukova et al., 2015) and offers an explanation for the apparent stability of LLSVPs. The formation of LLSVPs from SOC also appears in a paper by Huang et al. (2020).

LLSVPs and Terra

An exciting development relating to LLSVPs is the enhancement they provide to current Pangea breakup simulations using the terra code. Terra (Baumgardner, 1985) is a mantle dynamics simulation program that utilizes the equations of force balance, conservation of mass, and conservation of energy in the framework of a 3D spherical-shell grid of cells. The number of cells depends on the resolution chosen. The grid for the case described here has 1.35 million cells. Terra utilizes the finite-element method to solve these equations for the three components of velocity at each grid point plus pressure and temperature as the calculation steps through time. It employs a powerful solver technique known as multigrid to solve 5.4 million simultaneous equations for 5.4 million unknowns on each time step in about 0.5 seconds on a current generation laptop. It represents tectonic plates on the Earth's surface using particles that track each plate in a highly accurate manner. When terra cases are run using postulated initial conditions, the code simulates the breakup of the Pangea supercontinent during the Flood.

It must be understood that such Pangea breakup simulations have been discussed in previously published papers, namely Baumgardner (1993, 1994a, 2003). The following discussion is, however, an explanation of an attempt to improve simulation realism. The following results differ from previous calculations only slightly and yield slightly improved results.

Results

The African LLSVP anomaly was recently included in the terra Pangea calculations as a cluster of four distinct

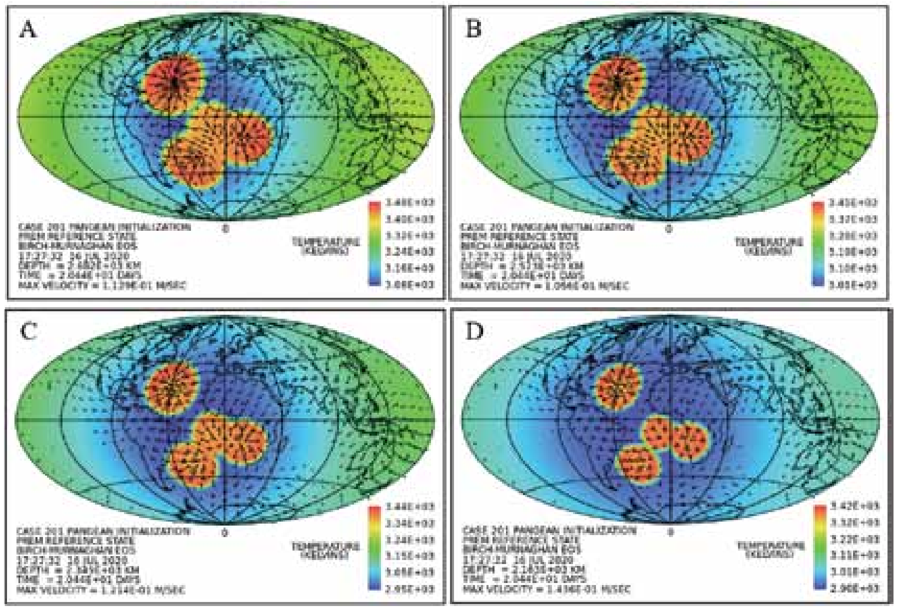

Figure 4. African LLSVP as a function of decreasing depth. (a) 2682 km (b) 2523 km (c) 2349 km (d) 2163 km.

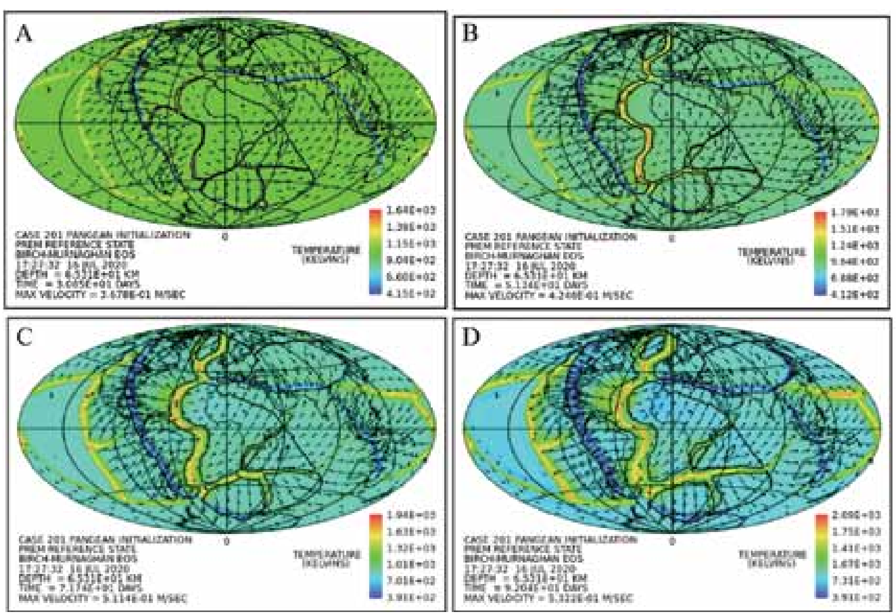

Figure 5. TERRA Pangea breakup simulation that includes the Africa LLSVP. (a) 31 days (b) 51 days (c) 72 days (d) 92 days.

blobs of buoyant mantle rock. Each was represented as a sphere with specified radius and specified distance of its center from the CMB. Figure 4 shows slices through the LLSVP blobs as a function of decreasing depth. Figure 5 displays a series of snapshots in time of the terra solution that includes the LLSVP implementation.

Discussion

While running these terra cases, it was realized that the principles of Catastrophic Plate Tectonics and the tumultuous upheaval during the Flood can provide a simple explanation for these enigmatic LLSVP structures. Let's briefly summarize these principles before we present our hypothesis for LLSVP formation.

Catastrophic Plate Tectonics, the Genesis Flood, and LLSVPs

Catastrophic plate tectonics (CPT) has demonstrated considerable explanatory power relative to the tectonic aspects of the Genesis Flood (Austin et al., 1994; Baumgardner, 1994a, 1994b, 2003). CPT relies on the experimentally measured properties of silicate minerals that show dramatic weakening under values of shear stress that can arise in Earth's mantle. This weakening allows runaway subduction to occur and catastrophic conditions for the wide-scale geological resurfacing during Noah's Flood to unfold (Austin et al., 1994; Baumgardner, 2003).

At the onset of the Flood, oceanic plates began to subduct along continental plate margins. The resulting geological upheaval simultaneously caused superheated steam jets to arise where plates pulled apart and tsunamis to form from the subduction zones. As subducted plates reached the core-mantle boundary, they began to push aside the hot rock just above that boundary and caused two antipodal patches of rock there to be squeezed together and then upwards akin to squeezing toothpaste from a tube. This hot material began to rise to the surface due to its buoyancy relative to the surrounding rock.

This, then, is the process we propose for LLSVP formation. When the runaway subduction had moved most of the cold plate material from Earth's surface and had carried it to the bottom of the mantle, the energy driving the process was largely exhausted. At this point, the high velocities plummeted and the silicate mantle viscosity, which had been temporarily dramatically reduced by the runaway process, then rapidly increased to modern levels. The newly emplaced hot material from the CMB, now also with dramatically higher viscosity, was essentially frozen in place—stable in terms of a time scale of a few thousand years—to become the LLSVPs of today.

LLSVPs Today

This explanation addresses the matters that are so problematic to the secular geoscience community, namely, LLSVP origin and stability. Indeed, LLSVPs have been shown to be in motion, though only at the rate of a few mm per year (Bono et al., 2019). Thus LLSVPs are buoyant and in motion, and this fact only reinforces the CPT explanation. Whereas the millions of years required by uniformitarianism leads to insurmountable difficulties in accounting for the apparent stability of LLSVPs, their formation only thousands of years ago eliminates this paradox. They have been mobile since their formation but have not traveled a substantial distance because that formation was very rapid and in the recent past, not millions of years ago.

Conclusion

Secular science has been unable to arrive at a reasonable explanation for the two antipodal structures that exist at the core-mantle boundary, originally known as superplumes but now known as Large Low-Shear-Velocity Provinces. Why are these structures so baffling? Psalm 19:1–3 (NKJV) states that "The heavens declare the glory of God; and the firmament shows His handiwork. Day unto day utters speech, and night unto night reveals knowledge. There is no speech nor language where their voice is not heard." Although this passage speaks of the heavens evoking the glory of the Creator, Earth bears such witness on a comparable scale. Earth does not show evidence for uniformitarian long ages, but loudly proclaims a recent global Flood cataclysm and bears witness to God's very real judgment on human sin. These elegant structures are simply additional features that testify to the truthfulness of God's Word, the power and sovereignty of God, and the reality of the global Flood. As Psalm 29:10 (NKJV) states: "The LORD sat enthroned at the Flood, and the LORD sits as King forever." We have endeavored to show that catastrophic plate tectonics offers a simple and reasonable explanation for the two structures, known as Large Low-Shear-Velocity Provinces, that are so baffling to the secular mind.

References

Austin, S.A., J.R. Baumgardner, D.R. Humphreys, A.A. Snelling, L. Vardiman, and K.P. Wise 1994. Catastrophic plate tectonics: A global Flood model of Earth history. In: Walsh, R.E. (editor), *Proceedings of the Third International Conference on Creationism*, pp. 609–621. Creation Science Fellowship, Pittsburgh, PA.

Baumgardner, J.R. 1993. 3-D numerical investigation of the mantle dynamics associated with the breakup of Pangea. In: Stone, D.B. and Runcorn, S.K. (editors), *Flow and Creep in the Solar System: Observations, Modeling and Theory*. NATO ASI Series (Series E: Applied Sciences), volume 391. Springer, Dordrecht. https://doi.org/10.1007/978–94–015–8206–3_14.

Baumgardner, J.R. 1994a. Computer modeling of the large-scale tectonics associated with the Genesis Flood. In: Walsh, R.E. (editor), *Proceedings of the Third International Conference on Creationism*, pp. 49–62. Creation Science Fellowship, Pittsburgh, PA.

Baumgardner, J.R. 1994b. Runaway subduction as the driving mechanism for the Genesis Flood. In: Walsh, R.E. (editor), *Proceedings of the Third International Conference on Creationism*, pp. 63–86. Creation Science Fellowship, Pittsburgh, PA.

Baumgardner, J.R. 1985. *A Three-Dimensional Finite-Element Model for Mantle Convection*. University of California, Los Angeles, CA. [No such book on Internet.]

Baumgardner, J.R. 2003. Catastrophic plate tectonics: The physics behind the Genesis Flood. In: Ivey, Jr., R. L. (editor). *Proceedings of the Fifth International Conference on Creationism*, pp. 113–126. Creation Science Fellowship, Pittsburgh, PA.

Becker, T.W., and L. Boschi. 2002. A comparison of tomographic and geodynamic mantle models. *Geochemistry, Geophysics, Geosystems* 3(1): 2001GC000168.

Bono, R.K., J.A. Tarduno, and H.-P. Bunge. 2019. Hotspot motion caused the Hawaiian-Emperor Bend and LLSVPs are not fixed. *Nature Communications* 10(1): 1–9.

Burke, K., B. Steinberger, T.H. Torsvik, and M.A. Smethurst. 2008. Plume Generation Zones at the margins of Large Low-Shear-Velocity Provinces on the core-mantle boundary. *Earth and Planetary Science Letters* 265(1–2): 49–60.

Deschamps, F., L. Cobden, and P.J. Tackley. 2012. The primitive nature of large low-shear-wave velocity provinces. *Earth and Planetary Science Letters* 349–350:198–208.

Fukao, Y., S. Maruyama, M. Obayashi, and H. Inoue. 1994. Geologic implication of the whole mantle P-wave tomography. *The Journal of the Geological Society of Japan* 100(1): 4–23.

Garnero, E.J., A.K. McNamara, and S.-H. D. Shim. 2016. Continent-sized anomalous zones with low seismic velocity at the base of Earth's mantle. *Nature Geoscience* 9(7): 481–489.

Houser, C., G. Masters, P. Shearer, and G. Laske. 2008. Shear and compressional velocity models of the mantle from cluster analysis of long-period waveforms. *Geophysical Journal International* 174(1): 195–212.

Huang, C., W. Leng, and Z. Wu. 2020. The continually stable subduction, iron-spin transition, and the formation of LLSVPs from subducted oceanic crust. *Journal of Geophysical Research: Solid Earth* 125(1): 1–20.

Kellogg, L.H., B.H. Hager, and R.D. van der Hilst. 1999. Compositional stratification in the deep mantle. *Science* 283(5409): 1881–1884.

Koelemeijer, P., J. Ritsema, A. Deuss, and H.-J. van Heijst. 2016. SP12RTS: A degree-12 model of shear- and compressional-wave velocity for Earth's mantle. *Geophysical Journal International* 204(2): 1024–1039.

Maruyama, S., M. Santosh, and D. Zhao. 2007. Superplume, supercontinent, and post-perovskite: Mantle dynamics and anti-plate tectonics on the core–mantle boundary. *Gondwana Research* 11(1–2): 7–37.

McNamara, A.K. 2019. A review of large low-shear-velocity provinces and ultra-low-velocity zones. *Tectonophysics* 760: 199–220.

McNutt, M.K. 1998. Superswells. *Reviews of Geophysics* 36(2): 211–244.

Mulyukova, E., B. Steinberger, M. Dabrowski, and S.V. Sobolev. 2015. Survival of LLSVPs for billions of years in a vigorously convecting mantle: Replenishment and destruction of chemical anomaly. *Journal of Geophysical Research: Solid Earth* 120(5): 3824–3847.

Niu, Y. 2018. Origin of the LLSVPs at the base of the mantle is a consequence of plate tectonics—A petrological and geochemical perspective. *Geoscience Frontiers* 9(5): 1265–1278.

Ritsema, J., A. Deuss, H.-J. van Heijst, and J.H. Woodhouse. 2011. S40RTS: A degree-40 shear-velocity model for the mantle from new Rayleigh wave dispersion, teleseismic traveltime and normal-mode splitting function measurements. *Geophysical Journal International* 184(3): 1223–1236.

Simmons, N.A., A.M. Forte, L. Boschi, and S.P. Grand. 2010. GyPSuM: A joint tomographic model of mantle density and seismic wave speeds. *Journal of Geophysical Research* 115(B12). https://doi.org/10.1029/2010JB007631.

Torsvik, T.H., R. van der Voo, P.V. Doubrovine, K. Burke, B. Steinberger, L.D. Ashwal, R.G. Trønnes, S.J. Webb, and A.L. Bull. 2014. Deep mantle structure as a reference frame for movements in and on the Earth. *Proceedings of the National Academy of Sciences* 111(24): 8735–8740.

Wignall, P.B. 2001. Large igneous provinces and mass extinctions. *Earth-Science Reviews* 53(1–2): 1–33.

Using Vardiman's Young-Earth Ice Sheet Model and a Simple Computer Code to Estimate Annual Layer Thicknesses

Jake Hebert*

Abstract

Unfortunately, uniformitarian models of the Greenland and Antarctic ice sheets are currently much more sophisticated than creation models. In fact, creation researchers are about sixty years behind uniformitarian scientists in this area. There is a great need for creation researchers to develop more sophisticated ice sheet and ice core models. Creation Ice Age models predict that annual layers at given depths in the deep Greenland and Antarctic ice cores will be considerably thicker than predicted by uniformitarian models. Here I use Larry Vardiman's 1993 analytical ice sheet model and a simple computer code to obtain estimates of annual layer thicknesses in Greenland's Camp Century ice core. These results are admittedly of limited usefulness, but it is my hope that this paper will help lead to better creation-based ice sheet models. I also hope that it serves a pedagogical purpose in enabling future creation researchers to quickly grasp important ice sheet concepts and to avoid misconceptions.

Introduction

In 1993, Larry Vardiman of the Institute for Creation Research published an analytical model for the rapid post-Flood formation of a thick ice sheet within the 4,500 years since the Genesis Flood (Vardiman, 1993, 1994, and 2001). Other creation researchers (Sherburn, Horsteymeyer, and Solanki, 2008) have used commercial software to model surging (short-term rapid advances) of glaciers. However, very little additional work has been done in this field by creationists, and creation research in this area lags secular research by about sixty years. In particular, there is a need for more sophisticated models for the rapid growth of post-Flood ice sheets, as well as a need to make predictions of annual layer thicknesses, to enable contrasts with the predictions of secular ice sheet models. This paper is a modest first step in that direction. Because of the much smaller number of available creation researchers, it is

* Jake Hebert, PhD, is a physicist and research associate at the Institute for Creation Research
Accepted for publication February 12, 2021

very important to clearly explain important concepts to future creation researchers in this field, so as to minimize the time needed for them to get "up to speed." Writing this paper has been a useful exercise that has helped clarify my thinking on a number of issues, and I hope that it may serve as a tutorial or primer that enables future creation researchers to quickly grasp ice sheet basics and to avoid misconceptions.

Ice Sheet Basics

Glaciologists often drill ice cores at geological features called *ice divides*. These features derive their name from the fact that ice on one side of the divide flows one way, and ice on the other side of the divide flows the other (Figure 1). Ice is deposited on the sheet in horizontal layers. Ice at the divide itself will flow neither to the right nor left, but will move straight down as additional layers are added, assuming no shifting of the ice divide during ice buildup. It is also possible for the ice to form a dome around the divide, so that ice flows radially outward from the divide, not just right and left.

Since the underlying bedrock is fixed (here we ignore possible isostatic adjustments), a horizontal layer that reaches bedrock can no longer move downward; it can only become thinner with time. If no melting occurs at bedrock, the total number of annual layers will equal the number of years since the ice sheet began forming. However, identifying the true number of annual layers is not trivial, since multiple distinct layers may be deposited per year (Alley and Koci, 1988; Alley, 1988). In fact, creation critic Bill Nye inadvertently highlighted why one *cannot* naively assume that each visible band in an ice core is an annual layer (Hebert, 2018a). The counting process has been described as an "art" that requires "trial and error" (Alley et al., 1997, pp. 26367, 26370). Hence uniformitarian glaciologists must make educated guesses about how many of these distinct bands should be grouped together and counted as a year. Unfortunately, these educated guesses are biased by long-age assumptions and circular reasoning (Alley et al., 1997, p. 26419; Oard, 2005; Hebert, 2014).

It should be mentioned in passing that it may technically be a misnomer to say that these ice layers are "compressed." Simple ice sheet models often ignore the variations in density due to the presence of bubbles in the uppermost parts of the ice (which is actually a combination of ice and granular snow called *firn*). The density of glacial ice is 917 kg/m^3, and temperature and pressure variations at the bottom of a four-kilometer-thick ice sheet will cause only slight increases in density (Cuffey and Paterson, 2010, pp. 12–13) to about 921 to 922 kg/m^3, a less than 1% difference. Hence, at most depths, the ice density will be very nearly constant, and the assumption of incompressibility (constant density and volume) is usually made (Paterson, 1980, p. 12).

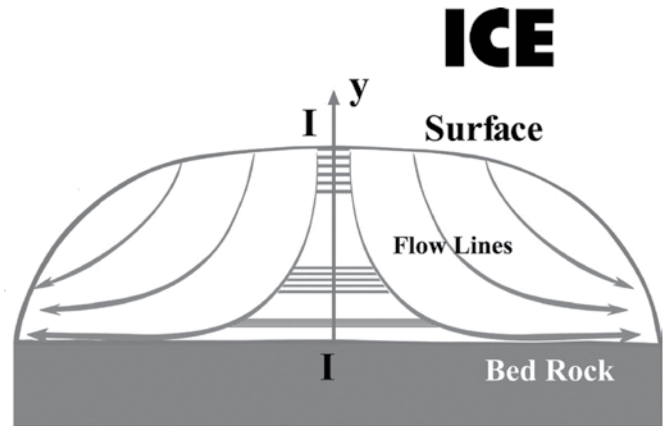

Figure 1. An idealized ice divide. Note that ice on the left of the divide flows to the left, and ice on the right of the divide flows to the right. Ice at the divide location must move straight down. Image courtesy of Michael J. Oard.

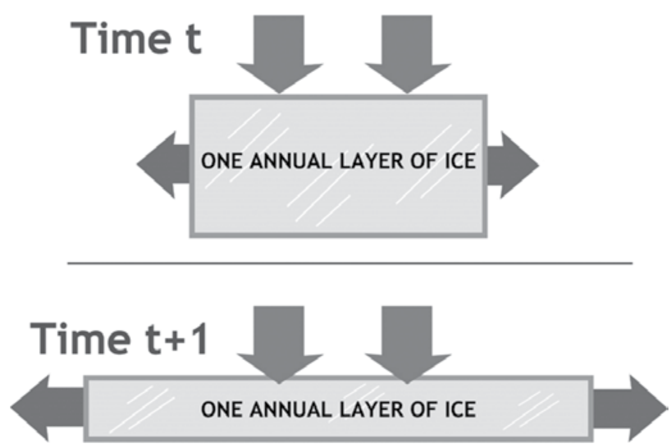

Figure 2. As more layers of ice are deposited at the site of the divide, the layers of ice become thinner, but in such a way that the total volume of each layer remains constant. Image courtesy of Michael J. Oard.

Hence, in the absence of melting or ablation, the total volume of an ice layer remains constant over time. The layer becomes thinner, but it does so in such a way that the total volume of the layer remains constant, with a corresponding increase in the upper and lower surface area of the layer (Figure 2). However, this may be somewhat pedantic, as even experts sometimes refer to vertical "compression" of the ice (i.e., Cuffey and Paterson, 2010, p. 357).

Annual Layer Thicknesses: Creation versus Uniformitarian Expectations

Uniformitarian age-depth models for thick ice sheets often make the simplifying assumption that the height of the ice sheet is constant, or nearly constant (Cuffey and Paterson, 2010, pp. 617–620). For instance, in his preliminary estimation of the amount of layer thinning in an ice sheet, Nye (1963, p. 786) implicitly assumed that the height of the ice sheet H is constant. Dansgaard and Johnsen (1969, p. 216) also made this assumption. At first glance, this does not seem to make sense. Regardless of whether one believes the ice sheet is thousands or millions of years old, its starting thickness *had* to be zero!

However, both creationists and uniformitarians agree that thick ice sheets can form relatively quickly, on the order of thousands or tens of thousands of years (Paterson, 1980, p. 40; Wilson, Drury, and Chapman, 2005). Not too surprisingly, the actual number is strongly dependent upon precipitation rates: the higher the precipitation rates, the less time is needed for the formation of the ice sheet. If one believes the ice sheet to be millions of years old, then one can *legitimately* simplify the calculations by treating the height of the ice sheet as constant. Any error introduced by ignoring the thousands of years for the ice sheet to grow to its steady-state height will be negligible in light of the ice sheet's multi-million-year history. Of course, if the ice sheet is just thousands of years old, then the time for the ice sheet's formation cannot be neglected.

Secular age-depth models predict much more thinning of the ice with depth than do young-Earth models, and some reflection upon Figure 1 shows why. In the absence of melting, all the annual layers are preserved in the ice, even if they cannot all be distinguished visually. In that case, the average thickness of an annual layer is simply the height of the ice sheet divided by the number of years it has been in existence. Naturally, subdividing the ice sheet height into millions of horizontal slices yields a much thinner average annual thickness than if you divided it into just 4,500 horizontal slices.

Although obtaining the average layer thickness is trivial, obtaining the true annual thicknesses as a function of depth is considerably more difficult, because these thicknesses depend upon the vertical strain rate (discussed below), which generally varies with time and depth (Cuffey and Paterson, 2010, pp. 614–617).

Hence, there is a need to be able to calculate the true thickness of an annual layer of ice in a creation model, in order to make comparisons between secular and creationist expectations. Oard (2005, p. 45) has already published some very rough estimates for the GRIP core in central Greenland (Figure 3), but there is a need to obtain more rigorous estimates for these thicknesses.

Creationists have already noted (Oard, 2005; Hebert, 2018b) that both the thicknesses and frequencies of tephra (volcanic ash and debris) layers in the deep ice cores make more sense in a creationist framework than in a uniformitarian one. Finding better estimates for annual layer thicknesses may help demonstrate other ways in which the creation model makes better sense of the data than do uniformitarian models.

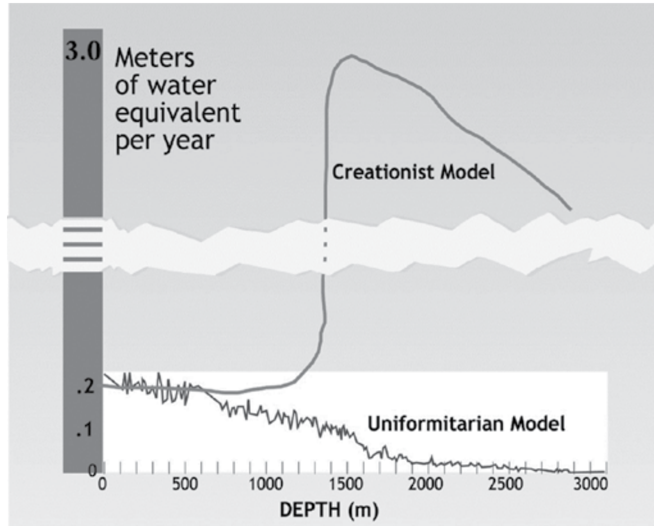

Figure 3. Rough estimates by Oard of annual layer thicknesses (in water equivalent) within Greenland's GRIP ice core, based upon uniformitarian and creationist expectations.

Governing Equation

In the absence of melting, the governing equation, at the divide location, for the growth rate of the ice sheet is:

$$\frac{dH}{dt} = \dot{b}(t) - w_s(t) \tag{1}$$

In Equation (1), H is the height of the ice sheet at the location of the ice divide, t is the time since the ice sheet began forming, and dH/dt is the time rate of change of the ice sheet divide height. $\dot{b}(t)$ is the accumulation rate at the surface of the divide (in meters of ice equivalent per year). $w_s(t)$ is the downward vertical speed of the ice sheet surface at the divide location, also in meters per year. In this discussion we will use z to represent vertical distance (in meters) above bedrock.

When the surface accumulation rate $\dot{b}(t)$ is greater than the downward vertical speed $w_s(t)$ of the ice sheet surface, the thickness of the ice sheet grows, so that the derivative in Equation (1) is positive. If the accumulation rate is equal to the downward surface speed, the derivative is equal to zero, and the ice sheet height remains constant in a "steady state" condition. Finally, if $\dot{b}(t)$ is less than $w_s(t)$, the height of the ice sheet divide will decrease.

Since the underlying bedrock prevents the bottom surface of the ice sheet from moving downward, one boundary condition is that the vertical velocity w is always equal to zero at height $z = 0$. The spatial derivative of vertical velocity is the vertical strain rate (Cuffey and Paterson, 2010, p. 615):

$$\frac{\partial w}{\partial z} = \dot{\varepsilon}_{zz}(t, z) \tag{2}$$

As we shall see later, the vertical strain rate is also (and is actually defined to be) the fractional change in thickness of an ice layer per unit time. In general, the strain rate at the divide is a function of both height z above bedrock and time t. Pioneering glaciologist J.F. Nye developed a simple thinning model (Nye, 1963) in which he assumed that the downward vertical speed increases linearly from zero at bedrock to a maximum value $w_s(t)$ at the surface. Or equivalently, the vertical velocity w has a maximum value of zero at the base, and this velocity decreases linearly with increasing z to a minimum value $-w_s(t)$ at $z = H(t)$. In this case, the strain rate is a function of time but not of depth.

$$\frac{\partial w}{\partial z} = \dot{\varepsilon}_{zz}(t) = -\delta(t) = -\frac{w_s(t)}{H(t)} \tag{3}$$

Vardiman's model is simpler still in that it treats the vertical strain rate $-\delta$ as a constant in both time and space. Not too surprisingly, vertical stress is greater at greater depths due to the greater weight of the overlying ice. However, the magnitude of the vertical strain rate is zero at a frozen base. For a frozen base, with horizontal velocity always zero at $z = 0$, the vertical strain rate must also be zero at $z = 0$, since the divergence of the ice velocity is zero (next section). Vertical strain rate is often approximated (Johnsen and Dansgaard, 1969) as a piecewise function whose magnitude increases from zero linearly up to some intermediate depth, and then remains constant all the way up to the surface. The strain rate also depends on time t. Future creation ice sheet models need to take into account space and time variations in the vertical strain rate.

Mass Balance

As implied by Equation (1), two competing processes influence the change dH in ice sheet height within a given time interval dt. The accumulation rate $\dot{b}(t)$ causes H to increase, but the thinning of underlying layers causes H to decrease.

Because we are treating the ice as incompressible, the divergence of ice velocity must everywhere be equal to zero. The ice core has a constant radius R and a cross-sectional area of πR^2 (Figure 4). Hence, any downward mass flux of ice (per unit time) at the top of the ice core must be balanced by the radially outward mass flux of ice (per unit time) occurring at $r = R$. For cylindrical coordinates, in the case of azimuthal symmetry, the divergence of the velocity (Griffiths, 1989, inside cover) is

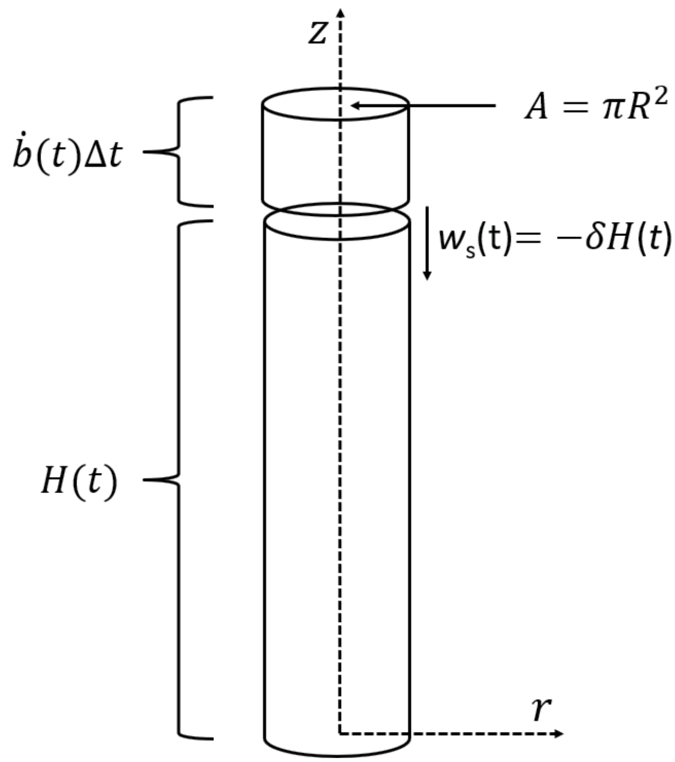

Figure 4. Diagram of an ice core of height *H* and radius *R*, at time *t*, just before the next layer of annual accumulation is deposited. The ice at $z = H(t)$ is moving downward with a speed of $\delta H(t)$. The next layer of ice accumulation will be deposited shortly after time $t + \Delta t$, after the already-deposited layers have been thinned.

$$\bar{\nabla} \cdot \bar{v} = \frac{1}{r}\frac{\partial}{\partial r}(r v_r) + \frac{\partial w}{\partial z} = 0 \tag{4}$$

Since the gradient of w is $-\delta$, we can solve Equation (4) to obtain the radially outward velocity of the ice:

$$v_r = \frac{\delta r}{2} = \frac{w_s(t) r}{2H(t)} \tag{5}$$

Note that, although $w_s(t)$ and $H(t)$ both depend on time, their ratio, δ, does not. The downward rate of mass flow (per unit time) into the cylinder's top face (Figure 4) is

Downward Mass Flow =

$$w_s(t)\rho A = [\delta H(t)]\rho A = \rho\delta H(t)\left(\pi R^2\right) \tag{6}$$

The radially outward rate of mass flow (per unit time) is the radial velocity evaluated at $r = R$, multiplied by the ice density ρ and the surface area of the cylinder's side:

Outward Mass Flow =

$$\rho\frac{\delta R}{2}[2\pi RH(t)] = \rho\delta H(t)\left(\pi R^2\right) \tag{7}$$

As expected, these two quantities are equal. In fact, mass balance is implied by Equation (1), since Equation (1) can be converted into a mass balance equation by multiplying both sides of the equation by ρA: the net change in mass of the ice core per unit time is the difference between the mass accumulation rate at the surface and the total mass outflow rate at the side of the core.

Vardiman's Model

Here we use Larry Vardiman's analytical ice sheet model (1993) and a simple computer code to estimate layer thicknesses in Vardiman's model. Vardiman wrote my Equation (1) as

$$\frac{dH}{dt} = \frac{\lambda(t)}{\tau} - \delta H \tag{8}$$

Here $\lambda(t)$ is the thickness of ice accumulation that occurs in a time increment $\tau = 1$ year. Since τ is always equal to 1, it may seem redundant to include it here, but we do so for purposes of dimensional consistency, as well as consistency with Vardiman's notation. As noted earlier, the vertical strain rate at the divide, $-\delta$, is constant in both time and space. By comparison with Equation (1), we see that Vardiman has implicitly assumed that the downward surface speed at the divide is always proportional to the height of the ice sheet.

Equation (8) may be rewritten as

$$\frac{dH}{dt} + \delta H = \frac{\lambda(t)}{\tau} \tag{9}$$

Vardiman reasonably assumed that the post-Flood ice accumulation rate would start very high and then smoothly decay over time to today's "slow and gradual" average accumulation

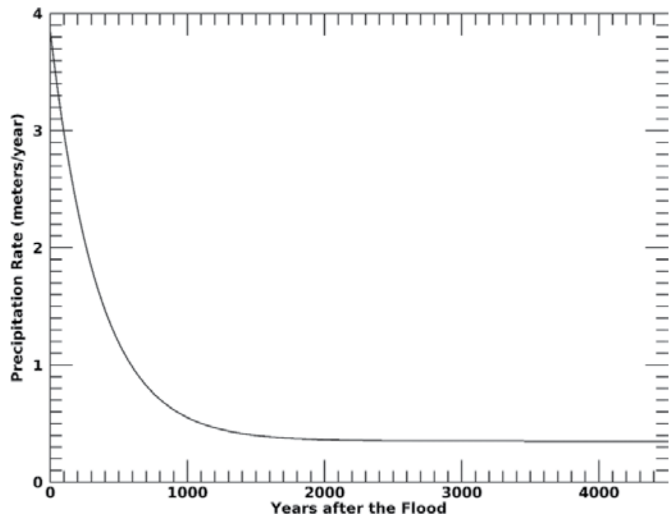

Figure 5. Vardiman's model for post-Flood ice accumulation at Greenland's Camp Century core, using parameter values of Φ = 10.0, Ψ = 350 years, H_∞ = 1370 meters, λ_H = 0.35 meters, and δ = 2.55×10^{-4} meters^{-1}.

rates. Therefore, he modelled the accumulation rate as a decaying exponential (Figure 5):

$$\dot{b}(t) = \frac{\lambda(t)}{\tau} = \frac{\lambda_H}{\tau}(\Phi e^{-t/\Psi} + 1) \tag{10}$$

Here λ_H/τ is today's accumulation rate, in meters of ice equivalent per year. Φ is a dimensionless number greater than 1 used to "scale up" the amount of Ice Age precipitation compared to today's average annual value. Likewise, t is the time since the ice sheet began forming, and Ψ is the e-folding time, the time for the initial post-Flood accumulation rate to drop to 37% of its original post-Flood value.

After including the expression for the accumulation rate, Equation (9) may be solved with the mathematical "trick" (Zill, 1989, p. 66) of multiplying both sides of the equation by an "integration factor," in this case, $e^{\delta t}$. This makes the left-hand side of Equation (9) the exact derivative of $He^{\delta t}$. Integration (see Vardiman, 2001 for details) yields this expression for $H(t)$:

$$H(t) = \frac{\lambda_H}{\tau\delta}\left(1 - e^{-\delta t}\right) + \frac{\Phi\lambda_H}{\tau\left(\delta - 1/\Psi\right)}\left(e^{-t/\Psi} - e^{-\delta t}\right) \tag{11}$$

Vardiman then imposed the boundary condition that the height of the ice sheet equal its steady state height H_∞ when $t \rightarrow \infty$. In particular, he used the Camp Century ice core from Greenland, whose current height is 1,370 meters and which would presumably have a frozen base (no melting) due to the low temperature near bedrock (Dansgaard and Johnsen, 1969, p. 216). This results in

$$H_\infty = \frac{\lambda_H}{\tau\delta} = 1370 \text{ m} \tag{12}$$

Using today's average accumulation rate of 0.35 meters/year, this allows us to solve for the parameter δ:

$$\delta = \frac{\lambda_H}{(1370 \text{ m})\tau} = 2.55 \times 10^{-4} \text{year}^{-1} \tag{13}$$

Figure 6 is a graph of $H(t)$ versus time since the Flood, using values of $\Phi = 10$, $\Psi = 350$ years, and a total time since the Flood of 4,500 years. The height of the ice sheet at $t = 4{,}500$ years is 1,362 meters, not quite the full 1,370-meter height obtained at $t = \infty$.

In passing, I should note that there appears to be an error in Vardiman's (2001) expression (his Equation 4.20, p. 49) for the vertical velocity. This is not intended as a criticism, but merely as a "guidepost" for future researchers in this area. Using my notation, his expression is

$$w(z) = -\delta \frac{z}{H_\infty} H(t) \tag{14}$$

Based on Equations (3) and (13), and the boundary condition that $w(z = 0, t) = 0$, it seems this expression should actually be

$$w(z) = -\delta z = -\frac{\lambda_H}{\tau H_\infty} z, \quad z \le H(t) \tag{15}$$

Note (Figure 4) that at $z = H(t)$, the downward velocity is $-\delta H(t)$, as indicated by Equation (15). Note also that the downward velocity is $-\lambda_H/\tau$ when $z = H_\infty$, as this is the downward velocity needed for the ice sheet to remain in steady state.

Numerically Obtaining Annual Layer Thicknesses

A simple computer code may be used to obtain the thickness of each annual layer at any given time, assuming that $H(t)$ and $\dot{b}(t)$ both are already known. I used the Interactive Data Language (IDL) to write my code. In this example, we use Vardiman's values for these quantities, calculated using the same parameter values used to produce Figures 5 and 6. The code uses double precision values for both constants and arrays to ensure numerical accuracy. However, in order to demonstrate the method in Figures 7–10, I do *not* practice rigorous adherence to significant figure rules. The reason for this is that rigid adherence to these rules, combined with rounding errors, will obscure the relationships between the numbers in Figures 7, 9, and 10, making it more difficult for the reader to follow the methodology I used.

The code establishes two arrays, each with 4,501 elements, each element corresponding to a particular time t since the Flood (and inclusive of $t = 0$). These arrays (Figure 7) give the values of $\dot{b}(t)$ and $H(t)$ at 4,501 particular times since the Flood, with an increment $\Delta t = t = 1$ year between each of these times. We are using a discrete numerical process to simulate a continuous process, so to keep our thinking straight, it is important to explicitly note the *precise* meaning of these $H(t)$ values. Each value of $H(t)$ is the total ice-core-divide height at the very start of a time increment, just *before* any of that year's ice accumulation has been deposited. Furthermore, we can imagine the entire year's worth of accumulation occurring just a tiny fraction dt of a year later. After the ice layer has been deposited, the thinning process begins and occurs continuously throughout Δt until the start of the next time interval.

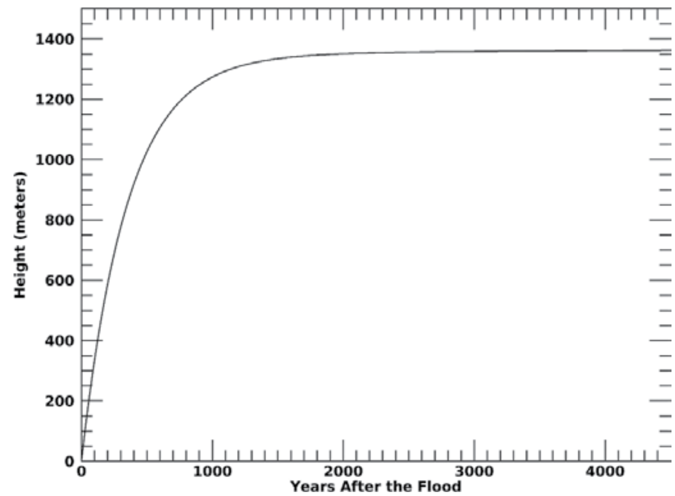

Figure 6. Height of the Camp Century (Greenland) ice sheet as a function of time since the Flood, using Vardiman's ice sheet model, with the same parameter values used to produce Figure 5.

Time *t* after Flood (in years)	Annual Precipitation $\dot{b}(t)$ (meters of ice equivalent/year)	Height of Ice Sheet *H*(*t*) (meters)
4,500	0.35000913	1362.1697
4,499	0.35000915	1362.1677
4,498	0.35000918	1362.1657
4,497	0.35000920	1362.1637
3	3.8201282	11.500715
2	3.8300570	7.6780746
1	3.8400143	3.8445134
0	3.8500000	0.00000000

Figure 7. Vardiman's model is used to calculate the values of *H* and $\dot{b}(t)$ in advance for the 4,500 years since the Flood.

We also establish an array λ, with 4,500 elements, each element corresponding to the current thickness of each one of the 4,500 annual layers deposited since the Flood. Since no layers have yet been deposited at time $t = 0$, all the elements in λ are initially set to 0. These values will be updated iteratively as the code runs.

The infinitesimal vertical strain ε_{zz} of a layer of ice is defined as the fractional change in the thickness of that particular layer:

$$\varepsilon_{zz}(z,t) = \frac{d\lambda}{\lambda(z,t)} \tag{16}$$

Since the layer thins, $d\lambda$ is negative, as is the strain. Taking the derivative of both sides gives the strain rate, the fractional change in thickness per unit time (Cuffey and Paterson, 2010, p. 615):

$$\dot{\varepsilon}_{zz}(z,t) = \frac{d\varepsilon_{zz}}{dt} = \frac{1}{\lambda}\frac{d\lambda}{dt} \tag{17}$$

Separation of variables and integrating from time t to time $t+\Delta t$ yields

$$\lambda(t+\Delta t) = \lambda(t)e^{\left(\int_{t}^{t+\Delta t} \dot{\varepsilon}_{zz}(t)dt\right)} \tag{18}$$

In other words, the thickness of a given ice layer after thinning will be the thickness prior to thinning, multiplied by the exponential, which I am calling "the fraction of thickness retained." Since $\dot{\varepsilon}_{zz}(t)$ is inherently negative (or zero), this fraction will always be less than or equal to 1, which implies that the thickness of the layer after thinning cannot be greater than it was before thinning. Note that Equation (18) is applicable to all 4,500 annual layers of the ice sheet, even if a layer has not yet been deposited. In that case, the fraction is simply multiplied by 0 meters, leaving the original thickness of that (not yet deposited) layer as still 0.

Two things should be noted regarding Equations (17) and (18). First, since the strain rate does not depend on height z in Vardiman's model, and because the total thickness of the ice sheet H is equal to the sum of the thicknesses of the individual layers, it is also true that

$$\text{Fraction of thickness retained} = \frac{\lambda(t+\Delta t)}{\lambda(t)} = \frac{H(t+\Delta t)}{H(t)} \tag{19}$$

Second, remember that conceptually we are imagining that the entire year's worth of ice accumulation occurs just a tiny fraction of a year *after* the start of the time interval. Since the thinning process does not begin until the year's accumulation has been deposited, we should, when calculating the fraction of retained thickness (Figure 8), replace *H(t)* with *H(t)* + $\dot{b}(t)\tau$, since this is the true thickness just before the thinning process begins:

$$\text{Fraction of thickness retained} = \frac{\lambda(t+\Delta t)}{\lambda(t)} = \frac{H(t+\Delta t)}{H(t)+\dot{b}(t)\tau} \tag{20}$$

Demonstration of the Method

As noted earlier, at the start of the program ($t = 0$), all of the 4,500 cells in the λ array are assigned a value of zero, indicating that all 4,500 annual layers currently have a thickness of 0

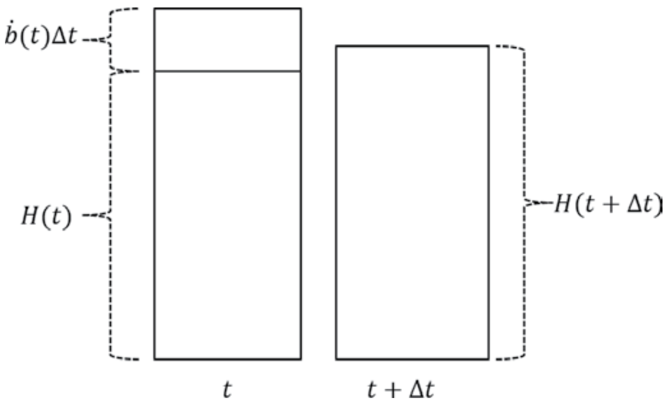

Figure 8. Due to thinning, the height of the ice sheet at time $t + \Delta t$ will be less than the sum of the previous height and the thickness of ice that was deposited just after t. Note that $\Delta t = \tau = 1$ year.

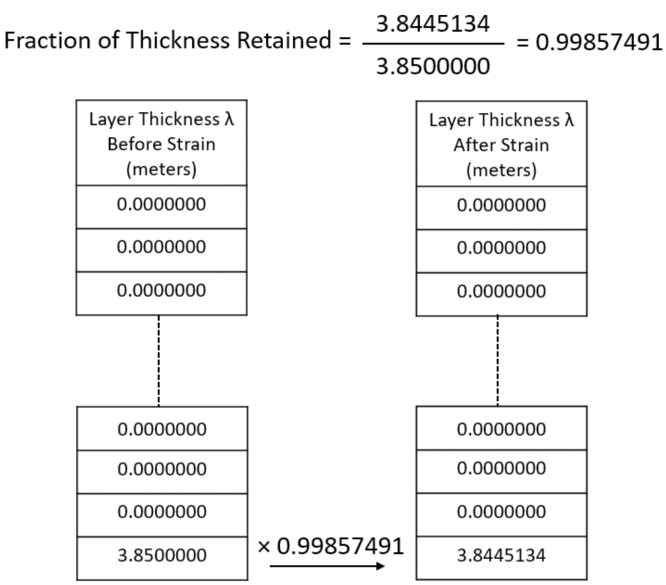

Figure 9. Illustration of how Equation 20 and Figure 7 are used to calculate the thickness of the first annual layer after thinning.

meters. All 4,501 values of $H(t)$ and $\dot{b}(t)$ have been calculated from Vardiman's model and stored in the appropriate arrays (Figure 7).

During the first year, exactly 3.85 meters of ice is deposited (Figure 7). Conceptually, we can imagine that all 3.85 meters of this ice is deposited at an infinitesimal time dt after $t = 0$. This is the layer thickness λ before the thinning that occurs

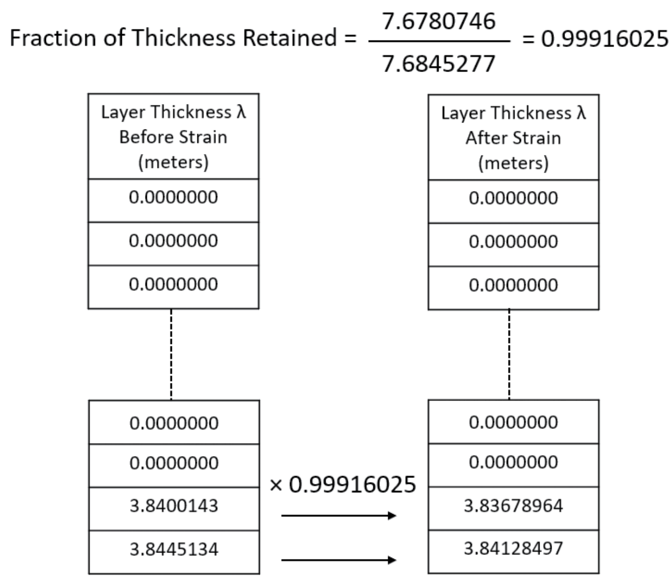

Figure 10. Illustration of how Equation 20 and Figure 7 are used to calculate the thicknesses of the first two layers, after the second annual layer has been deposited and both of the two layers have been thinned.

between $t = 0$ and $t = 1$. The fraction of the layer thickness retained will be

$$\begin{aligned}\text{Fraction of thickness retained} &= \frac{H(1)}{H(0)+\dot{b}(0)\tau} \\ &= \frac{3.8445134\text{ m}}{0\text{ m} + 3.8500000\text{ m}} \\ &= 0.99857491\end{aligned} \tag{21}$$

Note that the first values of $H(t)$ and $\dot{b}(t)$ are designated by the index $i = 0$, not $i = 1$, because IDL requires its array indices to start at 0, rather than 1. From Equations (18) and (20), and Figure 9, we see that the thinned thickness of this first layer will be

$$\begin{aligned}\lambda_{after}(1\text{ year}) &= \lambda_{before} \times 0.99857491 \\ &= 3.8500000\text{ m} \times 0.99857491 \\ &= 3.8445134\text{ m}.\end{aligned} \tag{22}$$

In this particular case, the starting value of λ is equal to $\dot{b}(t)\tau$. This will always be true for the uppermost layer, which

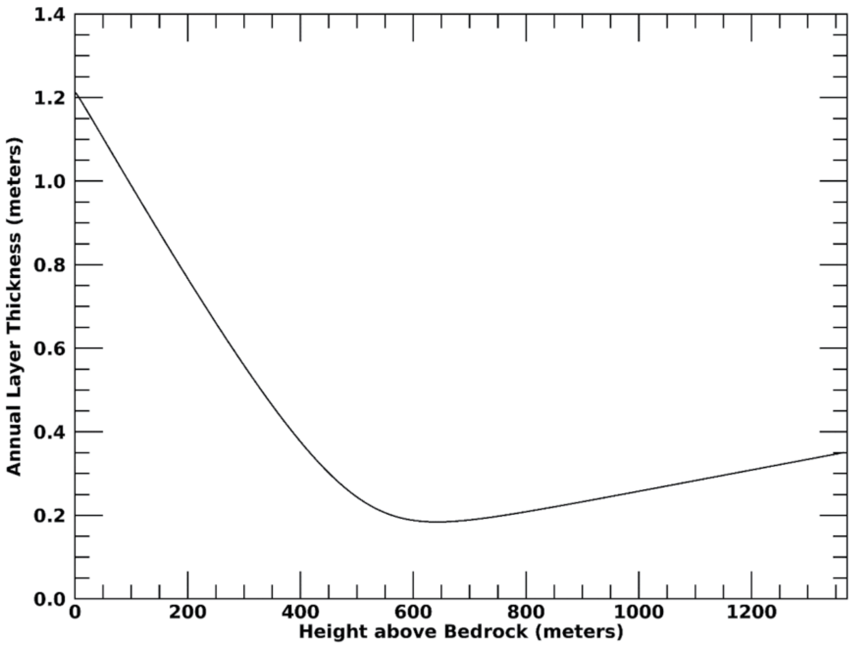

Figure 11. Resulting Camp Century annual layer thickness as a function of height above bedrock. The sum of the thicknesses of all 4,500 layers is 1,362.1697 meters, the height of the ice sheet at t = 4,500 years (see Figure 7).

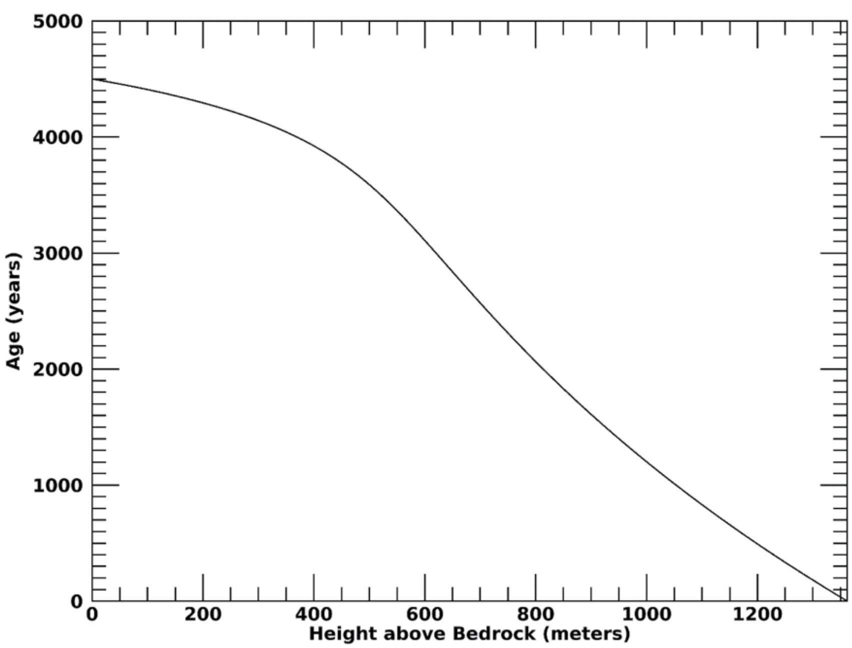

Figure 12. Age of Camp Century annual layers as a function of height above bedrock.

has just been deposited, but it is not true for the layers below it. Note that the ending thickness of this first layer (Figure 9) is equal to the height H (Figure 7) at the start of the next time increment (t = 1 year), as it should be.

This process is then repeated. A second layer $\dot{b}(1)\tau$ of thickness 3.8400143 meters (Figure 10) is deposited. Equations (18) and (20), together with the updated thickness $\lambda(0) = H(1)$ of the bottom layer, gives us a "fraction of thickness retained" of

$$\text{Fraction of thickness retained} = \frac{H(2)}{\left(H(1)+\dot{b}(1)\tau\right)} = \frac{H(2)}{\left(\lambda(0)+\dot{b}(1)\tau\right)} \tag{23}$$

Substituting the appropriate values into Equation (23) yields a fraction of 0.99916025. Multiplying both current thicknesses of these two layers by this fraction gives their new thicknesses (Figure 10). Note that the sum of these two new thickness is 3.84124897 m + 3.83678964 m = 7.6780746 m, which is the height of the ice sheet at t = 2 years (Figure 7), as it should be. The process is repeated until all 4,500 layers have been filled. As a consistency check, the height of the ice sheet at t = 4,500 years is 1,362.1697 meters, which is also the final sum of all 4,500 individual layer thicknesses.

Results

Figure 11 is the resulting graph of annual layer thickness as a function of height above bedrock. Note that the annual layer thickness at the top of the ice sheet is ~0.35 meters, as it should be, since the present-day accumulation rate is ~0.35 meters per year, and the uppermost layer has undergone negligible thinning. The bottommost layers have been thinned quite a bit, but are still much thicker than one would expect from a uniformitarian model.

That the minimum layer thickness in Figure 11 occurs, not at the very bottom of the core, but at an intermediate depth, makes physical sense. The much higher precipitation rates shortly after the Flood will tend to make the deepest annual layers much thicker than those at the top of the core. On the other hand, the deepest layers have also been thinning for the longest amount of time. These two competing processes will cause the minimum thickness to occur, not at the very bottom of the ice sheet, but at an intermediate depth, in this case about 600 meters above bedrock.

Since we know the exact time at which each layer was deposited, it is also possible to obtain the age of the ice as a function of height above bedrock (Figure 12).

An Alternate Method

We may simplify Equation (18) to obtain another expression for the final annual layer thickness for a layer having an age equal to (4,500 – t) years. Since $-\delta$ is constant, it may be "pulled out" of the integral:

$$\begin{aligned} \lambda &= \lambda_0 e^{-\delta \times age} \\ &= \dot{b}(t)\tau \cdot e^{-\delta \times (4500\text{-}t)} \end{aligned} \tag{24}$$

In words, the final thickness is the original thickness of the layer at the time it was deposited, multiplied by an exponential thinning factor that depends on the layer's age. Use of Equation (24) yields final layer thicknesses that are in very good agreement with Figure 11.

Discussion

These results should not be taken too seriously, as they were derived from the assumption that downward surface speed at the divide is proportional to the height, which is unrealistic (Vardiman himself acknowledged that his work was a preliminary effort). Nevertheless, it illustrates some important ice core basics. Hopefully this will become the springboard for more sophisticated creation ice sheet models in the future. The Mahaffy (1976) model may be a good place to start, as it allows for a time-varying accumulation rate and does *not* assume steady-state, as do most uniformitarian ice sheet models.

References

Alley, R.B. 1988. Concerning the deposition and diagenesis of strata in polar firn. *Journal of Glaciology* 34(118): 283–290.

Alley, R.B., and B.R. Koci. 1988. Ice-core analysis at Site A, Greenland: Preliminary results. *Annals of Glaciology* 10: 1–4.

Alley, R.B., C.A. Shuman, D.A. Meese, A.J. Gow, K.C. Taylor, K.M. Cuffey, J.J. Fitzpatrick, P.M. Grootes, G.A. Zielinski, M. Ram, G. Spinelli, and B. Elder. 1997. Visual-stratigraphic dating of the GISP2 ice core: Basics, reproducibility, and application. *Journal of Geophysical Research* 102 (C12): 26367–26381.

Cuffey, K.M., and W.S.B. Paterson. 2010. *The Physics of Glaciers* (4th ed.). Butterworth-Heinemann (an imprint of Elsevier), Amsterdam, Netherlands.

Dansgaard, W., and S.J. Johnsen. 1969. A flow model and a time scale for the ice core from Camp Century, Greenland. *Journal of Glaciology* 8(53): 215–223.

Griffiths, D.J. 1989. *Introduction to Electrodynamics* (2nd ed). Prentice Hall, Englewood Cliffs, New Jersey.

Hebert, J. 2014. Ice cores, seafloor sediments, and the age of the Earth, Part 2. *Acts & Facts* 43(7).

Hebert, J. 2018a. Bill Nye, PBS highlight young-Earth evidence. *Creation Science Update*. Posted on ICR.org. April 27, 2018. https://www.icr.org/article/bill-nye-PBS-young-earth (accessed July 7, 2020).

Hebert, J. 2018b. Tephra and inflated ice core ages. *Journal of Creation* 32(3): 4–6.

Mahaffy, M.W. 1976. A three-dimensional numerical model of ice sheets: Tests on the Barnes Ice Cap, Northwest Territories. *Journal of Geophysical Research* 81(6): 1059–1066.

Nye, J.F. 1963. Correction factor for accumulation measured by the thickness of the annual layers in an ice sheet. *Journal of Glaciology* 4(36): 785–788.

Oard, M.J. 2005. *The Frozen Record: Examining the Ice Core History of the Greenland and Antarctic Ice Sheets*. Institute for Creation Research, Santee, CA.

Paterson, W.S.B. 1980. Ice sheets and ice shelves. In: Colbeck, Samuel C. (editor). *Dynamics of Snow and Ice Masses*. Academic Press, New York, NY.

Sherburn, J.A., M.F. Horstemeyer, and K. Solanki. 2008. Simulation analysis of glacial surging in the Des Moines Ice Lobe. In: *Proceedings of the Sixth International Conference on Creationism*. Snelling, Andrew A. (editor). Creation Science Fellowship, Pittsburgh, PA, and Institute for Creation Research, Dallas, TX, pp. 263–273.

Vardiman, L. 1993. *Ice Cores and the Age of the Earth*. Institute for Creation Research, San Diego, CA.

Vardiman, L. 1994. An analytic young-Earth flow model of ice sheet formation during the "Ice Age." In: *Proceedings of the Third International Conference on Creationism*. Walsh, Robert (editor). Creation Science Fellowship, Pittsburgh, PA, pp. 561–568.

Vardiman, L. 2001. *Climates Before and After the Genesis Flood: Numerical Models and Their Implications*. Institute for Creation Research, El Cajon, CA, pp. 41–68.

Wilson, R.C.L., S.A. Drury, and J.L. Chapman. 2005. *The Great Ice Age: Climate Change and Life* (electronic version). Routledge and the Open University, London, UK, and New York, NY.

Zill, D.G. 1989. A *First Course in Differential Equations with Applications* (4th ed.). PWS-Kent Publishing Company, Boston, MA.

Supernova Light Curves and Accelerated Decay

Eugene Chaffin*

Abstract

Neutrinos and antineutrinos are emitted in great quantity in supernova explosions. In a previous paper they were linked to a hypothetical acceleron field and the variations in this acceleron field as the blast reached earth were investigated as a cause for accelerated nuclear decays. In this paper, the nuclear decays, which are thought to be primarily decays of Nickel-56 and Cobalt-56, which power the light curves of supernovae are investigated. The half-lives and other properties of Nickel-56 and Cobalt-56 have been measured in the laboratory, and the theory of the ground state and other levels of these nuclei are investigated to see if they are sensitive to changes in the acceleron field. One cannot induce stars to explode, but supernovae are often observed in distant galaxies and their study may be used to infer what the possible behaviors are. Nuclear theory is examined to see what the characteristics of Ni-56 and Co-56 might be, including whether the ground states of these nuclei have a pairing gap in their energy states. The calculations indicate that Ni-56 has no pairing gap and the neutrons in Co-56 have no pairing gap. There is a weak pairing gap for protons in Co-56. The implications of this for whether accelerated decay would result for these nuclei, and hence whether accelerated decay would be compatible with the observed light curves if the acceleron mechanism is adopted.

Introduction

In order to match the evident amount of decay that has occurred in Earth rocks, and fit the Biblical timescale, the RATE project emphasized an accelerated decay episode, beginning early in the year of the Genesis Flood, and tapering off somewhere between a minimum of about ten years and a maximum somewhat less than a thousand years after the Flood (Vardiman, Snelling, and Chaffin, 2005).

In this article, we will consider some isotopes such as Nickel-56 and Iron-56 which are of astrophysical interest (Rehm, 1998; Thielemann, Hashimoto and Nomoto, 1990). They are thought to be involved in nuclear reactions in the interiors of stars which go supernova. Also, they are the most important contributors to the light output during early

* Eugene Chaffin, retired physics professor currently serving as vice president of the CRS
Accepted for publication February 9, 2021

stages of various types of supernovae, the "light curves" (Pinto and Woosley, 1988).

Fardon, Nelson, and Weiner (2004) proposed that the neutrino mass could vary with the strength of a hypothetical "acceleron field." Chaffin (2017) considered whether this theory, or an adaptation of it, could enable the passage of the neutrino burst by Earth to give a consistent picture for an accelerated decay episode. In a paper submitted to the *Quarterly*, some issues raised by this scenario are considered (Chaffin, 2020). In this article, we concentrate on a few nuclei, including Nickel-56 and Cobalt-56, which are observed via the light curves of supernovae.

The consideration of the contributions to supernova light curves by nuclear decays necessarily leads away from pure astronomy into the field of nuclear physics. Nuclear physics calculations, while greatly aided by modern computing abilities, do not give exact numerical results. However, some answers are found which we do not think would be changed by the exact numbers. The reasons for the numerical uncertainties include our inability to give equations for the forces of attraction between the nuclear particles which are valid in all cases, but also due to our inability to solve some problems to exact mathematical precision. We are often forced, in nuclear physics, to become familiar with approximation techniques such as perturbation expansions, Hartree-Fock-Bogoliubov methods, mean field methods, and effective field theory (Rowe, 1970; Krane, 1987). Hence, the reader may be led into some interesting areas of study.

Supernova Light Curves and Radioactive Decay

According to current, state of the art, simulations and models, the light output from a supernova remnant is thought to be largely due to the energy from the radioactive decay of ^{56}Ni (half-life $t_{1/2}$ = 6.075±0.010 days, Cruz et al., 1992) and its daughter ^{56}Co (half-life $t_{1/2}$ = 77.08±0.08 days, Lesko et al., 1989, Yang et al., 2018, p. 2). This expectation has been supported by the observation (Pinto and Woosley, 1988) of the approximate 77.1-day exponential decay of the light output from supernova 1987A, and other observations including those of SN 2014J in M82 by Yang et al. (2018).

Yang et al. (2018, p. 2) wrote: "The decay chain of ^{56}Ni → ^{56}Co → ^{56}Fe provides the main source of energy deposition into the ejecta of Type I SNe (Arnett, 1982)." Assuming this is factual, one seems well advised to consider the extent to which the half-lives of ^{56}Ni and ^{56}Co are affected by accelerated decay.

The Nickel-56 nuclear ground state has a spin and parity of 0^+, decaying nearly 100% of the time by electron capture with a 6-day half-life, producing an excited state of Cobalt-56, usually the 1^+ state with 1.72 MeV excitation (Nudat 2.8 online interactive chart). This is not a forbidden transition. The Cobalt-56 ground state is 4^+, usually decaying under laboratory conditions by electron capture to various excited states of Iron-56 with either 4^+ or 3^+ spin and parity. However, there is evidence (McLaughlin and Wijers, 2002; Nadyozhin, 1994) that some fraction of the time, around 19%, Cobalt-56 undergoes beta-plus decay instead of electron capture. In that case, positrons are emitted. None of the prevalent Co-56 decays are forbidden decays, although the half-life is 77 days. It should be pointed out that in the hot environment of a star, the atoms may be completely ionized, and then, there being no electrons to capture, the electron capture gives place to beta-plus decay.

Sur et al. (1990) established a lower limit of 2.9×10^4 yr for the half-life of fully ionized ^{56}Ni nuclei in cosmic rays. Denoting neutron number as N and proton number as Z, the N = Z = 28, doubly closed shell, nuclide ^{56}Ni is the most abundantly produced isotope in many supernova case scenarios (Fisker, 1999, p. 8; Clayton et al., 1992, p. 155; Thielemann et al., 1990, p. 222; Jones et al., 2019, Table 4, p. 13). Neutral ^{56}Ni decays to ^{56}Co via an allowed electron capture transition. Fully ionized ^{56}Ni must undergo beta-plus decay with the much longer half-life of at least 2.9×10^4 years as the prevalent decay. A similar expectation exists for ^{56}Co. Neutral ^{56}Ni decays to the 1720-keV energy level in ^{56}Co with a ~100% branch and a half-life of 6.0 days. A half-life value of 6.076±0.010 days was reported by Cruz et al. (1992).

Yang et al. (2018) observed that the luminosity of the supernova SN 2014J in M82 appeared to follow, from days 200 to about 800 after the explosion, the exponential decay with an approximate 77-day half-life, matching the ^{56}Co half-life. This would imply that the ^{56}Co nuclei had attracted surrounding electrons to become a neutral atom or a least a partially ionized ion which could undergo electron capture decay. It would also imply that any episode of accelerated decay of ^{56}Co had largely passed. Otherwise, the graph decline would not correspond to the 77-day half-life. After 800 days one finds a flattening of the curve, apparently from the decline of Co-56 abundance as it decayed and consequent rise in importance of additional energy input from other radioisotopes, presumably ^{57}Co, ^{44}Ti and others (Suntzeff, 1992).

In the laboratory, *neutral* ^{56}Ni decays by electron capture (Fisker et al., 1999). The ^{56}Ni that we find is synthesized in nuclear reactions in extremely hot environments as a fully-ionized nucleus. Fully ionized ^{56}Ni nuclei in a low-density environment cannot decay by the laboratory mode of electron capture, there being then no electrons to capture, but instead can only undergo beta-plus decay with its attendant much longer half-life. However, the ^{56}Ni-rich material in most astrophysical situations rapidly expands and cools, and thus ^{56}Ni does not remain fully ionized for long. Hence, we find a ready explanation for the observed exponential decay of many supernova light curves from 200 to 800 days after the explosion.

Using given data for luminosity versus time it is possible to find the half-life by analyzing the graph for the linear portion between about 150 days and 500 days (Figure 1). The graph of the log to base ten of luminosity versus time in days should be linear if the decline is truly due to radioactive decay. From the data shown in the visual magnitude versus Julian day graph of Gehrz (1988, Gehrz's Figure 1) I find a trendline slope yielding a half-life of 68.5 days. Gehrz himself states that his data yields 72.5 days, which is very close to the laboratory value of 77 days for the half-life of ^{56}Co. From the graphs of Woosley and Phillips (1988) and Woosley and Weaver (1989), I find values of 75.2 days and 66.9 days, respectively. Of course, these authors were studying SN1987A, which was a Type II supernova.

Catchpoole et al., (1988) presented SN1987A data of bolometric luminosity versus time after 100 days. For the linear part of the curve from 160 days to 260 days, for four different methods of integrating the flux distribution, the corresponding half-lives are 76.5 days, 73.0 days, 75.6 days, and 71.9 days. These four values are all less than the Cobalt-56 laboratory value of 77.2 days.

Yang et al. (2018, their Figure 3), gave some data for SN2014J, which occurred in the galaxy numbered M82 in the Messier numbers list. M82 is a relatively nearby galaxy (12 million light-years), only slightly further away than Andromeda (2.5 million light-years). The SN2014J supernova was a Type Ia, and data presented include Hubble Space Telescope data labelled the F475W band and the F775W band. From these data, fitted with a trendline, I find 54.7 days and 59.0 days, respectively, for the corresponding half-life.

Hence, the data indicate that the half-life of Co-56 in these explosive environments is not orders of magnitude different from the current laboratory value of 77 days, but it is not necessarily exactly the same, averaging around 10% smaller than the 77 days. Is this what we would expect? We will come back to this question after a brief digression about nuclear forces.

Nuclear Force?

In order to overcome the electrical repulsion between protons and hold both neutrons and protons together in a nucleus, a nuclear force is required. Feynman (1985, p. 131) wrote: "There was also the problem of what holds neutrons and protons together inside the nucleus. It was realized right away that it could not be the exchange of photons, because the forces holding the nucleus together were much stronger—the energy required to break up a nucleus is much greater than that required to knock an electron away from an atom…"

Consider a process in which an electron goes between two points, as in Figure 2. In part (a.) on the left, it simply proceeds without interaction. In the middle part (b.), a virtual photon is emitted and absorbed and the electron still ends up at the same final point. In part (c.) on the right the electron emits one virtual photon, and then before reabsorbing it, it emits another. These are drawn following Feynman (1985), the Figure 77 in his book, *QED*.

Feynman points out in his book *QED* that the mass of virtual electrons

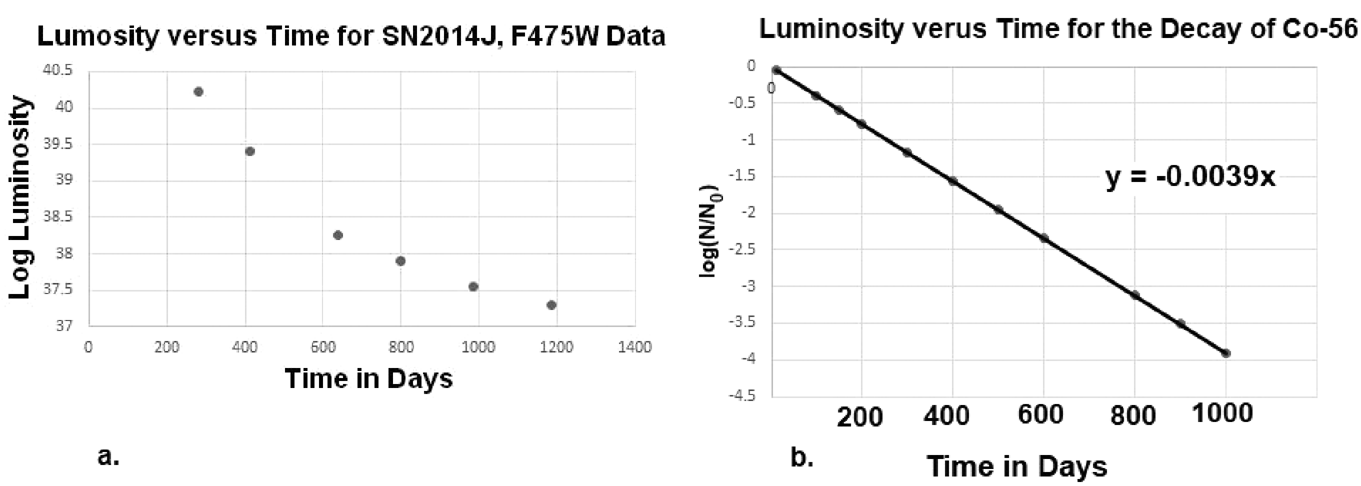

Figure 1. a. Log of Luminosity versus time for SN2014J for the dates 200 to 1200 days. Data from Yang et al., 2018), b. A graph for the decay of Co-56 plotted with a logarithmic scale for N/N_0, the fraction that has not decayed, versus time. The SN2014J data are only linear within a certain time interval, because other decays than Co-56 power it at other times.

is not the same as that of real electrons. This goes for W particles or any particle with rest mass as well. These intermediate particles, whose lines do not extend outside of the diagram, called virtual particles, are not constrained to have the same mass as a real particle, whose lines extend to infinity, and thus whose mass can be measured in the laboratory. If we note this fact, then there is a sense in which energy is not conserved if we insist on imagining the virtual particles to have the same mass as the real ones, which Feynman denies. However, energy must be conserved in the final states. On page 126 Feynman wrote: "Since the mass and charge of an electron are affected by these and all other alternatives, the experimentally measured mass, m, and the experimentally measured charge, e, of the electron are different from the numbers we use in our calculations, n and j." On page 128, Feynman adds: "So it appears that the only things that depend on the small distance between coupling points are the values for n and j, theoretical numbers that are not directly observable anyway;… " Thus the virtual particles do not have the same mass as real particles, which makes one wonder whether the mental pictures we associate with the mathematics are adequate.

Prior to Feynman's work, Hideki Yukawa (1935) introduced the conceptual framework for a systematic approach to the nucleon-nucleon interaction. His then postulated "U field" later became the pion field. This provided the basic mechanism of charge exchange between proton and neutron. From the form of the potential, $e^{-\mu r}/r$, and from the estimated range of the nuclear force, the mass of the U particle was predicted to be about 200 times that of the electron (Feynman, 1985, p. 132, 143). This is about the mass of the pions, which come with positive, negative and zero charge. The π^0 (pi nought) has a mass about 264 times the electron mass (135 MeV/c^2 = 264 x 0.511 MeV/c^2) while the charged pions ($\pi^\pm$) are slightly heavier.

This U particle was initially identified with the muon discovered in 1937, but which it turns out has nothing to do with nuclear forces. The "real" U particle was the π meson which was discovered a decade later (Occhialini et al., 1947) in cosmic rays and then produced for the first time (Lattes et al., 1947) at the Berkeley, California cyclotron.

Subsequent to Yukawa's original work, the 1950's saw an impressive effort to investigate whether the meson-exchange theory could match the facts. The evidence was investigated via a large number of papers in the Japanese journal *Progress of Theoretical Physics*, with some spill over into *Physical Review* and other journals. Taketani et al. (1951), considering the graph of potential versus distance between nucleons (Figure 3) into various pieces. At large distance, exchange of a single pion was thought to prevail, whereas at shorter distances two-pion exchange became important. It is found that a theory of nuclear forces involving the exchange of pions, ω (omega) mesons, ρ (rho) mesons, etc. represents the nuclear force very well (McCarthy, 1968, p. 52). The quark-gluon theory is hardly needed.

The quark was not proposed until Gell-Mann (1964), who wrote (1964, p. 215):

> A search for stable quarks of charge -1/3 or +2/3 and/or stable di-quarks of charge -2/3 or 1/3 or +4/3 at the highest energy accelerators would help to reassure us of the non-existence of real quarks.

Today the theory of the strong nuclear force at shorter distances involves quarks and gluons, which were unknown in the 1950's. Hence it is interesting that, in the 1950's the Japanese theoretical physicists (Konuma et al., 1958; Taketani et al., 1951) were reluctant to say that the Yukawa theory was working at short distances. At larger distances, one-pion exchange was thought and still is thought to prevail (Brown and Rho, 1983; Dean and Hjorth-Jensen, 2003,

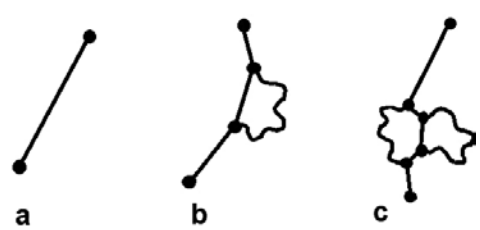

Figure 2. Three Feynman diagrams showing an electron going between two points with increasing complexity caused by photon emission. See the text.

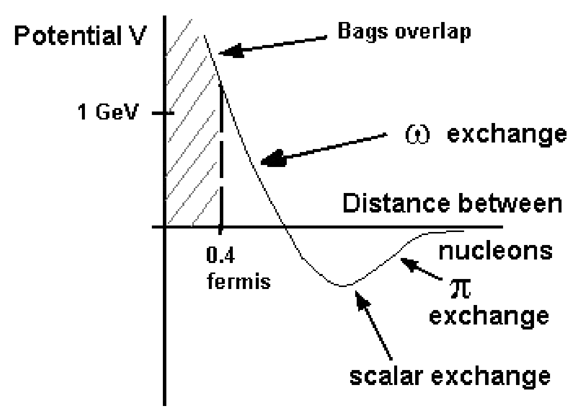

Figure 3. A graph of potential felt by a nucleon versus distance from a second nucleon, after Brown and Rho (1983).

p. 6) since the quarks are confined to a "bag" and should not matter at those distances. The quarks and gluons are thought to occupy a "core" of about 0.5 femtometers radius, while a meson cloud of pions and other mesons still prevails at larger distances (Brown and Rho, 1983, p. 51). The ρ (*rho*) meson, which consists of two pions, is thought to be a contributor, as is the ω (*omega*) meson.

According to the Pauli exclusion principle, two identical particles may occupy the same state only if they have opposite spins. However, the neutron and proton are not "identical." The nuclear force for neutron and proton approaching each other from opposite positions is stronger when the spins are parallel (Otsuka et al., 2005). The deuteron is the bound state of one neutron and one proton, ^{2}H. Evidently, there is only one bound state of the deuteron, and that is in the case where the spins of the neutron and proton are parallel, yielding +1 for the total spin quantum number (McCarthy, 1968, p. 51).

Nuclei and Superconductivity

Bardeen, Cooper, and Schrieffer (1957) (hereafter referred to as BCS) proposed that a very weak attractive force between pairs of electrons with opposite momentum was responsible for superconducting currents observed in many materials at low temperature. This at first appears counterintuitive since electrons are negatively charged, and two like charges should repel each other. However, the BCS theory is not concerned with two electrons moving in a vacuum, but in a crystalline solid where the medium includes a regular arrangement of positive ions. We picture the solid as a three-dimensional arrangement of positive ions called the *lattice*, surrounded by a gas of free electrons. The idea is that one electron attracts the positive ions near to it, causing a distortion of the crystal lattice, which may be transmitted through the solid in the form of quantized elastic waves, called *phonons*.

As the electron moves through the lattice, the positive ions nearby are displaced, forming a thin tube of displacement which follows the electron as it moves through the lattice. A second electron may be attracted to the tube of concentrated positive charge, but the attraction is only large if an electron moves along the direction of the tube opposite to the direction of the first electron. Otherwise the encounter is too short and the attractive interaction is too weak. Also, this mechanism is only effective at low temperature, where other lattice motions do not interfere. The two electrons, together with their tubes of displaced ions trailing along behind them, form a quantum state called a *Cooper pair* (Cooper, 1956) or also a *quasiparticle*. The electrons in a crystal obey the Pauli exclusion principle, which states that no two electrons can occupy the same state unless they have opposite spins. Having the opposite spin also makes the state different, so taking spin into account enables the statement to be changed to the requirement that no two electrons can occupy the same state. Particles which obey the Pauli exclusion principle have half-integral spin and are called *fermions*. The other category of particles includes particles of integral spin, called *bosons*, and these particles do not obey the Pauli exclusion principle and can have more than one particle per quantum state. In a solid, there is an amount energy called the Fermi energy, named after Enrico Fermi, which at absolute zero would divide occupied electron energy states from unoccupied energies. At a finite temperature, the Fermi energy still divides occupied levels from unoccupied levels, but the boundary is not so sharp, the occupation numbers changing from one to zero only over a finite interval or spread of energy. This means that Cooper pairs can only be formed by electrons near to the Fermi energy, because the energy from the weak attractions of one electron for another can only be effective if the electrons can change their quantum states to unoccupied levels. Cooper (1956) showed that two fermions of opposite spin attract each other to form a bound state, and that this Cooper pair has zero spin and behaves like a boson.

The adoption of BCS theory into nuclear physics followed the tentative plans offered by Bohr, Mottelson, and Pines (1958) and the more detailed form given by Belyaev (1959). Bohr et al. explained the energy gap observed in the spectra of even-even nuclei in terms of the BCS ideas, and then Belyaev used the mathematics of field theory, and approximations that followed from it that made possible simple calculations of the effects of pairing in nuclei in terms of independent quasi-particles.

In nuclei pairs of neutrons and also pairs of protons couple to a total spin of 0, giving a little extra binding energy. This has been noticed in several lines of research. Experimentally we find that nuclei with an even number of protons and also an even number of neutrons have a total angular momentum of zero in their ground states. The nuclear force just naturally leads to this. It is thought to be due to the short-range portion of the interaction between nucleons. The ground states of the majority of nuclei are very well described in terms of "superfluid condensates," in which pairs of protons or pairs of neutrons form.

Since they do not have to obey the Pauli exclusion principle, a neutron and a proton of parallel spin will be attracted to each other and pair up when in states of opposite orbital angular momentum. Also, two protons of antiparallel spin can pair up, or two neutrons of antiparallel spin can pair up. The pairing forms what are called "quasiparticles" and the formation of large numbers of these pairs of particles into quasiparticles is a "condensation" which lowers the overall energy of the nucleus, forming a "pairing gap," a lowering of the overall nuclear energy (Bohr, Mottleson, and Pines, 1958).

Is Nickel-56 a Special Nucleus?

Nuclei with doubly-closed shells are only a small fraction of the nuclei which have been charted. In theory, Nickel-56 has proton number and neutron number Z = N = 28, which would be doubly closed because of the filling of the $f_{7/2}$ orbital with the required eight particles, both for neutrons and protons, which filling brings the total number of particles to 28 counting the 20 particles in subshells of lower energy. Of course, then 28+28 is 56. However, if the ground state of this nucleus were deformed, the orbital energies could be modified and could destroy this property. This has been documented to occur for nuclei far from stability (Datta et al., 2018; Diriken et al., 2014). Evaluations of experimentally measured rates of excitation and subsequent gamma emission of a nucleus to the excited 2^+ state by electron collision have been used to infer the amount of deformation for the 2^+ state to ground state transition. This spheroidal deformation is measured by the "quadrupole deformation parameter β_2" (Pritychenko et al., 2016). The quadrupole deformation parameter for the ^{56}Ni transition determined in this way ranges from 0.144 according to Yanagisawa et al., (1998, quoted in Pritychenko et al., 2016, p. 43), to 0.173 according to values tabulated by Raman et al., 2001, p. 38, Table I). The 0.173 value originated with Kraus et al. (1994, p. 1775), who inferred the value from experimentally measured transition rates between the ground state and the first 2^+ excited state, using phenomenological equations (Raman et al., 2001, p. 14). This value is found from a transition rate between two states, more precisely the reduced electromagnetic transition rate B(E2: $0^+ \rightarrow 2^+$), and does not give the deformation of the 0^+ ground state of ^{56}N (Elliott, 1958, p. 576; Burcham, 1963, p. 690; Blatt and Weisskopf, 1979, p. 30; Bethe and Morrison, 1947, p. 175). On the other hand, very powerful computer calculations by Möller et al. (2016, p. 87) gave zero for the deformation parameter for the ground state. Also, we shall see below that even-even nuclei in their ground states invariably have zero spin and zero quadrupole moment. This does not necessarily mean zero deformation, as Burcham (1963, p. 690) pointed out:

> Quantum mechanical states with I = 0 and I = 1/2 have spherically symmetrical charge distributions and electric (E) moments are not observed for such states. This does not mean that a nucleus in such a state is necessarily a spherical object, since the spherical symmetry may arise because of the averaging over spin directions.

The nucleus in such a quantum state would have a deformation and react accordingly if it could be observed at rest, but its motion causes an averaging to zero effect. An example where the ground state has zero spin and zero quadrupole moment but still is deformed is ^{42}Si, which according to Möller et al., (2016, p. 53) is an oblate spheroid in the ground state.

Atomic nuclei, with their discrete energy levels, sometimes follow the "rigid rotor model" (Segre, 1965, p. 254; Burcham, 1963, p. 85). In such a case, for even neutron and proton number, the various energy levels form "bands" with spin I = 0, 2, 4, 6, etc. and have energies which increase in proportion to I(I+1). In some nuclei, such as ^{20}Ne and ^{22}Ne, the transition quadrupole moments found from the reduced electromagnetic transition rates B(E2: $0^+ \rightarrow 2^+$), B(E2: $2^+ \rightarrow 4^+$), and B(E2: $4^+ \rightarrow 6^+$) remain constant consistent with a rigid rotor model of the nucleus (Schwalm et al., 1972, p. 482 and their Table 5). Other nuclei, such as ^{24}Ne, exhibit a spherical state or a small oblate deformation for I = 0^+ and 2^+, while a prolate deformation is found at I = 4^+ (Bottoni et al., 2012, p. 5–6 and their Figure 7). Although no experimentally measured B(E2: $2^+ \rightarrow 4^+$), and B(E2: 4+ → 6+) values have been reported for Nickel-56, the trends indicate that it follows a more complicated behavior than the rigid rotor model.

Experimentally, one can use various indicators to provide evidence that closed shells, also called "magic numbers," do in fact exist. Taniuchi et al. (2019) discussed the size of the energy gap between the ground state, which invariably has a spin and parity of 0^+ in these even Z, even N cases and the first 2^+ excited state (see Figure 4).

Another line of evidence depends on values of the separation energies of the last pair of neutrons, as discussed by Thibault et al. (1975). An unexpected increase in this separation energy for Na-31 and Na-32 indicated nonexistence of a shell closure for these sodium isotopes. Rodriguez-Guzman et al. (2002) used these separation energies to show evidence for nonexistence of the N= 28 shell closure for the very neutron-rich nuclides Mg-40 (Z = 12, N= 28), Si-42 (Z = 14, N = 28, and S-44 (Z= 16, N = 28). However, Ni-56 is nearer the line of stability and is not neutron rich (Z = N = 28). The separation energies provide evidence for a shell closure in Nickel-56.

Pairing Phase Changes and Relevant Half-Lives

In modern physics, the nucleus, which consists of a finite number of neutrons and protons bound together by the strong nuclear force, is successfully treated using quantum theory, whereas exact equations for the nuclear interaction are not known. Various effective interactions, labelled GXPF1, the Kuo-Brown KB3, the Argonne V18 interaction, the Nijmegen interaction, the Gogny force, etc. have been found to give acceptable computational results (Lisetskiy et al., 2003; Langanke et al., 1995; Machleidt and Slaus 2001; Dechargé and Gogny, 1980). Although the nucleus consists only of a finite number of particles, the concept of a *phase transition* is useful for describing structure changes in the atomic nucleus (Chaffin, 2008, p. 180). The phase can consist of a state dominated by pairing forces in which the particles "condense out" into pairs of quasiparticles, referred to as a "superfluid." Alternatively, there are "shape transitions" in which the nucleus selects oblate, spherical, or prolate shapes (Figure 5). Some nuclei are said to be "soft," meaning that they may easily change to triaxial asymmetric shapes.

In the description of current nuclear physics models and theories, the term "residual interaction" refers to the leftover interaction after an average potential is assumed. "Pairing" is the part of this residual interaction of the pairs of particles in the correctly corresponding orbits are selected. When this interaction is strong enough, there can be a "condensation" of the particles into pairs which yields a "pairing gap" Δ, which is a reduction in energy of the nucleus resulting from the pairing. Typically, the pairing gap Δ is of the order of 1 MeV, which is smaller than the shell gap, which is several MeV depending on the particular gap to which we refer (see Figure 7). When the pairing interaction is not strong enough, then $\Delta = 0$ and the overall nuclear energy is not reduced. This does not mean that the pairing interaction vanishes, only that it is not strong enough to cause the condensation. This $\Delta = 0$ situation may occur in the ground state of some nuclei, whereas in other nuclei, at some excitation energy, there occurs a phase transition [second order] to a "heated" nucleus where the pairing effects may be neglected (Volya, Zelevinsky, and Brown, 2002).

In Chapter 7 of RATE, volume 2 (Chaffin, 2005a), quantum mechanical calculations were presented for an alpha particle in a nucleus. In quantum mechanics, the wavefunction is a quantity whose square gives the probability density for finding the particle, the alpha particle in this case. The calculations showed that, if the strength of the strong nuclear force were to change, the number of nodes in the effective wave function could change suddenly. This results in a jump in the decay constant (which is 0.693 divided by the half-life, and also the fraction of the nuclei decaying per unit time). Here we are concerned with changes in the weak nuclear force caused by an acceleron field pulse associated with a supernova burst. It is not the strong nuclear force that is affected, but nevertheless the weak force affects the nuclear particles.

In Chaffin (2017), it was considered that, during the nearby supernova event, the mass of U-238 nuclei could change, resulting in beta-minus decay becoming the predominate decay mode rather than alpha decay. This consequently results in a drastic change in nuclear half-life. The mass change of the U-238 nucleus was linked to the weak force rather than the strong nuclear force. However, the weak force also affects the dynamics of the nuclear particles. The weak force changes are hypothesized to be caused by the changes in the acceleron field.

In Chaffin (2008), the dependence of nuclear pairing phases on the strength of the nuclear force were discussed. For some nuclei it was shown that a slight change in nuclear force strength could cause a discontinuous change in half-life. For other nuclei, such as C-14, this was not the case. For C-14, the half-life is not as drastically altered. C-14 is exceptional in that there may be no pairing,

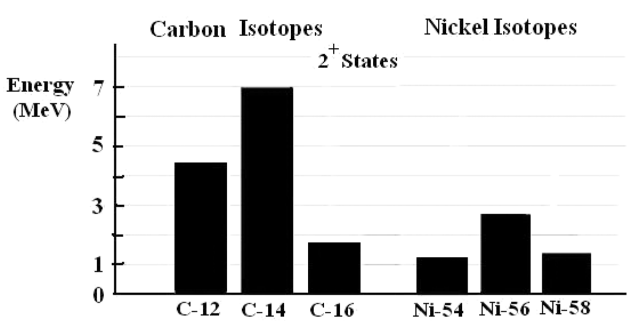

Figure 4. Energy gap between the 0^+ ground state and the first 2^+ excited state in even N-even Z carbon and nickel nuclei. Carbon-14, with neutron number N = 8 has a closed shell, whereas Carbon-12 and Carbon-16 do not. The smaller energy gap shown provides evidence that Carbon-14 does in fact have a closed neutron shell (Negret et al., 2006). Nickel-56 has doubly closed shells N=Z=28, and the bar height is higher for it than for its even N-even Z neighbors Nickel-54 and Nickel-58. This is experimental evidence for a closed shell (Taniuchi et al., 2019, their Figure 1].

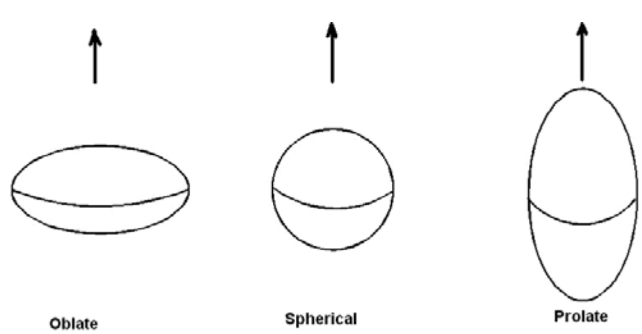

Figure 5. Oblate, spherical, and prolate ellipsoidal shapes. These are axially symmetric possibilities that a nucleus may assume depending on its energy level.

hence when the nuclear force strength changes, no phase change of the nucleus occurs. This implies that that half-life may change slightly, but not drastically.

Nickel-56 is important in the supernova explosion, since this nuclide is the most abundantly produced isotope in many supernova case scenarios (Yang et al. (2018, p. 2). As discussed above, Ni-56 is a *doubly closed-shell* nucleus with both neutron and proton numbers equal to 28. Empirically (and theoretically) one expects closed shells for nucleon numbers 8, 20, 28, 50, 82, 126, etc., and Ni-56 happens to have Z = N = 28. Figure 6 shows a graph, the result of computer calculations as in Chaffin (2008), of pairing gap versus pairing strength for Ni-56, assuming a spherical shape.

The actual pairing strength is thought to be 0.343 MeV, hence the pairing gap should be zero and there would be no "pairing condensate" or the Nickel-56 ground state would not exist in the pairing phase.

This zero-pairing gap for ^{56}Ni agrees with the results shown in Figures 5 and 6 of Li et al. (2015). Their graph shows the pairing gap curves on both sides ($N < 28$ and $N > 28$) dropping off precipitously to zero for N = 28. Terasaki and Engel (2006) presented a similar graph (their Figure 9), but the theoretical part used the Skyrme interaction. It also gave a zero-pairing gap for Nickel-56.

As explained in Chaffin (2008), Nilsson, et al. (1969, p. 17), found that the overall mass number A-dependence of the pairing strength G was found to be proportional to A^{-1}. Nilsson et al. gave the equation for G times A:

$$GA = g_0 \pm g_1(N\text{-}Z)/A,$$

with g_0 = 19.2 MeV and g_1 = 7.4 MeV. For the ± sign, the plus sign is for protons, the minus sign for neutrons. However, when more involved theoretical studies have been done, better, more precise calculations than this empirical approximation may be possible.

Ni-56, with proton number Z = 28 and neutron number N = 28, has an expected pairing strength of 0.343 MeV for both protons and neutrons, which according to my results is too small, and there is no expected pairing gap for this doubly-closed-shell nucleus. This would imply that, like Carbon-14, the half-life of Ni-56 is not sensitive to changes in either the weak or strong nuclear forces, since changes in these forces could not cause a phase transition since none is available. The single particle energy levels that should be used in these computer calculations are not precisely given, hence estimating the uncertainty in the critical pairing strength, given above as 0.41 MeV for a spherical nucleus, could be done by varying these single particle energies. For example, Gade et al. (2005, p. 4) and Sagawa et al. (2013, their Figure 1) gave some different sets of single particle energies for Nickel-56 which could be adopted for the calculation of these uncertainty intervals. For neutrons we find that the critical pairing strength G_p is between 0.36 and 0.42 MeV, while for protons in Nickel-56 it is between 0.36 and 0.41 MeV. Thus, the actual value of 0.343 MeV is well outside this range, indicating that small variations will not cause a phase change.

Gambacurta and Lacroix (2014) presented a graph, their Figure 2, showing that the pairing gap should be zero for Nickel-56. There calculations showed that their "Skyrme energy density functional" is minimized for a spherical shape with zero pairing gap, thus confirming my results.

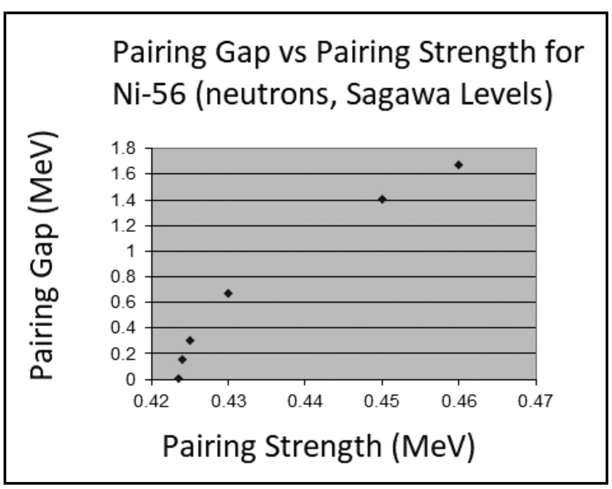

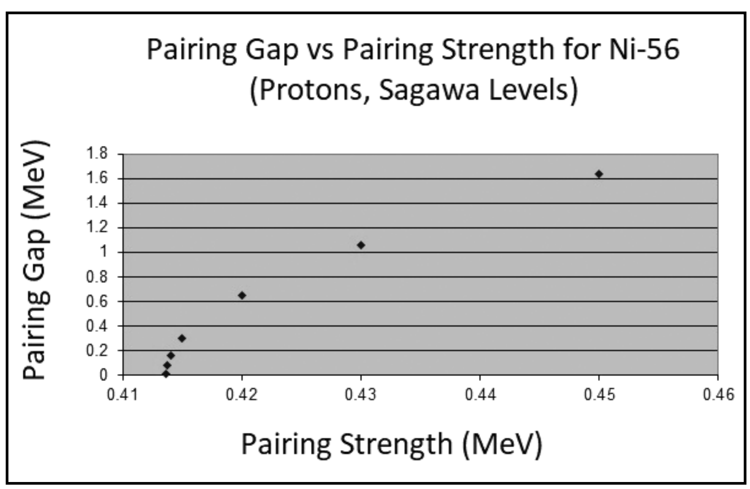

Figure 6. Pairing gap versus pairing strength for the doubly-closed shell nucleus Nickel-56, Z=N=28, neutron results on the left, protons on the right. For pairing strengths below 0.41 MeV, which includes the actual value, the pairing gap vanishes. The single-particle levels were adjusted using data given in Sagawa, Tanimura, and Hagino (2013).

However, the situation for Ni-56 is clouded by the fact that, it exhibits "shape-coexistence." In other words, according to this concept, a nucleus in some excited states has a deformation even though the ground state is a spherically symmetric shape (Chiba and Kimura, 2014, 2015). Blatt and Weisskopf (1979, p. 26) gave an interesting proof that an even Z, even N nucleus will have zero angular momentum and must have a zero-quadrupole moment in their ground state. This is borne out in experimental tables (Stone, 2005). The "electric quadrupole moment" which Blatt and Weisskopf defined more precisely than we will here, measures the amount of spheroidal deformation of the nucleus. A prolate (cigar-shaped) spheroid has a positive quadrupole moment, whereas an oblate (pancake-shaped, see Figure 5) spheroid has a negative quadrupole moment. Chiba and Kimura found that the Nickel-56 nucleus is "soft" against oblate deformations, and that the potential energy surface also had minima for prolate deformations. Rudolph et al. (1999) found bands of energy levels correspond to inferred deformations. Thus, although the ground-state is spherical and has zero angular momentum, Ni-56 is easily excited to energy levels with nonzero angular momentum and nonzero quadrupole moment. This idea is supported by the results of some earlier theoretical calculations of Otsuka et al. (1998) which indicated that the ground state of Ni-56 was not a pure doubly-closed-shell configuration but contained an appreciable mixture of something else. Honma et al. (2004, p. 24) characterized it as a 68% doubly-closed nucleus with a mixture of one particle excited across the shell gap, leaving one hole in the "core." They did not speculate on whether this meant there was a deformation, although their Figure 18 shows a value of about 20 e•fm^2 for the quadrupole moment of the first excited 2^+ level. However, as we discussed above, experimental data involving 2^+ excited states and two-neutron separation energies speaks in favor of the existence of the doubly-closed shell. Also, the calculations of Chiba and Kimura (2014, p. 6) led to a transition probability from the first excited 2^+ state to the ground state, the so-called B(E2) value, larger than the experimental value. They therefore concluded that "the actual deformation of ^{56}Ni is smaller than the present result." Rudolph (1999, p. 3764), Heyde and Wood (2011, p. 1496) and Horoi et al. (2006, p. 1) divide the levels of ^{56}Ni into a "spherical" ground state band and two "superdeformed," prolate bands. No experimental evidence for an oblate band has been found. Also, the shell gap shown in Möller, Nix, and Kratz (1997, p. 172) for either neutrons or protons at N or Z = 28, is slightly larger for the spherical shape than for the oblate deformation ($eps_2 = -0.40$). One could also reiterate the findings, from theoretical calculations, of Möller et al. (2016, p. 87), mentioned above, which gave zero for the deformation parameter for the ground state of ^{56}Ni. Therefore, the factuality of a doubly-closed shell, spherical or at least nearly spherical configuration for Ni-56 is not appreciably modified.

Another complication for Ni-56 concerns possible pairing between neutrons and protons, called *np*-pairing. In most nuclei, only proton-proton pairing (*pp*-pairing) or neutron-neutron (*nn*-pairing) is of any importance. However, for nuclei with N = Z the states of the neutrons and protons are very similar and *np*-pairing can be important. The *np* Cooper pairs are not deuterons (^{2}H nuclei), but involve an attractive interaction in which the particles of the pair remain further apart (Isaule, et al., 2016). In neutron star interiors both these *np* states are thought to occur, but at nuclear densities the deuteron state is not favored (Rubtsova et al., 2017). Cederwall et al. (2011) wrote:

> For all known nuclei, including those residing along the N = Z line up to around mass 80, a detailed analysis of their properties such as binding energies [9] and the spectroscopy of the excited states [10] strongly suggests that normal isovector (T = 1) pairing is dominant at low excitation energies.

Here, the term "isovector pairing" refers to a type of *np*-pairing in which the neutrons and protons couple in a certain way, as opposed to the other type called isoscalar pairing. Frauendorf and Macchiavelli (2014) wrote: "The *np* pairs can couple to angular momentum zero and isospin T = 1 (isovector), or, since they are no longer restricted by the Pauli exclusion principle, they can couple to T = 0 (isoscalar) and J = 1." We need not concern ourselves with the details here, but the interested reader can refer to the Cederwall et al. (2011) paper and references therein. The relevant theory states that *np*-pairing could exist for N = Z nuclei such as Ni-56. However, for the ground state of Ni-56, indications are that the pairing of this type does not materialize.

Martinez-Pinedo, Langanke, and Vogel (1999), in a numerical study of iron isotopes (proton number Z = 26), found that the strength of *np*-pairing decreased as the neutron number N increased away from the N = Z = 26 nucleus ^{52}Fe. For the closed shell nucleus N = 28 (^{54}Fe), where the $f_{7/2}$ subshell is full with 8 neutrons and the entire N = 28 shell is full, they found that the strength of the $f_{7/2}$ isovector and isoscalar pairing was substantially less (Martinez-Pinedo et al., 1999, their Figure 7). As other subshells, associated with higher neutron single particle energies (see Figure 7) across the shell gap, begin to fill, the overall *np*-pairing strength increases again.

Discussing nuclei with N ~ Z nuclei near the A = 56 mass number of Nickel-56, Poves and Martinez-Pinedo (1998, p. 207) wrote: "Finally we discard the presence of isoscalar pairing condensates everywhere in the region, as well as the existence of isovector pairing condensates at N = Z." In heavier nuclei, with proton numbers from 55 to 70, such *np*-pairing condensates have been found (Gezerlis, et al., 2011), but not near proton number Z = 28. Also, for short-lived nuclei with either very large or very small numbers of neutrons, relative to the proton number, *np*-pairing has not been ruled out. Nevertheless, in the doubly closed N = Z = 28 nucleus ^{56}Ni, there is no *np*-pairing gap or it is zero since the strength of *np*-pairing is not enough for this nucleus. Thus, a small change in nuclear attraction will not change the nuclear phase and will not drastically affect the half-life of this nucleus.

Nickel-56 decays to Co-56. For the case of Co-56, proton number Z = 27 and neutron number N = 29, and with the 77-day half-life and with a slight deformation, I have done computer calculations similar to those reported in Chaffin (2008), for both neutrons and protons, investigating the existence of pairing correlations. According to computer calculations, based on a liquid drop model corrected by single-particle microscopic methods, Möller et al. (1995, p. 235), found that Co-56 has a slight quadrupole deformation, measured by a parameter $eps_2 = 0.083$. More refined work (Möller et al., 2016, p. 85) gave $eps_2 = 0.07$. Taking the quadrupole deformation as factual leads to modified single particle levels (Möller, Nix and Kratz, 1997, p. 172). A prolate ellipsoidal shape occurs (Peng and Chen, 2018, p. 4). This deformation was taken in to account using the single particle level graphs presented in Möller, Nix and Kratz (1997), which show the shift in the levels as a result of the quadrupole deformation parameter. My results are shown in Figure 8.

Due to uncertainties in the single particle energy levels, there are corresponding uncertainties in the possible pairing gaps. For Co-56, G_p the limit point for neutrons is about 0.405 MeV, below which the pairing gap is zero. The limit point for protons is around G_p = 0.26 MeV. The actual pairing strength is G_p = = 0.338 MeV for neutrons and G_p = 0.347 MeV for protons. Thus, there should be no pairing gap for neutrons. For protons there would be a pairing gap of around 0.8 MeV. Co-56 is an odd-odd nucleus in that both the proton and neutron numbers 27 and 29 are odd numbers. For particle number N = 29, there

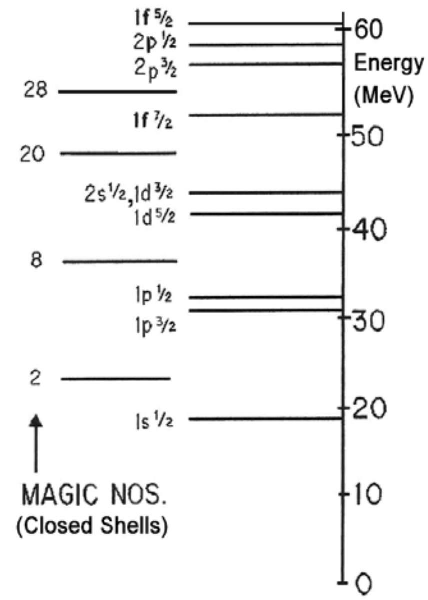

Figure 7. Nuclear single particle levels in the shell model plotted using their energies and showing the shell gaps. Nickel-56 would have a filled shell corresponding to the N = 28 shell gap.

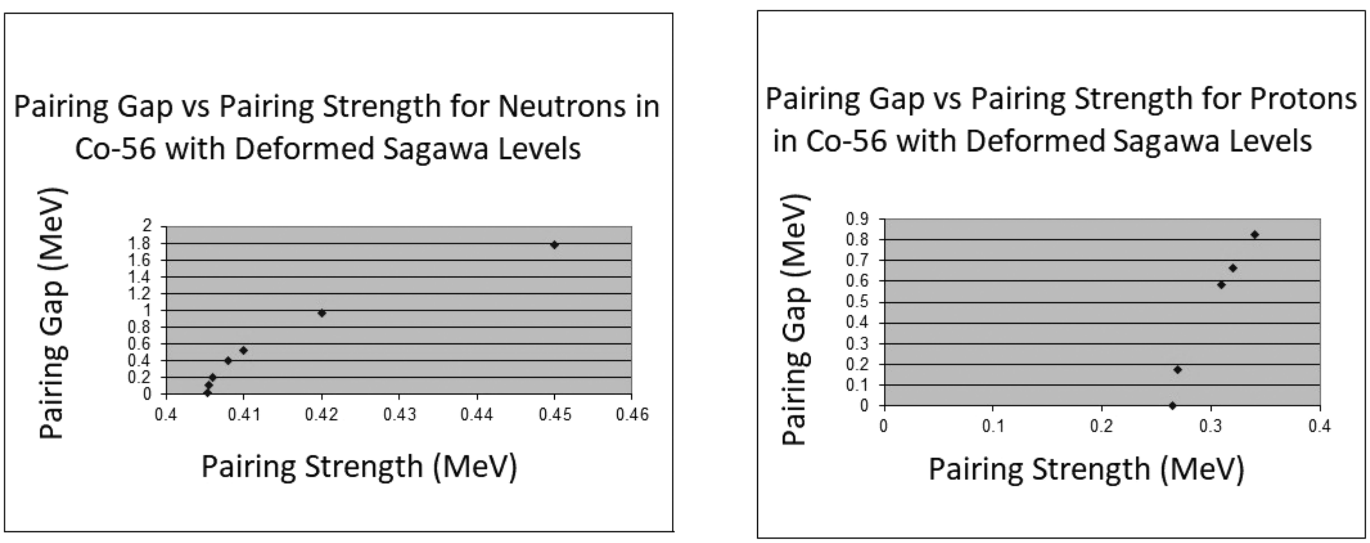

Figure 8. The two graphs show the pairing gap as a function of the pairing strength, in Co-56, Z = 27, N= 29, showing neutrons for the left pane and protons for the right pane. The single-particle levels were adjusted using data given in Sagawa, Tanimura, and Hagino (2013).

is one neutron outside the closed shell at N = 28, which odd neutron is more likely to be at larger distance than the others, hence has less of a pairing probability. On the other hand, the subtraction of one proton from the closed shell at Z= 28 does not decrease the likelihood of proton pairing as much as for the neutrons. Hence, we find the limit point for protons (0.26±.02 MeV) is smaller than for neutrons (0.405±.02 MeV). This is an example of what is called "blocking" (Rowe, 1970, p. 194). Rowe wrote: "If one particular single-particle state μ is singled out and occupied by a physical particle, that state is no longer available for the pair correlations of the other particles. In other words, the single-particle state μ is blocked." Compared to Ni-56, there is more of a likelihood that the pairing phase for protons persists as the weak nuclear force changes (a change we think is due to the acceleron field). Thus, the sensitivity of Co-56 to changes in nuclear forces should be somewhat more than Ni-56, but not as pronounced as for some other nuclei.

The pairing gap may be plotted against neutron number as shown in Figure 9. The pairing gap is seen to drop precipitously to zero as the neutron number nears the N = 28 closed shell.

Langanke et al. (1995) performed a type of improved calculation for nuclei that are of interest for supernova studies such as those of interest here. The Langanke et al. (1995) figure [Fig. 6 in the original article, Fig. 12 when essentially the same figure was reproduced in Dean and Hjorth-Jensen (2003)] shows that pairing strength in even-even nuclei is smallest in the closed shell nucleus. Langanke et al. studied the BCS-like pairing content of the ground states of even-even nuclei $^{52,54,56,58,60}Fe$ [Z=26], $^{56,58,60,62,64}Ni$ [Z=28], and $^{60,62,64}Zn$ [Z=30] by measuring the expectation values for the pairing fields, which was their expression $<\Delta^{\dagger}\Delta>$, for proton-proton and neutron-neutron pairing. Nuclei such as cobalt have Z=27, an odd number, and thus cannot be even-even, regardless of neutron number. However, these calculations show that the pairing correlations get smaller as you approach a closed shell.

The size of the pairing gap is determined by the density of single particle states close to the "Fermi surface," or the position (energy) separating occupied from unoccupied levels. We find that the total energy is lowered when there is an unusually high-level density, since the higher the level density, the larger the number of levels into which pairs can be scattered. At a closed shell, the level density is small and consequently pairing gets weaker.

Dean and Hjorth-Jensen (2003, p.2) stated: "Second, there is a critical value of the pairing-force strength for which no non-trivial solution exists." This was viewed as a negative aspect of the BCS approximation which could be "corrected" by the Lipkin-Nogami "trick." This "trick" involves an extra term in the constraint equation from which the working approximations are derived (Nogami, 1964, 1965). However, phase transitions are still expected, although this does not necessarily imply vanishing of all correlations, such as neutron-proton correlations (Clark and Macchiavelli, 2008). A nucleus, after all, has a finite number of particles, not the very large numbers usually encountered in the thermodynamics of phase transitions. Clark and Macchiavelli found evidence that the doubly-closed-shell nucleus, Pb-208, is very close to the critical-point of the pairing phase transition. Although the sharpness of a pairing to no-pairing phase transition remains an uncertainty, nevertheless the occurrence of such transitions can be considered as an important event.

Conclusion: Expectation for Changed Half-Life

As the strength of the nuclear force changes, a half-life may either increase or decrease Chaffin (2005a, Figure 3, p. 530). The half-life is not a steadily changing (monatonic) function of one parameter. However, when the nucleus undergoes a phase change, a dramatic alteration in half-life is to be expected rather than a miniscule alteration. Hence, these studies point to very little change in the doubly-closed shell Nickel-56 half-life. For Cobalt-56, the neutrons are not condensed into the pairs called quasiparticles, hence a slight change in nuclear parameters

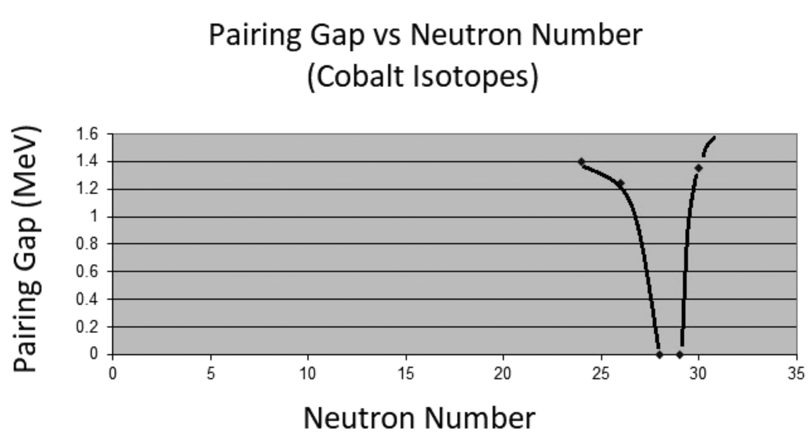

Figure 9. The calculated pairing gap is plotted versus neutron number, showing how the gap drops to zero as the number of neutrons approaches the N = 28 closed-shell value.

would probably not produce dramatic phase change and/or associated half-life change. According to the present study, for the Co-56 protons a slight change caused by the acceleron field or any other factor affecting the nucleus is more likely to alter the half-life, and this is a subject for future studies.

References

CRSQ: Creation Research Society Quarterly

Arnett, W.D. 1982. Type I supernovae. I. Analytic solutions for the early part of the light curve. *Astrophysical Journal* 253: 785–797.

Bardeen, J., L.N. Cooper, and J.R. Schrieffer. 1957. Theory of superconductivity. *Physical Review* 108: 1175–1204.

Belyaev, S.T. 1959. Effect of pairing correlations on nuclear properties. *Matematisk-Fysiske Meddelelser Udgivet Af Det Kongelige Danske Videnskabernes Selskab* 31(11): 1–55.

Bethe, Hans A. and Philip Morrison. 1947. *Elementary Nuclear Theory*. John Wiley and Sons. New York.

Blatt, John M. and Victor F. Weisskopf. 1979. *Theoretical Nuclear Physics*. Dover Publications. New York. Originally published 1952.

Bohr, A., B.R. Mottleson, and D. Pines. 1958. Possible analogy between the excitation spectra of nuclei and those of the superconducting metallic state. *Physical Review* 110: 936–938.

Bottoni, S., G. Benzoni, S. Leoni, D. Montanari, A. Bracco, F. Azaiez, S. Franchoo, I. Stefan, N. Blasi, F. Camera, F.C.L. Crespi, A. Corsi, B. Million, R. Nicolini, E. Vigezzi, O. Wieland, F. Zocca, L. Corradi, G. DeAngelis, E. Fioretto, B. Guiot, N. Marginean, D. R. Napoli, R. Orlandi, E. Sahin, A.M. Stefanini, J.J. Valiente-Dobon, S. Aydin, D. Bazzacco, E. Farnea, S. Lenzi, S. Lunardi, P. Mason, D. Mengoni, G. Montagnoli, F. Recchia, C. Ur, F. Scarlassara, A. Gadea, A. Maj, J. Wrzesinski, K. Zuber, Zs. Dombradi, S. Szilner, A. Saltarelli, G. Pollarolo. 2012. Reaction dynamics and nuclear structure of moderately neutron-rich Ne isotopes by heavy-ion reactions. *Physical Review* C 85(6): 064621 [7 pages].

Brown, Gerald E. and Mannque Rho. 1983 The structure of the nucleon. *Physics Today* 36(2): 24–32.

Burcham, W.E. 1963. *Nuclear Physics An Introduction*. McGraw-Hill. New York.

Catchpoole, R.M. et al. 1988. Spectroscopic and photometric observations of SN1987A - III. Days 135 to 260. *Monthly Notices of the Royal Astronomical Society* 231: 75–89.

Cederwall et al. 2011. Evidence for a spin-aligned neutron-proton paired phase from the level structure of ^{92}Pd. *Nature* 469: 68–71.

Chaffin, E.F. 2001. A model for the variation of the Fermi constant with time. *CRSQ* 38: 127–138.

Chaffin, Eugene F. 2005a. Accelerated decay: theoretical considerations. In Vardiman, L., A.A. Snelling, and E.F. Chaffin (editors), *Radioisotopes and the Age of the Earth, Volume 2, Results*. Institute for Creation Research and Creation Research Society, Dallas, TX and Chino Valley, AZ., pages 525–585.

Chaffin, E.F. 2005b. Accelerated decay: Theoretical models. In Ivey, Robert L. (editor) *Proceedings of the Fifth International Conference on Creationism*. Creation Science Fellowship. Pittsburgh, PA, pages 3–15.

Chaffin, E.F. 2008. Studies of the dependence of nuclear half-lives on changes in the strength of the nuclear force. In Snelling, Andrew A. (editor) *Proceedings of the Sixth International Conference on Creationism*. Creation Science Fellowship. Pittsburgh, PA and Institute for Creation Research, Dallas, TX., pages 179–192.

Chaffin, E.F. 2017. Variable neutrino mass, supernovae, and accelerated decay. *CRSQ* 53: 180–190.

Chaffin, E.F. 2019. A discontinuous change in half-life seems to characterize many findings regarding accelerated decay. *CRSQ* 55: 248–251.

Chaffin, E.F. 2020. Supernova driven accelerated decay confronts the evidence. *CRSQ* 57: 98–112.

Chiba, Y. and M. Kimura. 2014. Collectivity and instability of the N=Z=28 shell gap and strongly deformed bands with $g_{9/2}$ configuration in ^{56}Ni. *Physical Review* C 89(5) 054313 [9 pages].

Chiba, Y. and M. Kimura. 2015. Collectivity and instability of the N = Z= 28 shell gap in ^{56}Ni. In *Proceedings of the Conference on Advances in Radioactive Isotope Science (ARIS2014)*. *Journal of Physics Conference Series Proceedings* 6: 030047 [4 pages].

Clark, R. M. and Macchiavelli, A. O. 2008. Exact and collective treatments of the pairing phase transition. *Physical Review* C77(5): 057301 [4 pages]

Clayton, D.D., M.D. Leising, L.-S. The, W.N. Johnson, and J.D. Kurfess. 1992. The ^{57}Co abundance in SN1987A. *Astrophysical Journal* 399: L141–L144.

Cooper, L. N. (1956). Bound electron pairs in a degenerate Fermi gas. *Physical Review* 104: 1189–1190.

Cruz, M.T.F. da, Y. Chan, R.-M. Larimer, K.T. Lesko, E.B. Norman, R.G. Stokstad, F.E. Wietfeldt, I. Zlimen. 1992. Half-life of Ni-56. 1992. *Physical Review* C46: 1132–1135.

Datta, U. A. Rahaman, S. Chakraborty, B.K. Agrawal, T. Aumann, K. Boretzky, C. Caesar, H. Emling, H. Geissel, C. Langer, T. Le Bleis, Y. Leifels, J. Marganiec, G. Münzenberg, C. Nociforo, R. Plag, V. Panin, R. Reifarth, M.V. Ricciardi, D.Rossi, C. Scheidenberger, H.Simon, S.Typel, V. Volkov, F. Wamers, J.S. Winfield, H. Weick, B. Jonson, H.Johansson, T.Nilsson, A. Wagner, G.De.Angelis, and B.V.Carlson. 2018. Weakly Bound Neutron-Rich Nuclei and Cosmic Phenomena. Available at arXiv.org: 1810.08996 [nucl-ex].

Dean, D. J., M. Hjorth-Jensen. 2003. Pairing in nuclear systems: from neutron stars to finite nuclei. *Reviews of Modern Physics* 75: 607–656. arXiv.org nucl-th/0210033.

Dechargé, J. and D. Gogny. 1980. Hartree-Fock-Bogolyubov calculations with the D1 effective interaction on spherical nuclei. *Physical Review* C 21: 1568–1593.

Diriken, J., N. Patronis, A.N. Andreyev, S. Antalic, V. Bildstein, A. Blazhev, I.G. Darby, H.De Witte, J. Eberth, J. Elseviers, V.N. Fedossev, F. Flavigny, Ch. Fransen, G. Georgiev, R. Gernhausen, H. Hess, M. Huyse, J. Jolie, Th. Kroll, R. Krücken, R. Lutter, B.A. Marsh, T. Mertzimekis, D. Muecher, F. Nowacki, R. Orlandi, A. Pakou, R. Raabe, G. Randisi, R. Reiter, T. Roger, M. Seidlitz, M. Seliverov, K. Sieja, C. Sotty, H. Tornvist, J. Van De Walle, P. Van Duppen, D. Voulor, N. Warr, F. Wenander, and K. Wimmer. 2014. Study of the deformation-driving $\nu d_{5/2}$ orbital in ${}^{67}_{28}Ni_{39}$ using one-neutron transfer reactions. 2014. *Physics Letters* B 736: 533–538. Erratum *Physics Letters* B 743: 543–543.

Elliott, J.P. 1958. Collective motion in the nuclear shell model II. The introduction of intrinsic wave-functions, *Proceedings of the Royal Society, Series A, Mathematical and Physical Sciences* 245: 562–581.

Fardon, R., A.E. Nelson, and N. Weiner. 2004. Dark energy from mass varying neutrinos. *Journal of Cosmology and Astroparticle Physics* 10 (005): 75–100. arXiv.org: astro-ph/0309800.

Feynman, Richard P. 1985. *QED: The strange theory of light and matter*. Princeton University Press: Princeton, NJ.

Fisker, Jacob Lund. 1999. Large Scale Shell Model Calculations of The Forbidden β^+ Decays of ^{56}Ni and The Thermonuclear Reaction Rates of The rp-Process on Nuclei in The Intermediate Mass Range. MS Thesis, Institute of Physics and Astronomy, University of Aarhus Denmark.

Fisker, J. L., G. Martinez-Pinedo, K. Langanke. 1999. Halflife of Ni-56 in cosmic rays. *European Physical Journal* A5: 229–231.

Frauendorf, S. and A.O. Macchiavelli. 2014. Overview of neutron-proton pairing. *Progress in Particle and Nuclear Physics* 78: 24–90. arXiv.org 1405.1652 [89 pages].

Gade, Alexandra, A. Becerril, C,M, Campbell, J.M. Cook, D.J. Dean, D.-C. Dinca, T. Glasmacher, G.W. Hitt, M.E. Howard, W.F. Mueller, H. Olliver, J.R. Terry, and M.E. Yoneda. 2005. Quadrupole deformations of the self-conjugate nucleus ^{72}Kr. *Physical Review Letters* 95: 022502 [4 pages].

Gambacurta, D. and D. Lacroix. 2014. Deformation effects on the coexistence between neutron-proton and particle like pairing in N = Z medium mass nuclei. *Physical Review C* 91(1): 014308 [14 pages] arXiv.org: 1411.1891.

Gehrz, Robert D. 1988. Supernova 1987A. Casting light on the ejecta. *Nature* 333: 705–706.

Gell-Mann, M. 1964. A schematic model of baryons and mesons. *Physics Letters* 8: 214–215.

Gezerlis, Alexandros, G.F. Bertsch, and Y.L. Luo. 2011. Mixed-Spin Pairing Condensates in Heavy Nuclei. *Physical Review Letters* 106: 252502 [4 pages].

Heyde, K. and J.L. Wood. 2011. Shape coexistence in atomic nuclei. *Reviews of Modern Physics* 83: 1467–1521.

Honma, M. T. Otsuka, B. A. Brown, and T. Mizusaki. 2004. New effective interaction for pf-shell nuclei and its implications for the stability of the N=Z=28 closed core. *Physical Review* C 69 034335 [34 pages].

Horoi, M., B.A. Brown, T. Otsuka, M. Honma, and T. Mizusaki. 2006. Shell model analysis of the ^{56}Ni spectrum in the full *pf* model space. *Physical Review* C73(6): 061305R [4 pages].

Isaule, F., H.F. Arelano, and A. Rios. 2016. Di-neutrons in neutron matter within a Brueckner-Hartree-Fock approach. *Physical Review* C 94: 034004 [26 pages] arXiv.org 1602.05234.

Jones, S., F.K. Röpke, C. Fryer, A.J. Ruiter, I.J. Seitenzahl, L.R. Nittler, S.K. Ohlmann, R. Reifarth, M. Pignatari, and K. Belczynski. 2019. Remnants and ejecta of thermonuclear electron-capture supernovae. Constraining oxygen-neon deflagrations in high-density white dwarfs. *Astronomy and Astrophysics* 622: A74 [22 pages].

Konuma, M., H. Miyazawa, and S. Otsuki. 1958. Two-pion-exchange nuclear potential. *Progress of Theoretical Physics* (Kyoto) 19: 17–30.

Krane, K. S. 1987. *Introductory nuclear physics*. New York: John Wiley.

Kraus, G. P. Egelhof, C. Fischer, H. Geissel, A. Himmler, F. Nickel, G. Miinzenberg, W. Schwab, A. Weiss, J. Friese, A. Gillitzer, H. J. Korner, M. Peter, W. F. Henning, J.P. Schiffer, J.V. Kratz, L. Chulkov, M. Golovkov, A. Ogloblin and B.A. Brown. 1994. Proton Inelastic Scattering on ^{56}Ni in Inverse Kinematics. *Physical Review Letters* 73(13): 1773–1776.

Langanke, K., D. Dean, P. Radha, Y. Alhassid, and S. Koonin. 1995. Shell-model Monte Carlo studies of fp-shell nuclei. *Physical Review* C 52: 718–725.

Lattes, C.M.G., H. Muirhead, G.P.S. Occhialini and C. F. Powell. 1947. Processes involving charged mesons. *Nature* 159: 694–697.

Lesko, K.T., E. B. Norman, B. Sur, and R.-M. Larimer. 1989. Half Life of ^{56}Co. *Physical Review* C40: 445–448.

Li, Jia Jie, Jérôme Margueron, Wen Hui Long, and Nguyen Van Giai. 2015. Pairing phase transition: A finite-temperature relativistic Hartree-Fock-Bogoliubov study. *Physical Review C* 92: 014302, arXiv 1506.04507 [13 pages].

Lisetskiy, A.F., N. Pietralla, M. Honma, A. Schmidt, I. Schneider, A. Gade, P. von Brentano, T. Otsuka, T. Mizusaki, and B.A. Brown. 2003. Experimental evidence for ^{56}Ni—core breaking from the low-spin structure of the N=Z nucleus ${}^{58}_{29}Cu_{29}$. *Physical Review* C 68: 034316 [10 pages] arXiv.org: nucl-ex/0306032

Machleidt, R. and I. Slaus. 2001. The nucleon-nucleon interaction. *Journal of Physics G: Nuclear and Particle Physics*, 27(5): R69-R108.

Martinez-Pinedo, G., K. Langanke, and P. Vogel. 1999. Competition of isoscalar and isovector proton neutron pairing in nuclei. *Nuclear Physics* A 651: 379–393. arXiv.org: nucl-th/9811060.

McCarthy, I.E. 1968. *Introduction to Nuclear Theory*. John Wiley & Sons: New York.

McLaughlin, G.C. and R.A.M.J. Wijers. 2002. Delayed nickel decay in gamma-ray bursts. *Astrophysical Journal* 580: 1017–1023.

Möller, P., J. R. Nix, W. D. Myers, and W. J. Swiatecki. 1995. Nuclear ground-state masses and deformations. *Atomic Data and Nuclear Data Tables* 59, 185–381.

Möller, P., J. R. Nix, and K.-L. Kratz. 1997. Nuclear properties for astrophysical and atomic beam applications. *Atomic Data and Nuclear Data Tables* 66: 131–343.

Möller, P. A.J. Sierk, T. Ichikawa, H. Sagawa. 2016. Nuclear ground state masses and deformations: FRDM(2012). *Atomic Data and Nuclear Data Tables* 109–110: 1–204. arXiv.org 1508.06294.

Nadyozhin, D.K. 1994. The properties of Ni → Co → Fe decay. *Astrophysical Journal Supplement Series*, 92: 527–531

Negret, A. et al. 2006. Gamow-Teller strengths in the A= 14 multiplet: A challenge to the shell model. *Physical Review Letters* 97: 062502 [4 pages].

Nilsson, S.G., C.F. Tsang, A. Sobiczewski, Z. Szymanski, S. Wycech, C. Gustafson, I-L. Lamm, P. Möller, and B. Nilsson. 1969. On the nuclear structure and stability of heavy and superheavy elements. *Nuclear Physics* A 131: 1–60.

Nogami, Y., 1964, Improved superconductivity approximation for the pairing interaction in nuclei. *Physical Review* 134B, 313–321.

Nogami, Y. 1965. On the superconductivity theory of the nuclear pairing interaction. *Physics Letters* B15(4): 335–337.

NuDat 2.8 (accessed 2020)

Occhialini, G.P.S. and C.F. Powell. 1947. Nuclear disintegrations produced by slow charged particles of small mass. *Nature* 159: 186–190.

Otsuka, T., M. Honma, and T. Mizusaki, 1998. Structure of the N = Z = 28 closed shell studied by Monte Carlo shell model calculation. *Physical Review Letters* 81: 1588–1591.

Otsuka, T., T. Suzuki, R. Fujimoto, H. Grawe, and Y. Akaishi. 2005. Evolution of nuclear shells due to the tensor force. *Physical Review Letters* 95, 232502 [4 pages].

Peng, J. and Q. B. Chen. 2018. Exploring nuclear multiple chirality in the A ≈ 60 mass region within covariant density functional theory. *Physical Review* C 98 024320 [13 pages]. arXiv.org 1808.03776.

Pinto, P.A. and S. E. Woosley. 1988. The theory of gamma-ray emergence in supernova 1987A. *Nature* 333: 534–537.

Poves, A. and G. Martinez-Pinedo. 1998. Pairing and the structure of the *pf*-shell N ~ Z nuclei. *Physics Letters* B 430: 203–208. arXiv.org nucl-th/9802047

Pritychenko, B., M. Birch, B. Singh, M. Horoi. 2016. Table of transition probabilities from the first 2^+ states in even-even nuclei. *Atomic Data Nuclear Data Tables* 107: 1–175. arXiv.org: 1312.5975.

Raman, S., C. W. Nestor Jr., P. Tikkanen. 2001. Transition probability from the ground to the first-excited 2^+ State of even–even Nuclides. *Atomic Data and Nuclear Data Tables* 78: 1–128.

Rehm, K.E., F. Borasi, C.L. Jiang, D. Ackermanm, I. Ahmad, B.A. Brown et al. 1998. Study of the ^{56}Ni(d,p)^{57}Ni reaction and the astrophysical ^{56}Ni(p,g)^{57}Cu Reaction Rate. *Physical Review Letters* 80: 676–679.

Rodriguez-Guzman, R., J. L. Egido, and L. M. Robledo. 2002. Quadrupole collectivity in N ≈ 28 nuclei with the angular momentum projected generator coordinate method. *Physical Review* C 65: 024304 [14 pages].

Rowe, D.J. 1970. *Nuclear collective motion: models and theory*. Methuen, London.

Rubtsova, O. A., V.I. Kukulin, V.N. Pomerantsev, and H. Müther. 2017. In-medium bound states and pairing gap. *Physical Review* C 96: 034327 [10 pages] arXiv.org 1706.05299.

Rudolph, D., C. Baktash, M. J. Brinkman, E. Caurier, D.J. Dean, M. Devlin, J. Dobaczewski, P.-H. Heenen, H.-Q. Jin, D. R. LaFosse, W. Nazarewicz, F. Nowacki, A. Poves, L. L. Riedinger, D. G. Sarantites, W. Satula, and C.-H. Yu. 1999. Rotational Bands in the Doubly Magic Nucleus ^{56}Ni. *Physical Review Letters* 82: 3763–3766.

Sagawa, H., Y. Tanimura, and K. Hagino. 2013. A competition between T = 1 and T = 0 pairing in pf-shell nuclei with N = Z *Physical Review* C87: 034310 [4 pages] arXiv.org 1212.5992.

Schwalm, D., A. Bamberger, P. G. Bizzeti, B. Povh, G. A. P. Engelbertink, J. W. Olness and E. K. Warburton. 1972. Reorientation measurements using the Doppler shift method: static quadrupole moments of ^{20}Ne, ^{22}Ne, ^{24}Mg, ^{26}Mg, and ^{28}Si. *Nuclear Physics* A192: 449–495.

Stone, N.J. 2005. Table of nuclear magnetic dipole and electric quadrupole Moments *Atomic Data and Nuclear Data Tables* 90: 75–176.

Suntzeff, N.B. 1992. The energy sources powering the late-time bolometric evolution of SN1987A. *Astrophysical Journal* 384: L33–L36.

Sur, Bhaskar, Eric B. Norman, K. T. Lesko, Edgardo Browne, and Ruth-Mary Larimer. 1990. Reinvestigation of ^{56}Ni decay. *Physical Review* C 42(2): 573–580.

Taketani, Mituo, Seitaro Nakamura and Muneo Sasaki. 1951. On the Method of the Theory of Nuclear Forces. *Progress of Theoretical Physics* 6(4): 581–586.

Taniuchi, R., C. Santamaria, P. Doornenbal, A. Obertelli, K. Yoneda et al. 2019. ^{78}Ni revealed as a doubly magic stronghold against nuclear deformation. *Nature* 569(7754): 53–58. arXiv.org: 1912.05978 [nucl-ex].

Terasaki, J. and J. Engel. 2006. Self-consistent description of multipole strength: Systematic calculations. *Physical Review* C74(4) 044301 [19 pages].

Thibault, Catherine, R. Klapisch, C. Rigaud, A.M. Poskanzer, R. Prieels, L. Lessard, and W. Reisdorf. 1975. Direct measurement of the masses of ^{11}Li and $^{26-32}$Na with an on-line mass spectrometer. *Physical Review* C12: 644–657.

Thielemann, F.-K., M. Hashimoto and K. Nomoto. 1990. Explosive nucleosynthesis in SN1987A. II. Composition, radioactivities, and the neutron star mass. *Astrophysical Journal* 349: 222–240.

Vardiman, L., A.A. Snelling, and E.F. Chaffin, (editors) 2005. *Radioisotopes and the Age of the Earth, Volume 2, Results*. Institute for Creation Research and

Creation Research Society, Dallas, TX and Chino Valley, AZ.

Volya, Alexander, Vladimir Zelevinsky, and B. Alex Brown. 2002. Coherent and chaotic properties of nuclear pairing. *Physical Review* 65: 054312 [11 pages].

Woosley, Stan E. and M.M. Phillips. 1988. Supernova 1987A! *Science* 240 (4853): 750–759.

Woosley, Stan and Tom Weaver. 1989. The great supernova of 1987. *Scientific American* 261(2): 32–40.

Yanagisawa, Y., T. Motobayashi, S. Shimoura, Y. Ando, H. Fujiwara, I. Hisanaga, H. Iwasaki, Y. Iwata, H. Murakami, T. Minemura, T. Nakamura, T. Nishio, M. Notani, H. Sakurai, S. Takeuchi, T. Teranishi, Y. X. Watanabe, and M. Ishihara. 1998. Coulomb excitation of ^{56}Ni. In B. Sherrill, D. Morrissey, and C. Davids, editors, *Proceedings of the Conference on Exotic Nuclei and Atomic Masses 98 (ENAM 98)*, Bellaire, Michigan, June 23–27, *American Institute of Physics Conference Proceedings* 455, p. 610–613.

Yang, Yi, Lifan Wang, Dietrich Baade, Peter.J.Brown, Aleksandar Cikota, Misty Cracraft, Peter A. Höflich, Justyn R. Maund, Ferdinando Patat, William B. Sparks, and Jason Spyromilio. 2018. Late-time Flattening of Type Ia Supernova Light Curves: Constraints from SN2014J in M82. *Astrophysical Journal* 852: 89–98.

Yukawa, Hideki. 1935. On the interaction of elementary particles. I. *Proceedings of the Physico-Mathematical Society of Japan*. 17 (1935), 48–57.

Baraminic Classification of the Tuatara *(Sphenodon punctatus)* among Reptiles Based on Whole-Genome K-mer Signature Comparison

Matthew Cserhati*

Abstract

The baraminic status of the tuatara (*Sphenodon punctatus*), the only extant species of the reptilian order Rhynchocephalia, is an intriguing question for creation science. This animal superficially resembles lizards in its anatomy, yet has special physical and genomic characteristics which make it discontinuous with all other reptiles. A previous morphological baraminology study strongly suggested that the tuatara belongs to its own distinct group. In this study, the genomic analysis of 61 reptile genomes using the whole-genome k-mer signature reinforces this conclusion.

Introduction

The tuatara (Figure 1) is a unique reptile found on approximately 30 small islands around New Zealand (Evans, 2003). Its name comes from the Māori language and refers to the spiny crest on its back. It has a host of unique morphological and genomic features. For example, its brain fills only half of its endocranium. A row of pyramid-shaped acrodont teeth are on its lower jaw; two rows of blade-like teeth are on the upper jaw, which fit over the lower teeth when chewing. A parietal eye with retina and lens-like structures detects light, and is nested between the scales on the back of its head. It has no penis, rather sperm enters the female's body when the cloaca of the male and the female meet together. The tuatara also has a cold-adapted physiology, temperature-dependent sex determination, and can also live up to 80 years (Young, 1950, p. 384; Jones and Cree, 2012).

The tuatara is the sole living member of the reptile order Rhynchocephalia ("beak-head" in Latin), although some researchers recognize a second subspecies as a full species, *Sphenodon guentheri* (Hay et al., 2010). This order is thought to have had a worldwide distribution at one time in Earth's history (Evans, 2003). The tuatara allegedly shared a common ancestor with squamates (scaled reptiles, such as lizards, worm lizards, and snakes) some 250 million years ago (Gemmell et al., 2020). Many of its features were previously thought to be primitive but are now thought to be have been acquired over time (Jones et al., 2009). For example, the *Sphenodon* skull is held to be fully diapsid, and the lower bar of the temporal bone is thought to have been lost in its descendants, only to reappear later in recent species (Evans, 2003).

Evolutionists consider the tuatara to be an important link to those alleged stem reptiles which they claim gave rise to dinosaurs, modern reptiles, birds, and mammals. Interestingly, the tuatara resembles several sphenodontine fossils, allegedly from the Cretaceous, classifying it as yet another living fossil (Hay, 2008). Over forty rhynchocephalians exist in the fossil record, and it is possible that *S. punctatus* is the sole survivor of its kind from the Genesis Flood. Considering that dinosaurs have all gone

* Matthew Cserhati has a Ph.D. in biology and a B.Sc. in software development. He has been a member of CRS for six years. His main interest is molecular baraminology.

Accepted for publication February 8, 2021

Figure 1. The tuatara *(Sphenodon punctatus)*. Source: animals.sandiegozoo.org/animals/tuatara

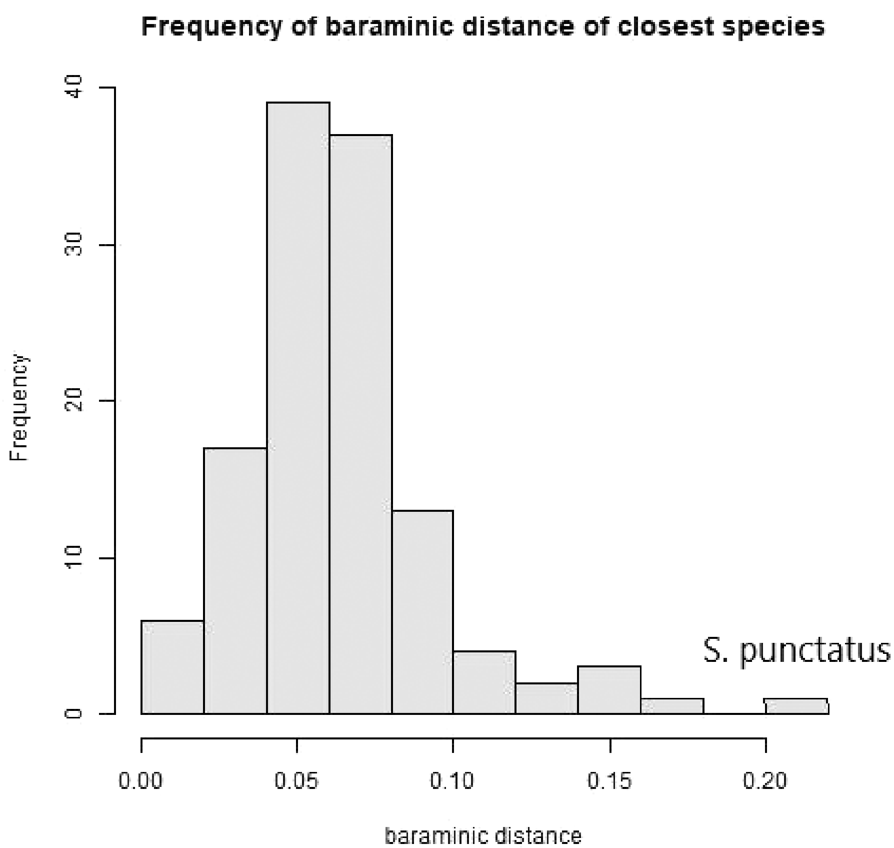

Figure 2. Histogram of closest baraminic distance values for each of the species in the morphological analysis of Cserhati, 2020a. The baraminic distance was noted for all species in that study and the species closest to it. These closest baraminic distances are then depicted as a histogram.

extinct, it is reasonable that something similar could have happened in Rhynchocephalia.

A previous baraminology study by Hennigan (2014b) places the tuatara into its own baramin. He bases his classification based on a number of skull characteristics which separate the tuatara from all other squamates. He also refers to the delay of hatching from eggs as much as 16 months after laying, and the lowest incubation temperature of all extant reptiles. In Figure 3 of Cserhati, 2020a, *S. punctatus* is fairly separate from all other species.

Upon examination of the baraminic distance matrix, the distance between *S. punctatus* and the species closest to it is 0.206. For each of the species in the study, the baraminic distance to the closest species to it was noted, and is visualized in the histogram in Figure 2. As we can see, the largest (closest) baraminic distance is that of *S. punctatus* (0.206, with *Physignathus cocincinus*, the Chinese water dragon). The next highest (closest) baraminic distance is 0.168, which belongs to *Anniella pulchra* (the California legless lizard, with *Sphenomorphus solomonis*, a skink species). This means that morphologically, *S. punctatus* is discontinuous with (or distinct from) all other reptiles, despite some superficial resemblance to lizards. But what about its genetics? Does a difference in phenotype also mean a difference in genotype as well?

Tuatara Genetics

Genetically, the tuatara is also a rather interesting animal. Its genome appears to be an amalgam, containing transposons from reptiles, monotremes, and placental animals. Its genome is 4.3 Gb in size with an estimated 17,448 genes, 75% of which are homologous to genes in birds, turtles, and crocodiles. Gene order is also similar between the tuatara, turtle, chicken and human. Furthermore, 64% of the tuatara genome is

Figure 3. Heat map showing Pearson Correlation Coefficient (PCC) values between species pairs among the 61 reptile species in this study. Darker colors denote higher PCC values, representing related species from the same cluster (baramin). Lighter colors denote lower PCC values, suggesting unrelated species from different baramins.

made up of repetitive elements, which are actually more similar to mammals than reptiles (Gemmell, 2020). If the tuatara genetically resembles reptiles and mammals, it cannot be an ancestor to either one of them. Rather, the evidence shows that the tuatara belongs to its own special group.

Remarkably, Hay and colleagues (2008) isolated mitochondrial DNA from tuatara fossils, suggesting from maximum likelihood analysis that the ratio and the sites of C to T and T to C substitutions are almost the same between modern and ancient tuatara populations (2.71 and 2.66 respectively). Furthermore, the positions where substitutions occur in the genome are also the same, another indication that the tuatara did not change much after its creation.

Object of this Study

The tuatara is interesting for baraminology studies because of its unique features. Some researchers believe that the tuatara most closely resembles squamates. A previous baraminology study on squamates showed that snakes and lizards are separate apobaramins (Cserhati, 2020a). It would be interesting to see how the tuatara can be classified, either as a member of its own or of another existing baramin. As we have seen, the tuatara is morphologically different from all other reptiles. Is the tuatara different genetically as well? Does the tuatara belong to an already existing reptile holobaramin, or does it form its own group? In this paper I will compare the tuatara with other reptile species by analyzing genomic data with a molecular baraminology algorithm to clarify its baraminic status.

Materials and Methods

Data availability

The whole-genome sequences (WGS) of 61 reptiles were downloaded from NCBI, which were then analyzed with the whole-genome k-mer signature (WGKS) algorithm. This algorithm has been used in previous molecular baraminology studies to measure the global genomic similarity between species to determine baraminic relationships. Octamers were analyzed, according to protocol in Cserhati, 2020b. A list of these species and a link to their whole-genome sequences are available in Supplementary File 1. Molecular and morphological data from a previous study on squamates was also included in this study on the tuatara (Cserhati, 2020a). This data is available at github.com/csmatyi/squamates. All supplementary files for the current study are available online at this web address.

All analyses were done using R version 4.0.1. Heatmaps were created using the heatmap command in R, using the 'ward.D2' clustering algorithm. Clustering was done using the Partition Around Medoids (PAM) algorithm, using the pam command in the cluster R library, with the algorithm parameter set to 'Forgy.' The PAM algorithm was designed to find a set of objects called 'medoids,' which are found in the middle of their own cluster. The algorithm classifies each object in such a way so as to minimize the dissimilarity between the object and their corresponding medoid. The Forgy algorithm is a widely used k-means clustering algorithm, which classifies entities based on their minimal distance to k previously determined centroids, each of which represents one of the k clusters, as selected by the user. The centroids can be determined by selecting those k entities which are the farthest from one another. In each iterative step, entities are assigned to one of the k centroids, after which the centroids are recalculated (Morissette and Chartier, 2013).

Results and discussion

Figure 3 is a heat map depicting the Pearson Correlation Coefficient (PCC) values. Darker, redder colors depict PCC values closer to 1, indicating two species from the same cluster. Lighter colors depict PCC values closer to 0, indicating two species from two different clusters. The PCC matrix has a Hopkins clustering statistic value of 0.863, which is very good for clustering. Several large and small clusters, and individual species can be seen in the figure. Using the PAM clustering method, 30 clusters were chosen; those with two or more species are listed in Table 1. In the following paragraphs, only clusters with three or more species will be viewed as putative baramins.

Cluster 1 consists of six turtle species (*Actinemys marmorata*, *Chrysemys picta*, *Malaclemys terrapin*, *Platysternon megacephalum*, *Terrapene carolina*, *Trachemys scripta*). These species belong to a group including the family Emydidae (terrapins), plus Platysternidae (big-headed turtles).

Cluster 2 is made up of four species from the order Crocodilia: *Alligator mississippiensis*, *Alligator sinensis*, *Crocodylus porosus*, *Gavialis gangeticus*. These species belong to a baramin comprised of reptiles with long bodies and long snouts. Hennigan (2014) puts crocodiles, alligators (caimans) and gharials into their own separate kinds because of strong cognita and reported interspecific hybridization within (but not across) some families. However, he suspects that Crocodilia possibly forms a holobaramin, despite the lack of hybridization data between the different families. The results in this paper support the latter.

Cluster 6 is made up of three species, *Chelonia mydas* (green sea turtle) from the family Cheloniidae, *Chelydra serpentina* (common snapping turtle), from the family Chelydridae, and *Dermatemys mawii* (Central American river turtle, or hickatee), from the family Dermatemydidae. The green sea turtle is a marine turtle, albeit the female comes to shore to lay eggs. The other two species are aquatic and sometimes submerge

Table 1. Statistics for 11 putative baramins with two or more species based on PCC values calculated for the 61 species.

Cluster	Species	Min	Mean	Max	Stdev	P-Value
1	6	0.792	0.899	0.977	0.062	4.36E-23
2	4	0.872	0.913	0.962	0.035	3.48E-09
4	2	0.831	0.831	0.831	NA	NA
6	3	0.642	0.652	0.662	0.01	3.00E-30
7	3	0.819	0.885	0.937	0.06	9.22E-4
8	4	0.843	0.902	0.978	0.055	3.14E-08
10	2	0.979	0.979	0.979	NA	NA
13	2	0.831	0.831	0.831	NA	NA
15	6	0.732	0.84	0.977	0.067	4.43E-18
16	5	0.727	0.831	0.977	0.101	9.16E-09
20	3	0.938	0.958	0.996	0.033	2.15E-06
28	3	0.6	0.739	0.899	0.151	0.039

into rivers. These three species may belong to different families, and therefore it is very tentative that they belong to the same baramin. However, both *D. mawii* and *Ch. mydas* both have a diploid number of 56, and their chromosomes can be arranged into groups A, B, and C following the 7:5:16 pattern (Carr et al., 1981).

Cluster 7 is made of three species, *Chelonoidis abingdonii*, *Gopherus agassizii*, and *Gopherus evgoodei*, the last two which are fossorial turtle species. All three species belong to the tortoise family (Testudinidae).

Cluster 8 is made of four species from the family Viperidae (vipers): *Crotalus horridus*, *Crotalus viridis*, *Protobothrops flavoviridis*, and *Protobothrops mucrosquamatus*.

Cluster 15 is made of six snake species from the superfamily Colubroidea, which includes colubrid and elapid snakes. These six species are: *Hydrophis cyanocinctus*, *Hydrophis hardwickii*, *Hydrophis melanocephalus*, *Notechis scutatus*, *Ophiophagus hannah*, and *Pseudonaja textilis*.

Cluster 16 is made of five lizard species, *Lacerta agilis*, *Lacerta bilineata*, *Lacerta viridis*, *Podarcis muralis*, and *Zootoca vivipara*. These species all belong to the family Lacertidae (true lizards), which may comprise a holobaramin.

Cluster 20 is made of three snake species, *Pantherophis guttatus*, *Pantherophis obsoletus*, and *Ptyas mucosa*. All three belong to the family Colubridae (colubrid snakes, which have grooved fangs in the rear of the upper jaw).

Cluster 28 is made of three more snake species, *Thamnophis elegans*, *Thamnophis sirtalis*, and *Thermophis baileyi*. All three species belong to the family Colubridae.

There are several species which are grouped by themselves. Some of these species also belong to families which contain species from other clusters listed here. It may be that these families are polybaraminic. Such species include *Crotalus pyrrhus* and *Vipera berus* (Viperidae), *Dermochelys coriacea* and *Dermatemys mawii* (Dermochelyidae), *Gekko japonicus* and *Paroedura picta* (Gekkonidae), *Emydocephalus ijimae*, *Laticauda colubrina*, *Laticauda laticaudata*, and *Naja naja* (Elapidae).

Figure 3 clearly shows that *Sphenodon punctatus* belongs to its own cluster. *S. punctatus* has a mean PCC of 0.206 with all 60 other reptile species in this study. The mean PCC value in the PCC matrix is 0.321. The species with the top five highest PCC values compared to the tuatara belong to *Emydura subglobosa* (0.309), *Alligator mississippiensis* (0.291), *Mesoclemys tuberculata* (0.283), *Crocodylus porosus* (0.275), and *Varanus komodoensis* (0.268). These are turtle, crocodile, and lizard species, indicating that *S. punctatus* is discontinuous with all other reptile groups.

Figure 4 is a histogram showing the number of species whose closest species (measured by the PCC value) is depicted on the x-axis. For species within the same holobaramin, the closest species would come from the same holobaramin and the PCC value would be very high. This is why there is a maximum at around 0.9. The species closest to *S. punctatus* is the turtle species, *Emydura subglobosa*, with a PCC value of only 0.309 between it and *S. punctatus*. In comparison, only one other species, *Anolis carolinensis*, has a PCC value lower than this when compared to any other species (namely *Zootoca vivipara*, with a PCC value of 0.248). This also illustrates the fact that *S. punctatus* is genomically discontinuous with all other reptiles.

Summary and Conclusion

According to this study, the tuatara is clearly genetically distinct from other reptiles. Therefore, I suggest putting it into its own holobaramin. The tuatara seems to be the sole survivor of its kind after the Flood. This is in agreement with a previous study based on morphological characteristics, as well as a previous creationist analysis. The current study illustrates how morphologi-

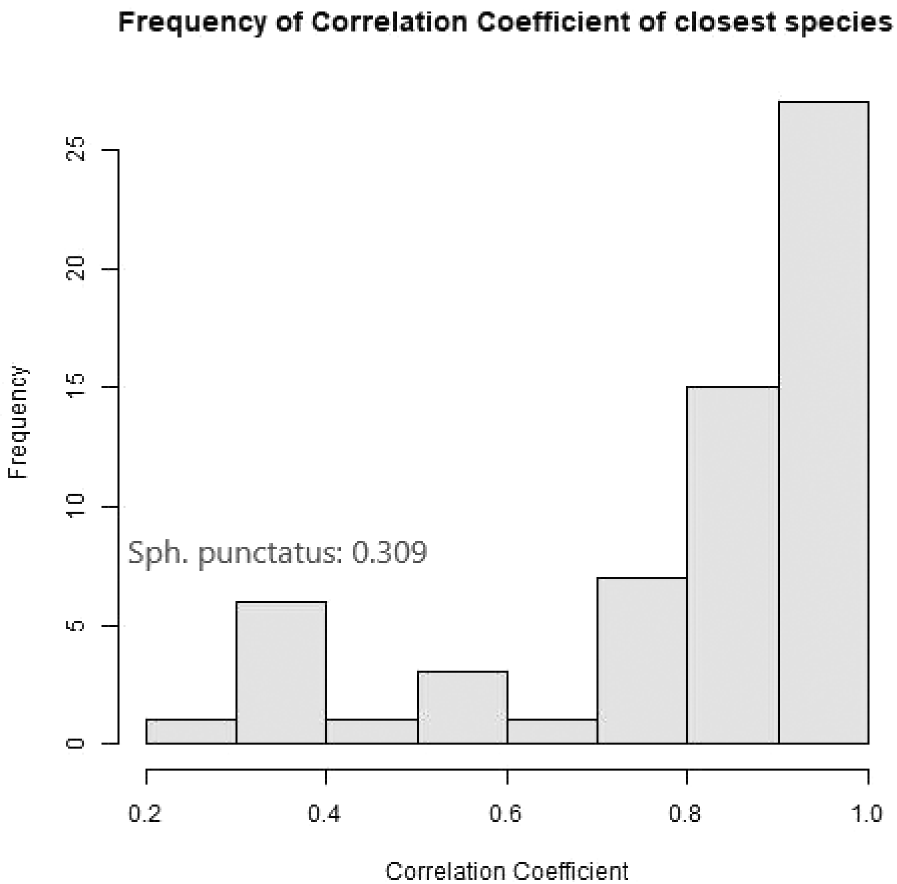

Figure 4. Histogram of PCC values of closest species to each of the 61 species in this study. In other words, for each species, the PCC of the species closest to it is noted, and all of these 61 'closest species PCC values' are depicted on the histogram.

cal and genomic baraminology studies can nicely complement one another. Besides morphology and genetics, fossil data also appears to support the discontinuity between the tuatara and all other reptile groups, consistent with the creationist narrative that distinct kinds of animals were created at the beginning of history.

Acknowledgements

This research was funded by Creation Research Society Grant #62.

References

Carr, J.L., J. Bickham, and R.H. Dean. 1981. The karyotype and chromosomal banding patterns of the Central American river utrtle *Dermatemys mawii*. *Herpetologica* 37: 92–95.

Cserhati, M. 2020a. Do lizards and snakes form separate apobaramins? *Journal of Creation* 34(1): 96–101.

Cserhati, M. 2020b. A new baraminology method based on whole-genome k-mer signature analysis and its application to insect classification. *Journal of Creation* 34(1): 86–95.

Evans, S.E. 2003. At the feet of the dinosaurs: The early history and radiation of lizards. *Biological Reviews of the Cambridge Philosophical Society* 78(4): 513–551.

Gemmell, N.J., K. Rutherford, S. Prost, M. Tollis, D. Winter, J.R. Macey, et al. 2020. The tuatara genome reveals ancient features of amniote evolution. *Nature* 584(7821): 403–409.

Hay, J.M., S. Subramanian, C.D. Millar, E. Mohandesan, and D.M. Lambert. 2008. Rapid molecular evolution in a living fossil. *Trends in Genetics* 24(3): 106–109.

Hay, J.M., S.D. Sarre, D.M. Lambert, F.W. Allendorf, and C.H. Daugherty. 2010. Genetic diversity and taxonomy: A reassessment of species designation in tuatara (*Sphenodon*: Reptilia). *Conservation Genetics* 11: 1063–1081.

Hennigan, T. 2014a. An initial estimate toward identifying and numbering the Ark turtle and crocodile kinds. *Answers Research Journal* 7(2014): 1–10.

Hennigan, T. 2014b. An initial estimate toward identifying and numbering extant tuatara, amphisbaena, and snake kinds. *Answers Research Journal* 7(2014): 31–47.

Jones, M.E., A.J. Tennyson, J.P. Worthy, S.E. Evans, and T.H. Worthy. 2009. A sphenodontine (Rhynchocephalia) from the Miocene of New Zealand and palaeobiogeography of the tuatara (*Sphenodon*). *Proceedings Of the Royal Society B, Biological Sciences* 276(1660): 1385–1390.

Jones, M.E., and A. Cree. 2012. Tuatara. *Current Biology* 22(23): R986–R987.

Morissette, L., and S. Chartier. 2013. The *k*-means clustering technique: General considerations and implementation in *Mathematica*. *Tutorials in Quantitative Methods for Psychology* 9(1): 15–24.

Robinson, D.A. 1997. A mitochondrial DNA analysis of the Testudine apobaramin. *Creation Research Society Quarterly* 33: 262–272.

Wise, K.P. 1992. Practical baraminology. *Creation Ex Nihilo Technical Journal* 6(2): 122–137.

Young, J.Z. 1950. *The Life of Vertebrates*. The Clarendon Press, Oxford, UK.

A Dam Breach Unlikely for the Origin of Grand Canyon

Michael J. Oard

Abstract

The origin of the Grand Canyon is still being debated by uniformitarian and creation scientists. Two uniformitarian scientists have recently used pieces of previous research to suggest that the Grand Canyon was finally formed when the Kaibab Plateau was breached by water piping through limestone—a difficult task with little or no evidence. Several creation and uniformitarian scientists have recently defended the dam-breach hypothesis against published objections. These are reviewed, and another flaw is introduced: the absence of a huge cobble and boulder delta at the mouth of Grand Canyon. The Bidahochi Formation is interpreted as containing Lake Hopi bottom sediments, but most of its deposits are currently higher than its proposed elevation. Furthermore, the lacustrine interpretation is equivocal. Problems with the breach event are discussed. The late-Flood runoff erosion model still seems the best explanation.

Introduction

The Grand Canyon is truly one of the most remarkable icons of geology on Earth. Visually fascinating (Figure 1), it defies uniformitarian explanations of its origin. Uniformitarians have spent nearly 150 years cycling through unworkable hypotheses. One of the main problems is the way in which the Colorado River defies typical principles of drainage:

> The course of the Colorado River and its tributaries are remarkably independent of topographic and structural control, with mountains discordant to the course of the streams, or as stated by Dutton (1882, p. 73): "They run in a majority of cases against the inclination of the topographic slopes. They cut through mountains and plateaus; they enter cliffs, they emerge from them; they enter the lifts of monoclines, they cross faults from the up-thrown to the downthrown [side]. They run here obliquely up or down the structural slopes, and then they course along the strike" (Hill and Polyak, 2020, p. 2).

Hill and Polyak (2020) list five enigmas for each of the three segments of the Canyon. The most substantial include:

1. Where was the Colorado River before 6 Ma?
2. Why does the Colorado River make a 90° bend from south to west in the Desert View area?
3. Why does the route through the central Grand Canyon seem unrelated to structure and not affected by the Hurricane or Toroweap faults?
4. Is long distance headward erosion a viable concept for this location?
5. Why is there no delta at the mouth of Grand Canyon?

However, they do not include the elephant in the room—the canyon cut through the high Kaibab Plateau at an

Accepted for publication February 19, 2021

intermediate altitude, not at its lowest points.

Like others before them, assumptions of uniformitarianism and deep time stand in the way of a viable explanation for the Grand Canyon. In contrast, creation scientists have only been working (with a fraction of the budget and man-hours) on a Biblical mechanism for about 40 years. I published evidence that the Grand Canyon was carved by channelized Flood runoff (Oard, 2010 a,b,c,d, 2011, 2016a), like any other water gap. However, Austin et al. (2020) and Hill and Polyak (2020) offer other mechanisms, from creationist and secular viewpoints.

Figure 1. Grand Canyon, northern Arizona (view north from Yavapai Observation Station, South Rim). The side canyon is Bright Angel Canyon, caused by the Bright Angel Fault which the North Kaibab trail runs down.

A Uniformitarian Piping Hypothesis

One of the greatest difficulties for uniformitarian Grand Canyon origin theories is the dating of basalt and ash in the Muddy Creek Formation, Hualapai Limestone, and Bouse Formation west and southwest of the Grand Canyon at about 6 Ma (Longwell, 1946; Howard et al., 2008, pp. 391–410). These dates mean that the Colorado River did not flow out of its canyon until that time, implying the western Grand Canyon eroded 1,600 m down in only 6 million years (Karlstrom et al., 2007, 2008). This is extremely rapid though exceeded at the Colorado River upstream from the Grand Canyon. Aslan et al. (2019) propose a phenomenal rate of 2,188 to 3,706 m/m.y. between 85–144 kyr for the Gunnison River after it quit cutting the Unaweep Canyon wind gap through the Uncompahgre uplift of southwest Colorado.

The 6 Ma date has triggered complicated and controversial scenarios. After chiding creation scientists for "misinterpreting" various aspects of the Grand Canyon (Hill and Davidson, 2016), Hill admits uniformitarian scenarios still fail to explain its origin (Hill and Polyak, 2020). It is worth noting that practically all challenges to a creation-science origin of the Grand Canyon are based on the authors' slavish beliefs in uniformitarianism and deep time (Woodmorappe, 2016).

Hill and Polyak (2020) offer a more complicated story. They begin with a deep "Laramide paleo Grand Canyon" carved by the uplift of the Hualapai Plateau on the southwest edge of Grand Canyon about 85 to 80 Ma (Figure 2). Drainage started at Peach Springs and flowed northeast into the "Western Interior Seaway" in central North America or into "paleolakes" in Utah. Part of the drainage was underground. But Wernicke (2011) envisions a river starting in California and called it the "California River." Hill and Polyak (2020) say there is no evidence for such a river, since there is no evidence it crossed the Kingman Uplift in northwest Arizona.

Between 85 and 65 Ma, the Kaibab arch uplifted and diverted the northeast drainage of this paleoriver from the Coconino Plateau northward along the southwestern portion of the Kaibab uplift. Then, between about 65 and 17 Ma, Great Basin faulting and Rocky Mountain uplift resulted in multiple closed basin lakes. They claim a paleo Little Colorado River, east of the Kaibab Plateau, flowed north and northeast into "Paleogene Glen Lake" around Glen Canyon just northeast of Lees Ferry, although there is no field evidence for such a lake (Hill and Polyak, 2020).

About 28 to 18 Ma, the "Arizona river" flowed southwest to the Pacific Ocean and spread orthoquartzite to the southern California coast, now found in the Sespe Formation (Sabbeth et al., 2019). The only plausible source is the 1.1 Ga Shinumo Formation in the Mesoproterozoic Grand Canyon Supergroup strata, exposed only between Colorado River mile 75 and 109. River miles start with zero at Lees Ferry and go to 277 at the western entrance to the Grand Canyon. The existence of the Arizona River contradicts a paleo river not flowing out of the western Grand Canyon until after 6 Ma. Hill and Polyak (2020) do not resolve this problem.

Between 17 to 6 Ma, a complex series of events are believed to have

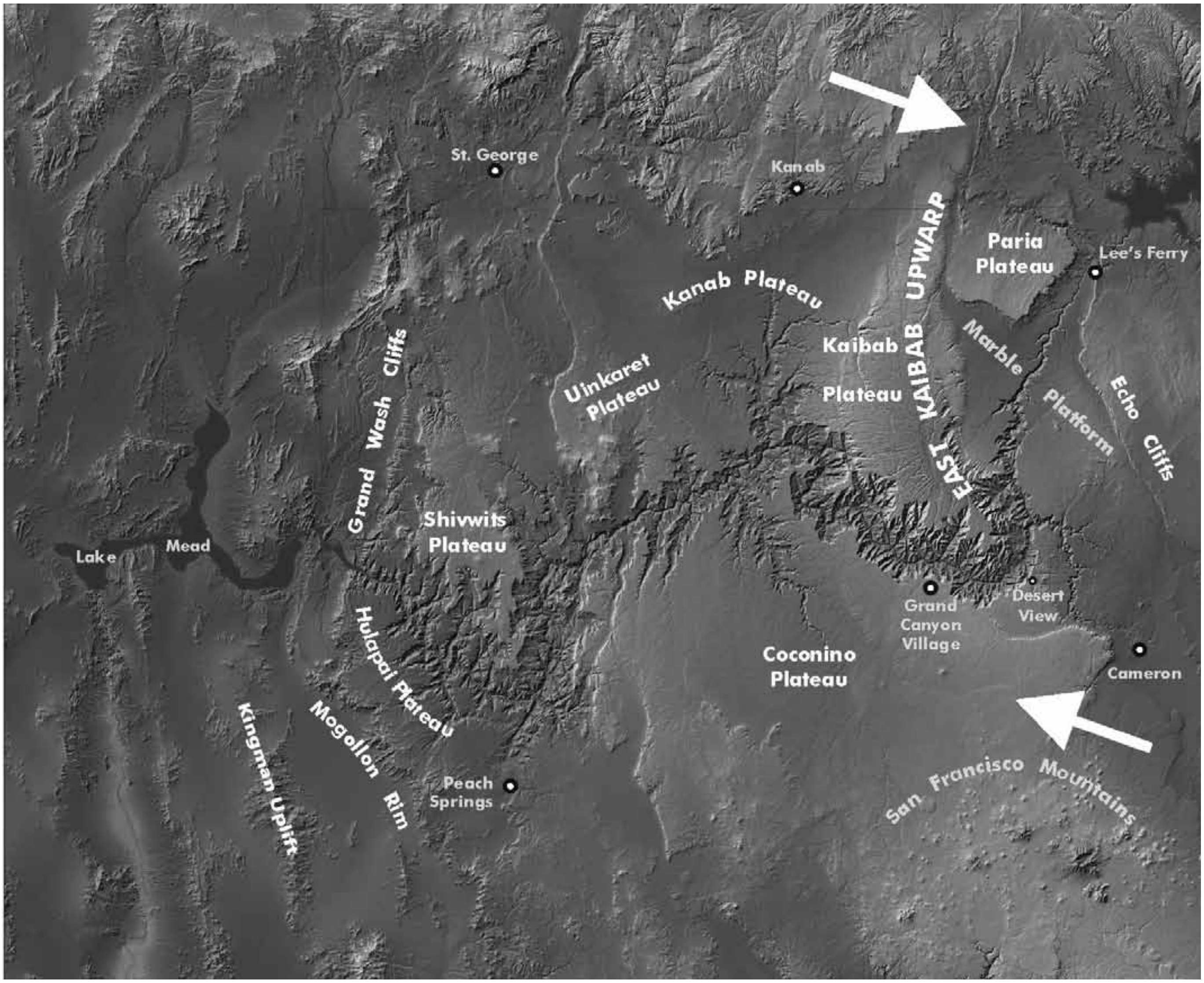

Figure 2. The Grand Canyon and the surrounding area with the main plateaus and prominent topographic features. The low point of about 1,700 m (5,577 ft.) asl of the northern Kaibab Plateau and the low point a little above 1,830 m (6,000 ft.) on the eastern Coconino Plateau marked by arrows (map background provided by Ray Sterner and drawn by Peter Klevberg).

taken place. It was at this time that a "precocious gully" supposedly eroded headward from the mouth of the Grand Canyon at the Grand Wash Cliffs all the way to the Kaibab Plateau, about 322 km (200 mi) (Larson et al., 2017), possibly following the Laramide paleo Grand Canyon. Hill and Polyak (2020) claim this, but many geologists believe that headward erosion, even in soft sediments, is slow, rare, and overutilized (Larson et al., 2017). At the same time, the deep Kanab and Cataract Creek tributary canyons, about 80 km long, also eroded headward from the "precocious gully." This scenario presents many challenges (Hill and Polyak, 2020). Then the Little Colorado River deposited the Bidahochi Fm in the eastern part of the "Lake Hopi" basin. Hill and Polyak (2020), along with many other geologists, maintain that the lower member of the Bidahochi was deposited in a playa lake (the middle member is volcanic and the upper member, fluvial). This is contrary to the views of Austin et al. (2020), who believe that the lacustrine Bidahochi is in the *upper* member.

Integrating prior research to address the most difficult uniformitarian prob-

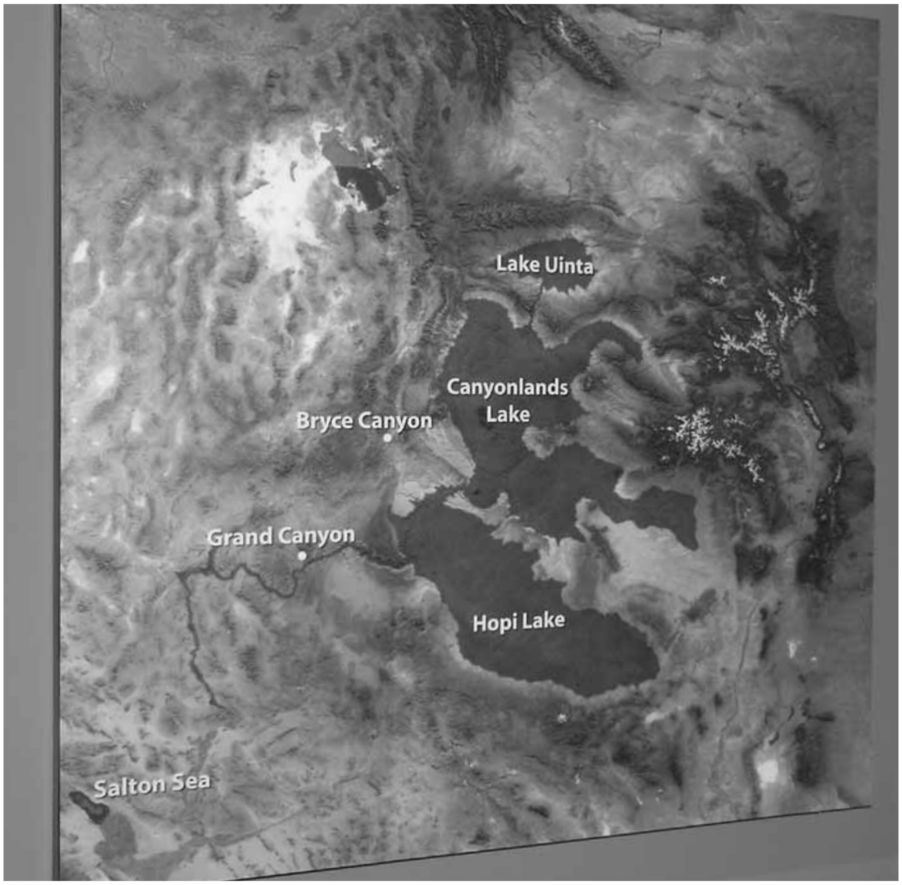

Figure 3. The three lakes that supposedly breached to carve Grand Canyon (from AiG museum display).

lem, eroding across the high Kaibab Plateau, Hill and Polyak (2020) propose that the Little Colorado River, flowing north at the time, diverted into a sinkhole near the southern Kaibab Plateau between 8 and 6 Ma (Hill et al., 2008). The river sank down to the Redwall/Muav limestones and then was piped westward under the high Kaibab Plateau to the westward drainage off the Kaibab Plateau. This is similar to Austin's early suggestion (1994, pp. 102–104) of piping that passed under the high Kaibab Plateau, where the Grand Canyon occurs at the current elevations of 2,285 m (7,500 ft) above sea level (asl) at Grandview Point along the south rim and about 2,500 m (8,200 ft) asl along the north rim (the plateau slopes down to the south). Austin et al. (2020) now advocate flow over the top of the plateau at a time when the Kaibab Plateau was 300 m lower (see below). There is no evidence of a sinkhole at the confluence of the Colorado and Little Colorado River today, which is said to be due to collapse of the strata all along the piping route. Hill and Polyak (2020) point to a dry sink hole, called the Hol Sah sinkhole/breccia pipe, on the northern Marble Platform, as an analog. They are the only uniformitarian researchers proposing this piping model. For other problems with the path of the Colorado River, see Oard (2010, 2016).

I have summarized only the main points of Hill and Polyak's complex hypothesis and only dealt with the most obvious difficulties. Each step of their complicated scenario is difficult to accomplish in reality. But if nothing else, the necessity of such a theory shows that previous explanations are not having much success. It will be interesting to see how other uniformitarian geologists respond.

Some Creation Scientists Sticking with the Dam-Breach Mechanism

Uniformitarians are not the only ones working on an explanation for Grand Canyon. One creationary idea is the dam-breach hypothesis, which has two versions (Austin, 1994, pp. 83–110; Austin et al., 2020; Brown, 2008). I will address Austin et al.'s (2020) version, that is a little different from his previous version. The original Austin (1994) version believed that three lakes formed after the Flood, southeast and northeast of Grand Canyon. Those included: (1) Hopi Lake in the Little Colorado River Valley, (2) Canyonland Lake over Canyonlands National Park and vicinity, and (3) Uinta or Vernal Lake in northern Utah (Figure 3). In the Austin et al. (2020) version, the third lake is no longer included. It is very likely that the Green River Formation and its equivalents suggested as deposits from Lake Vernal are very likely from the Flood (Oard and Klevberg, 2008). Therefore, I will only be addressing the southern two lakes.

The southern lakes continued to fill for a while after the Flood, then emptied via dam breaching, and carved the Grand Canyon. The time for filling depends critically on the precipitation of the area, which I had previously estimated was roughly four times the current precipitation based on the warm Pacific Ocean (Oard, 1993). At this rate it would take a few hundred years to fill the lakes to overflowing from a lower level right after the Flood. Hypercanes could potentially increase the precipitation rate an order or two of magnitude.

Hypercanes are super-hurricanes that need sea surface temperatures in excess of 40°C (104°F) over an area greater than 500 km (310 m) in diameter. Multiple hypercanes per year would fill the lakes in a decade or two. However, hypercanes are very unlikely after the Flood, especially over the Colorado Plateau, for at least four reasons. First, a large source of hot sea surface temperatures off the Pacific Coast of the United States is unlikely. Second, the ocean currents and atmosphere must be close to rest for days (Emanuel et al., 1995). Hypercanes take time to develop, just like a hurricane. So, the initial storm would intensify *slowly* over the hot water. The developing storm must remain over the hot spot. This is unrealistic after the Flood. Third, if the tracks of hypercanes are similar to those of hurricanes, then hypercane erosion would be confined mainly to the east coasts of continents between about 40°N and 40°S. Fourth, as a hypercane moves inland, it would rapidly lose its moisture source.

Austin et al. (2020) apparently abandoned the piping idea and advocate that the Grand Canyon was carved at intermediate altitudes of the Kaibab Plateau when the southern part of the plateau was 300 m (1,000 ft) lower and the northern part 300 m (1,000 ft) higher.

I was once favorably disposed to the dam-breach hypothesis, but recognized problems with it (Oard, 1993). While studying a real dam breach, the Lake Missoula flood (Oard, 2004, 2014c), I became more skeptical of that explanation for the Grand Canyon. Out of about a dozen problems, three seemed fatal to the dam-breach hypothesis: (1) the lack of bottom sediments, (2) the deep tributary canyons of Kanab and Havasu Creeks, and (3) the lack of ancient shorelines. Austin et al. (2020) address the first two, and for the third claim that tufa near Cape Solitude and the Bidahochi formation are evidence of an old shoreline. Clarey (2020a) has recently pointed out that actual wave-cut terraces at generally the same altitude are required for the hypothesis to work, and they are missing.

Setting the Record Straight

Austin et al. (2020) disparage Clarey and me for our analysis, implying that we cannot be trusted in our critique of the dam-breach hypothesis or in the alternative of late-Flood channelized erosion. Before continuing, I will answer their objections.

Did Henry Morris Believe in the Dam-Breach Hypothesis?

Austin et al. (2020) claim that Henry Morris affirmed the dam-breach hypothesis in Vail (2003), and they criticize me for saying that Morris favored the channelized Flood-runoff hypothesis. Whitcomb and Morris, (1961, p. 153 and caption to their Figure 6) stated after Flood sediment deposition and rapid uplift:

> Subsequent rapid canyon downcutting then ensued while the sediments were still relatively soft and the rivers were carrying much larger discharges. … Following the Flood, while the rocks were still comparatively soft and unconsolidated, the great canyons were rapidly scoured out as the waters rushed down from the newly-uplifted peneplains to the newly-enlarged ocean basins.

This could be taken to mean channelized erosion during Flood runoff, depending upon what Whitcomb and Morris meant by "rivers" and "Following the Flood." Looking back on it now, the statements are equivocal, and I should not have used Whitcomb and Morris as directly advocating channelized Flood runoff.

I suppose then that Peter Sheele (2010) and/or myself (Oard, 2010 a,b,c,d, 2011) may be the originator(s) of the late-Flood channelized erosion hypothesis. Regardless, it does not matter whether Henry Morris advocated the dam-breach hypothesis or not. What matters is, do the available data support a particular hypothesis?

Who First Originated the Dam-Breach Hypothesis?

Austin et al. (2020) take me to task for not recognizing that Newberry was the first to advocate the dam-breach hypothesis back in about 1860, instead of Blackwelder (1934):

> A misstatement of historical fact occurs in Oard 2016, 39: "Geologist Eliot Blackwelder was the first to propose that Grand Canyon was eroded by rushing water derived from the spillover of a lake that was ponded northeast of the Kaibab Plateau." Mike Oard appears to be oblivious to the earlier work of John Strong Newberry (Austin et al., 2020, p. 157, note 5).

Blackwelder (1934, p. 562) was a bit obscure when he says that lakes ponded in the desert basins and "the lakes rose until they overflowed the lowest points of their rims and spilled into adjacent basins." He was most likely thinking of the multiple basins in the Lower Colorado River drainage west and southwest of Grand Canyon, and he may have also been thinking of Grand Canyon itself. This is probably why Blackwelder is given credit for the overspill hypothesis, although Grand Canyon did not spill over at the current lowest points on the Kaibab Plateau, as expected, but at an intermediate altitude.

I checked the Newberry (1862) paper referenced by Austin et al. (2020) and did not find any mention of the origin of Grand Canyon. Newberry's 1861 paper was too difficult to obtain. Regardless, overflow advocates Douglass et al. (2020, p. 2), clear up the situation:

> Blackwelder (1934) is often cited by others for proposing overflow to explain the formation of the Grand Canyon. However, in his paper, *he never directly states that overflow accounts for Grand Canyon incision.*

> Blackwelder proposed a model of drainage development eloquently described as, "a chain of lakes strung upon a river" (1934, p. 562). Newberry (1861) proposed a similar model, but again, *not directly related to Grand Canyon incision* (emphasis mine).

So, the history of the origin of the dam-breach hypothesis is confusing. Scientifically, it is not important who first suggested the hypothesis. Did Austin et al. (2020) mention this trivial point to discredit what I have said about the dam-breach hypothesis?

Bottom Sediments

Austin et al. (2020) criticize me for saying that there is no evidence for the lakes, no lake-bottom sediments, and no shorelines (Austin et al., 2020, p. 182, and note 55). The *CRSQ* was also criticized for letting "no evidence" statements be published. Clarey (2020b is also taken to task for agreeing with me on the origin of Grand Canyon, although he admitted there could be a *little* evidence (Austin et al., 2020). Clarey has mentioned the Bidahochi Formation as possible evidence, but believes it is weak at best.

However, Austin et al. (2020) need to carefully read Oard (2010, 2016a). It is easy to miss something important in a manuscript. I do mention the Bidahochi Formation, as being potential lake bottom sediments, but point out that "there does not seem to be enough sediments to justify a lake as large as 'Lake Hopi'" (Oard, 2010, pp. 296–297). This statement is based on many uniformitarian scientists, who have claimed that only a small part of the formation is considered lacustrine and generally from a small playa lake (Dickinson, 2013). Moreover, the formation today (Figure 4) on the northeast edge of "Lake Hopi" is near and well above the suggested shoreline. The elevation of Lake Hopi is said to be about 1,860 m (6,100 ft.), but the Bidahochi Formation is as high as 2,250 m (7,380 ft) asl (Douglass et al., 2020).

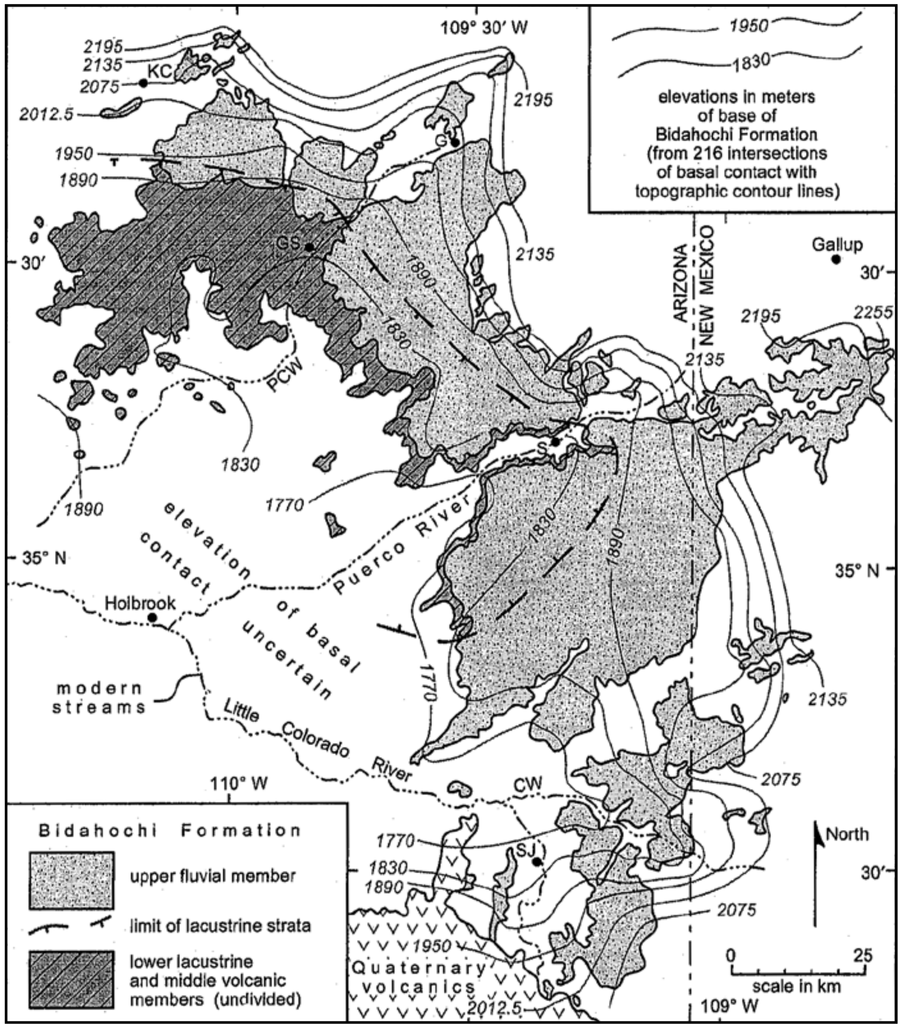

Figure 4. The lower/middle and upper Bidahochi Formation of Arizona and New Mexico, USA. The Hopi Buttes are in the lower/middle member in the northwest part of the formation (Copyright Dickinson, 2013, p. 3). Used in accordance with federal copyright (fair use doctrine) law. Usage by *CRSQ* does not imply endorsement of copyright holder.) Note that the Bidahochi Formation is also found up to 2,250 m (7,380 ft.).

Also, in the reference to "no lake bottom sediments," I stated:

> While the Bidahochi lake sediments are located near the northern and eastern "shoreline," there is [sic] no deposits in what would have been the deepest part of the lake—exactly where they would be most expected. There should be thick sediments at the bottom of the Little Colorado River Valley (2010, p. 297).

In Oard (2016a, pp. 65–66), I did admit that the Bidahochi Formation could be considered evidence:

> I said earlier that there is almost no sedimentary evidence for the lakes. There is a claim, however, that some sediments still exist for Lake Hopi.

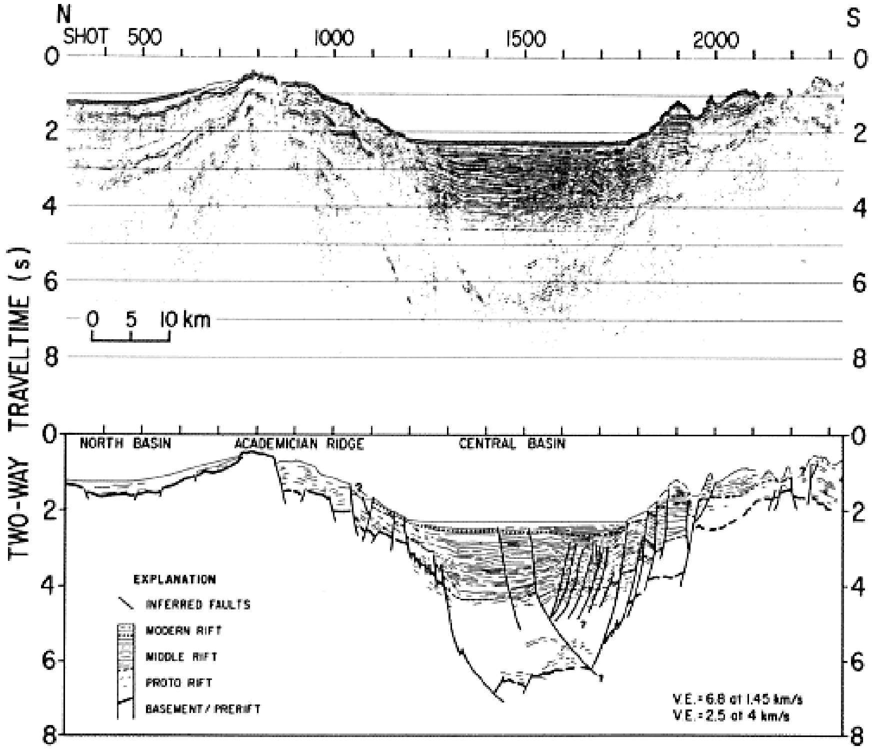

Multichannel seismic reflection line across central part of Lake Baikal showing seismic data (top) and interpretation (bottom). The thickest deposits are confined to a narrow trough that is 15 to 20 kilometers (9 to 12 miles) wide.

Figure 5. Interpreted north-south profile through Lake Baikal, southern Siberia through the Central Basin (USGS).

> The rocks in question are part of the Bidahochi Formation…

I still stand by these statements from personal observations, and it is the lack of bottom sediments in the *deepest parts* of the lake, for instance from Cameron to Holbrook, that I believe is a fatal problem for the dam-breach hypothesis. No advocate of the dam-breach hypothesis has claimed any bottom sediments in the deepest part of Hopi and Canyonland Lakes. When glacial Lake Missoula emptied, it failed to scour bottom sediments around Missoula, Montana, and especially north of Missoula. Lakes typically accumulate thick bottom sediments in the deepest parts, for instance the Central Basin of the very deep Lake Baikal with about 7 km of mostly Late Cenozoic sediments (Figure 5). Lake Baikal is about 100 km (60 mi) wide perpendicular to the Central Basin, which is probably close to the width of Lake Hopi, but Lake Baikal is much deeper than Lake Hopi.

No Geologists Have Proposed a Superimposed Submarine Canyon

Austin et al. (2020, p. 178) say that no geologist has proposed a superimposed submarine canyon model:

> In Mike Oard's view, Grand Canyon is a superposed submarine canyon! Oard's hypothesis is completely new to geologists, never before proposed in 150 years of Grand Canyon discussion.

At its heart, this is an appeal to authority. It assumes past geologists would have conceived of, and examined, every possible origin theory. We are always confronted with what uniformitarian interpretation we can accept (Oard and Reed, 2019). In this case, a superposed submarine canyon is not even on the uniformitarian radar. I would not expect them to have suggested such a hypothesis because it may imply channelized Flood runoff. We are looking for a *Biblical* solution, and the proposed mechanism is logically consistent with the Biblical account and is one that can be shown to consistently explain many geomorphological features on the Earth's surface (Oard, 2008, 2013).

I may also add that it does not matter whether uniformitarian scientists have suggested a submarine canyon model or that the dam-breach hypothesis is a creationist mechanism, as touted by Austin et al. (2020). If the dam-breach hypothesis is not consistent with the field data, it should be rejected.

The Lack of Lake Bottom Sediments

Austin et al. (2020) propose that an analog for their model is the breaching of Lake Manix, filled with water by the Ice Age Mojave River. The rock dam breached and carved a 135 m (440 ft.) deep outlet canyon, called Afton Canyon. Austin et al. (2020) note that there is a lack of fine-grained bottom sediments associated with the Afton subbasin just west of the dam breach, although there is coarse-grained sediment. This is thought to justify the lack of bottom sediments for Hopi Lake.

However, this example is flawed, since the breaching of Lake Manix not only cut down to the level or near the level of the bottom of the Afton subbasin, but also the canyon was almost the same width as the subbasin. During this dam breach, the fine-grained bottom sediments could easily have been scoured out, especially since the Afton subbasin is narrow (see Figures 13 to 16 in Austin et al., 2020, pp. 170–171).

This example is contradicted by the Little Colorado River Valley, a narrow slot canyon (Figures 6 and 7). Except for this narrow slot canyon, the wide valley of the Little Colorado River southeast of Cameron is surrounded by high terrain. It is true that the canyon was carved down to the level of potential lake bottom sediments, but because this canyon is so narrow and Lake Hopi so large, the narrow slot canyon would have prevented hardly any bottom sediments from being scoured out. If Hopi Lake filled to 2,135 m (7,000 ft.) asl, as estimated by Austin et al. (2020, p. 173) during the dam breach, the lake would have had an area of 51,200 km^2 (20,000 mi^2). Rapid currents through the narrow canyon of the Little Colorado River, before it enters Grand Canyon, would not have scoured out hardly any bottom sediments (Figure 8), if they existed.

Lake Hopi should have left tens of meters of bottom sediments in the deepest parts, since the formations around the putative lake are often soft. During the likely existence of the lake likely for several hundred years, erosion would have easily produced thick sediments in the deepest parts of the lake. This problem still stands, and by itself should tell us that Lake Hopi never existed, despite properties of the Bidahochi Formation (see below). It is no surprise that Austin et al (2020) ignore the absence of bottom sediments in what should have been the deepest parts of the lake, but instead focus on the Bidahochi Formation.

"Canyonland Lake," even larger than Lake Hopi, should also have left a record of massive bottom sediments. If the lake reached an elevation of 1,940 m (6,400 ft.) asl, as believed by Austin et al. (2020) (see below), many valleys would have been filled by the lake, including the San Juan River Valley into northwest New Mexico, the Colorado River Valley well past Grand Junction, and the Green River Valley up to the Book and Roan Cliffs (not counting the water gap through the Book and Roan Cliffs into the wide area with the Green River Basin in "Lake Vernal"). These valleys vary in width. The geological maps of the area often indicate the bedrock is Mesozoic sedimentary rocks. Figure 9 shows the bedrock around the confluence of the Green and Colorado Rivers showing no indication of expected lacustrine sediments.

Assuming a rock dam east of Lees Ferry (a late development in the hypothesis), the bursting of Canyonland Lake would have eroded this dam over a width of several kilometers, emptying the top half of the lake. However, the erosion of rock may have been slow and not a dam breach, as shown by the breaching of Lake Bonneville at Red Rock Pass, Idaho. But as Canyonland Lake lowered to the top of the western Marble Platform, the drainage would have been confined to

Figure 6. The narrow valley of the Little Colorado River Valley at a scenic overlook at milepost 285.7 on highway 64. The canyon at this point is a slot-like canyon about 365 m (1200 ft) deep.

Figure 7. Top of the slot-like canyon of the Little Colorado River Valley at milepost 277.7 on Highway 64.

the narrow Marble Canyon (Figure 10, also see Figure 11 in Austin et al. (2020)). So, just like with Lake Hopi, the current would be strong enough to have eroded and transported lacustrine sediments through Marble Canyon. However, upstream, the currents would have been sluggish, and lake bottom sediments would not have been scoured out during the dam breach. As far as I know, there are no bottom sediments associated with Canyonland Lake (personal observations). No matter what is claimed about the Bidahochi Formation, such lack of bottom sediments is strong evidence that the proposed lakes did not exist. If so, the dam-breach hypothesis lacks crucial evidence needed to argue its case.

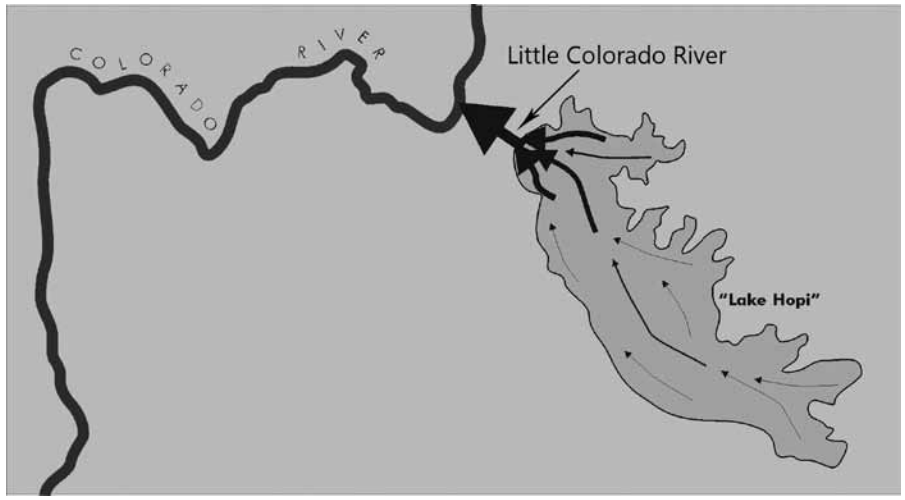

Figure 8. Schematic of postulated currents in "Lake Hopi" and the Little Colorado River Canyon (drawn by Peter Klevberg). The current would have been strong through the Little Colorado River Canyon because it is a narrow, slot canyon, but currents would have been very weak in the rest of the lake away from the entrance to the canyon and hence little erosion of lake bottom sediments would have occurred.

The Problem of Tributary Valleys

Austin et al. (2020) supposedly "answered" the argument that the long, deep Kanab and Havasu tributary valleys are inconsistent with the dam-breach hypothesis by claiming that tributary canyons were also formed during the March 19, 1982 mudflow in the upper Toutle River Valley, northwest of Mount St. Helens, Washington. They (pp. 168–169) state: "These big side canyons at Mount St. Helens are similar to Kanab Creek and Havasu Creek (see Figure 4) in the central Grand Canyon."

Their example does not satisfactorily answer the problem of deep tributary canyons at Grand Canyon. These tributary valleys are about 1,600 m (5,200 ft.) deep where they enter the Grand Canyon. There are several reasons to doubt their proposed analogy. First, the Little Grand Canyon, about 30 m (100 ft.) deep, and its tributaries of the Toutle River are a 1/40th scale of Grand Canyon. Second, they were curved by *a mudflow*. Third, they were cut into *unlithified landslide debris*. In contrast, Kanab and Havasu Creeks were likely carved in consolidated or near consolidated rock. Much evidence indicates the sediments through which the Grand Canyon and its tributaries were carved were lithified (Oard, 2016a). If the strata were unconsolidated, the sides of Grand Canyon, Kanab Creak, and Havasu Creek would have slumped inward. The problem still stands. On the other hand, tributaries (Kanab and Havasu Canyons)

Figure 9. View northeast from near the confluence of the Green and Colorado Rivers about a hundred meters above the river, showing no thick bottom sediments around the river within the area of "Canyonland Lake" (courtesy of Esther Fishbaugh). Alluvial fan on the left. River elevation about 1,370 m (4,450 ft.), well below the surface of the lake.

Figure 10. The Colorado River flowing through the beginning of the narrow Marble Canyon.

Figure 11. Shorelines from glacial Lake Missoula on Mount Jumbo, northeast of Missoula, Montana.

merging downstream with the main trunk channel (the Grand Canyon) is "a fundamental outcome of erosion by flowing water" over a broad area (Perron et al., 2012, p. 100).

The Problem of the Lack of Shorelines

Austin et al. (2020) mostly ignore the lack of shorelines (wave-cut terraces) and raised deltas that should be evident in the rocks surrounding Hopi and Canyonland Lakes. Based on the numerous shorelines associated with the short-lived glacial Lake Missoula (Oard, 2004) (Figure 11) and the numerous Ice Age lakes of the Great Basin (Figure 12), such shorelines should be abundant (Clarey, 2020a). Multiple Ice-Age lake terraces occur in the Great Lakes region, ponded south of the Laurentide Ice Sheet (Clarey, 2020a). The Great Lakes area gets far more precipitation than Arizona and eastern Utah today and presumably after the Flood, yet these shorelines are preserved and traceable. It seems highly unlikely that all of the expected shorelines would have been erased in the areas surrounding the two lakes since shorelines are not greatly eroded from the other locations. Austin et al. (2020) cannot claim that the rocks were too soft to retain shorelines, since glacial Lake Missoula cut shorelines into both hard and soft rocks, and that those shorelines were preserved (Oard, 2004).

Even if the presumed lakes existed for as little as 10–20 years, lake shoreline terraces should have formed, and still be visible, marking the perimeter of the lakes (Clarey, 2020a). Clarey (2020a) quoted John Wyatt, who spent 40 years building hydroelectric plants. Wyatt commonly observed wave cut terraces forming around the margins of new reservoirs in just a few days or weeks as the lakes reached a relatively stable level. However, we see no terraces around the perimeters of either Hopi or Canyonlands Lakes as drawn.

Figure 12. Lake Bonneville shoreline at base of mountains north of Salt Lake City, Utah.

Figure 13. Mammoth Hot Spring travertine from Yellowstone Park, Wyoming.

Austin et al. (2020) point to what Austin claims is a shoreline tufa deposit near Cape Solitude as evidence of Lake Hopi. Tufa is, "A variety of travertine that is commonly spongy or porous due to precipitation around a variety of floral strictures, such as reeds, plants, roots, leaves, etc." (Neuendorf et al., 2005, p. 688). Tufa is considered to have been deposited in water at ambient temperatures and can be deposited on other objects besides plants, while travertine is denser and believed to have been deposited by hydrothermal or warm water with rapid CO_2 degassing (Figure 13) (Felton et al., 2006). A good location for the study of tufa is Mono Lake, California, and it occurs around the shorelines of pluvial lakes in the Great Basin.

Austin was looking for silt and limestone on the east side of Kaibab uplift, which he considered to be the "smoking gun" for the dam-breach hypothesis with Hopi Lake at an elevation of about 1,830 m (6,000 ft.) asl. He does not tell us how silt and limestone would be a smoking gun. Austin noted a 1.5-m (5-ft.) thick deposit of calcium carbonate near Cape Solitude just east of Grand Canyon according to Scarborough and Hereford that "appears" to be a lake deposit, namely tufa. Limestone and other fine-grained sediment were also found elsewhere on the Marble Platform. That these limestones represent a shoreline of Hopi Lake is an unsubstantiated claim. Austin must show that the limestone is really a tufa; whether it is continuous at the same elevation, not from an ancient spring; and that it compares with tufa deposited at Mono Lake and Great Basin pluvial lakes.

The main factors for tufa precipitation include water agitation:

> Shore-zone lacustrine calcium carbonate deposition is a function of water temperature, clastic input, calcium concentration of the water body, and local water pH, all of which are influenced by biological facts and *water agitation* [emphasis mine] (Felton et al., 2006, p. 384).

Outgassing of CO_2 must occur, which can be caused by wave agitation, as expected along shorelines. However, fast currents and turbulence may also cause degassing of CO_2 in carbonate-rich water. Thick travertine speleothems, including dripstone, in caves is more rapidly deposited in fast currents with turbulence (Dreybrodt, 1988). Travertine is reported from upper Triassic sedimentary rock, interpreted as lacustrine (Leslie et al., 1992). Tufa is claimed from Lower Jurassic carbonate deposits within the Navajo Sandstone of the western United States (Totman-Parrish et al., 2017). The vast majority of Flood geologists would place these two occurrences in the Flood. So, tufa, or the interpretation of a tufa, is not necessarily a positive indicator of a shoreline, and could form during the Flood. Austin needs to show that tufa cannot form during the Flood.

A Fourth Problem—Lack of Coarse Deposits West of Grand Canyon

There are many other problems with the dam-breach hypothesis (Oard, 2010, 2016a). I will amplify one of these that I believe is also fatal: the lack of coarse-grained delta deposits at the mouth of the Grand Canyon. As shown by Austin et al. (2020), during the breach of pluvial Lake Manix, a large delta up to 55 m (180 ft.) thick was deposited just downstream of Afton Canyon. The delta thins eastward (Meek, 1989). If 4,100 km^3 (1,000 mi^3) of sedimentary rock was eroded from Grand Canyon, a huge delta should have formed at the mouth of the Grand Canyon, with thick, coarse sediments (boulders and cobbles) west of the Grand Wash Cliff and fining downstream sediments toward the Gulf of California. The delta should exist whether or not the water turned south toward the Gulf of California or continuing west/southwest toward the Pacific Ocean to be deposited in the Los Angelis Basin or the Anza Borrego Desert. This latter scenario assumes no significant ridges and mountains would block or divert the flow and that mountains and ridges rose after the dam breach. There is no delta west of the Grand Wash Cliffs (Hill and Polyak, 2020).

Austin (1994, p. 102) has pointed to fine-grained sediments, well downstream in the Imperial Formation west of the Salton Sea. The Imperial Formation is some 400 km (250 mi.) from the mouth of the Grand Canyon. There should be a generally continuous or at least contiguous sheet of fine-grained sediments from the mouth of the Grand Canyon to the Imperial Formation. But the sediments of the Imperial Formations could easily have been deposited during Flood runoff into deep basins and valleys. Regardless, thick, coarse sediments near the mouth of the Grand Canyon are *missing*, so the expected sediments from a dam breach and associated canyon erosion are not present.

The Bidahochi Formation

The claim for the existence of a post-Flood Lake Hopi seems to revolve around how one interprets the three members of the Bidahochi Formation (Figure 4). Many geologists claim that the Bidahochi Formation is weak evidence for such a lake (Love, 1989; White, 1990; Dickinson, 2013). The lowest of the three members of this formation has been considered lacustrine or from a playa lake, while the middle member is volcanic and the upper member, fluvial. Austin et al. (2020) see lacustrine sediments in the upper member, which Douglass et al. (2020) show was deposited up to 2,250 m (7,380 ft.) asl. Austin et al. (2020) point to the following as evidence that a post-Flood lake deposited some of the upper member of the Bidahochi Fm:

- tufa deposits and limestone
- 300 volcanic maar craters, at least one having an ejecta ring
- a high strontium isotope ratio
- fossils of fish, lake and pond-dwelling snails, frog, toads, bird tracks, and beavers

Tufa has already been mentioned. As discussed above, it is equivocal in defining a shoreline. "A maar is a low-relief, broad volcanic crater formed by multiple shallow explosive eruptions" (Neuendorf et al., 2005, p. 386). Austin et al (2020) interpret these maars and the surrounding sediments as formed within the sediments of a lake bottom in standing water. If there was a current toward the west, ejecta rings around the maars would be destroyed. As evidence that the lake was large, Austin et al. (2020) emphasize the fish fossils in the Bidahochi Formation. The fish fossils are not found in the Los Angeles Basin but have a striking similarity with those in the Pliocene of the Snake River of southern Idaho, presumably from "Lake Idaho." Let's examine these arguments.

The Upper Member Mostly Deposited by Moving Water

Despite Austin et al. (2020) and Douglass et al. (2020) interpreting the upper member as being lake sediments, most geologists have described this member as "fluvial" sediments. The uniformitarian emphasis on a fluvial environment may mean the upper member has numerous cross-beds with only local fine-grained sediments, interpreted as lacustrine (see Austin et al. (2020), Figure 20). Austin et al. (2020) do mention cross-bedded sandstones, but they think these local. Uniformitarian scientists automatically consider cross-bedded sandstone, along with rounded conglomerate and other water-laid features, as "fluvial," since they view all the rocks and fossils through the lens of uniformitarianism. So, "fluvial" would predominantly mean laid down by moving water, which could suggest Flood deposition. In one of Austin et al.'s (2020) references for a lake environment, White (1990, p. 45) actually says that the upper member is "*characterized* by quartzose sandstones deposited in a southwesterly flowing fluvial system (emphasis mine)." I would take this quote to mean that the upper member overwhelmingly shows sediments laid down in moving water.

What About the Maars?

Austin et al. (2020) make a point that the maars would have erupted in the lake floor sediments, where there were few, if any, currents to spread ejecta. There are a variety of other possibilities. Eruptions could have occurred during the Flood, underneath the Floodwater. This would get back to the stratigraphic end-of-Flood debate (Oard, 2016b, 2017a,b, 2018b, 2019; Clarey, 2017, 2020b; Clarey and Werner, 2019). Also, water may have been ponded or slow-moving during Flood runoff during the uplift of the Kaibab Plateau. This probably happened in many basins or valleys in the mountainous west during late-Flood uplift. Such tectonism would likely have resulted in local and briefly ponded or slow-moving water, such as around Maudlow, Montana. Uplift of the Horseshoe Hills to the west resulted in slow-moving water with gravel bars 60 m (200 ft.) high deposited where fast-moving water that created three water gaps to the east slowed in the ponded water (Oard, 2018a).

What About the High Strontium Isotope Ratio?

Austin et al (2020) claim a high strontium isotope ratio ($^{87}Sr/^{86}Sr$) of the Bidahochi Formation is not the seawater ratio, but that of adjacent streams. The ratio for the upper member is about 0.7102 (Douglass et al., 2020) while the ratio for seawater is 0.7091. Douglass et al (2020, p. 10) interpret this high ratio as coming, not from local streams, but from "the exotic surface water sourced from ancestral upper Colorado River watershed." The modern river waters on the Colorado Plateau are comparable to the strontium isotope ratio of the Bidahochi Formation (Dickenson, 2013). The high strontium isotope ratio of the upper Bidahochi Formation does not seem significant, since it comes from the upper Colorado River watershed, which can easily be explained by Flood runoff from the north and east of the Bidahochi Formation.

Freshwater Fossils

Austin et al. (2020) point out that the fossils found in the Bidahochi Formation are what would be expected in a post-Flood lake and that many of them are still found on the Colorado Plateau and other areas of the western United States. These transported fossils could have been spread during the drainage of the Floodwater from what had been a terrestrial pre-Flood environment, similar to other terrestrial fossils that are sometimes mixed with marine organisms (Clarey, 2019). Very similar fish fossils associated with "Lake Idaho" would also have been deposited in the Recessive Stage of the Flood.

I twice looked for evidence of Lake Idaho with Brent Carter, who advocated a Pliocene lake. Other than fine-grained sediments or sedimentary rocks along the Snake River in a few locations, I did not see any significant evidence for such a post-Flood lake. There were no shorelines and no breached lava dam at the entrance to Hells Canyon, as Carter thought. Features considered as positive evidence for the lake, such as oolites or pisolites, are equivocal and could have formed in the Flood. They are found in rocks of all uniformitarian ages (Pettijohn, 1975, pp. 83–87).

Bird Tracks

Bird tracks occur in the Bidahochi Formation (Breed, 1973). One would normally expect tracks of vertebrates during the Flooding Stage (Walker, 1994). So, maybe the Bidahochi Formation was deposited during the Flooding Stage, especially in view of the average 2,500–5,000 m (8,200–16,400 ft.) of erosion of the whole Colorado Plateau, including the Grand Canyon area (Schmidt, 1989). This erosion would be expected to occur during the Retreating Stage, leaving what is left behind from the Flooding Stage. It is also possible that birds and even some mammals, probably small mammals, could have survived on log mats for a while during the Recessive Stage of the Flood? Genesis 7:21–23 may refer to all air-breathing land animals being dead by Day 150. Or could these verses be a summary statement for the whole Flood? I would expect that the Bidahochi Formation was deposited during the Channelized Flow Phase—the last phase of the Flood, since it was deposited on the northern and eastern edge of a basin that probably had already formed. Further research into these issues is required.

Why is the Bidahochi Formation Mostly Above the "Shoreline"?

Austin et al. (2020) point out that we must be careful about using the current landscape to explain Flood runoff or a dam breach after the Flood. This is true, but we need evidence of post-Flood topographical changes. Otherwise, we can willy-nilly postulate a change in topography to support our hypothesis. So, it is possible that the Bidahochi Formation was faulted upward or raised by monoclinal uplift, but the question remains: is there any evidence of a significant uplift of the area? I doubt it, and it is up to Austin et al. (2020) to demonstrate such uplift.

Uniformitarian advocates of the dam-breach hypothesis do not appeal to the subsequent uplift of the Bidahochi Formation, but instead believe Lake Hopi rose to 2,250 m (7,400 ft.) based on the highest outcrop of the formation (Douglass et al., 2020). Such a lake would allow the breach to occur near the minimum elevation of 2,285 m (7,500 ft.) through the Kaibab Plateau. However, they need the low point across the Coconino Plateau, currently at 1,975 m (6,500 ft.) to be raised to 2,290 m (7,510 ft.) while the elevation at Grandview Point at 2,285 (7,500 ft.) remained the same (Douglass et al., 2020). This allowed the spillover point to occur at

Grandview Point. This scenario seems *ad hoc*.

To keep the water from spilling southwest down the current topographic slope and taking a northwest route along the same elevation, Douglass et al. (2020) propose a "half-circular cuesta scarp" that directed the spillover water to flow west and then northwest around the southern end of the Kaibab Plateau. Where is the evidence of such a pre-existing half-circular channel?

Another possibility for raising the Bidahochi Formation is isostatic rebound after Hopi Lake emptied. An analog would be pluvial Lake Bonneville. The isostatic rebound of Lake Bonneville, where scientists first discovered isostasy, has been about 80 m in the deepest part of the former lake, which was 300 m (1,000 ft.) deep (Austermann et al., 2020). Little rebound took place along the edge of the lake. Thus, the Bidahochi Formation, at the edge (and above) Lake Hopi, should not have been uplifted significantly by isostatic rebound.

The Mammal Problem in the Bidahochi Formation

Austin et al. (2020) only mention beaver mammal fossils in the Bidahochi Formation. However, there are also saber-toothed tiger, camel, antelope, rhino, and gomphothere fossils (Douglass et al., 2020). If the Flood ended at the end of the Cretaceous (Austin et al., 1994), mammals would have had to leave the "mountains of Ararat," multiply, spread, across the Bering Land Bridge, increase into the millions, die, and be buried in the top layer of sediments along the high Great Plains and in the mountain valleys and basins of the western United States.

How likely is this in the time available, especially since Austin et al (2020) believe the dam breach occurred only 10 to 20 years after the Flood? Migrating over the Bering Land Bridge early in the Ice Age soon after the Flood would have been feasible, since winters then would have been mild and a land bridge tectonically raised (Oard, 2020), but the rest is far-fetched. Furthermore, there is evidence that the mammal fossils in the top layer of the High Plains were buried (or re-buried) during Flood runoff (Oard, 2014b).

These mammals represent a significant diversification, as shown by Cenozoic fossils. This much diversity is unlikely soon after or any time after the Flood. Then there is the issue of the order of appearance and disappearance of numerous mammals at various times within the Cenozoic—*all over the world at the same time*, if the fossil order from the geological column is assumed to be a worldwide sequence. For instance, brontotheres are like rhinoceroses but with unique horns (Figure 14). They show up in the late Paleocene and go extinct at the very end of the Eocene. In addition, the end-Cretaceous position must address the evidence that very few mammal fossils would have been buried and fossilized during the Flood in the Mesozoic, but many millions of them would have been buried and fossilized *after* the Flood.

There are more than 35 evidences that the Flood/post-Flood boundary is in the late Cenozoic, often in the very late Cenozoic around the Pliocene/Pleistocene boundary (Oard, 2016b, 2017a,b, 2018b, 2019; Clarey, 2017, 2020b; Baumgardner, 2018, pers comm.; Clarey and Werner, 2019). A very late Cenozoic end-Flood time would imply that the Grand Canyon was formed by late-Flood channelized erosion (Oard, 2010, 2016a).

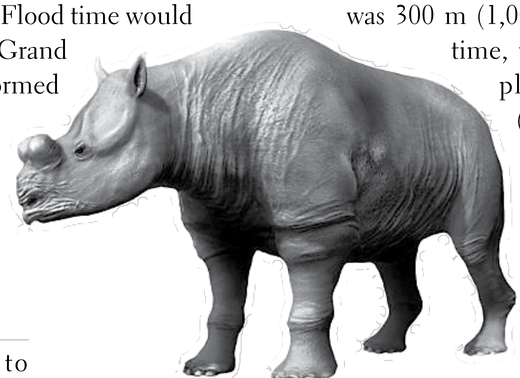

Figure 14. A brontothere, *Protitanops curryi* (Nobu Tamura, Wikipedia commons CC-BY-SA-4.0).

The Breach

In addition to all of these problems with the dam-breach hypothesis, there are questions about the actual event. When Holroyd (1994, pp. 243–254) first proposed water in the current basins northeast and southeast of Grand Canyon, he had Canyonlands Lake level at 1,700 m (5,577 ft.) asl (Figure 6 in Austin et al., 2020, p. 162). At this altitude, the lake would have been banked up to the pass on the northern Kaibab Plateau. Any higher, it would have spilled over the pass 32 km (20 mi.) east of Kanab, Utah. But Austin et al. (2020) propose a lake at 1,940 m (6,400 ft.) asl, held back by a rock dam east of Lees Ferry. This would keep the water from spilling over the pass on the northern Kaibab Plateau, assuming the same topography. However, Austin et al. (2020) claim this pass was 300 m (1,000 ft.) higher with the southern part of the Kaibab Plateau 300 m (1,000 ft.) lower.

Austin et al. (2020) say the breach occurred after the "higher" Canyonlands Lake spilled into the lower Lake Hopi; the currents producing the "fluvial" sediments of the Bidahochi and raising the level of Hopi Lake about 90 m (300 ft.). Hopi Lake then breached over the southern slope of the Kaibab Plateau at about 1,900 m (6,234 ft.) asl, significantly lower than advocated by Douglass et al. (2020). Today, the lowest point across the Kaibab Plateau on the south rim of the Grand Canyon is about 2,285 m (7,500 ft.) asl. Austin et al. (2020) then claim that the southern Kaibab Plateau was 300 m (1,000 ft.) lower at this time, while the northern plateau was 300 m (1,000 ft.) higher. It is as if the central part of the Kaibab Plateau was a fulcrum. This is supposed to account for the canyon being eroded at intermediate altitudes across the Kaibab Plateau. However, it needs to be demonstrated that such tectonic changes occurred after the Flood.

According to Austin et al. (2020), Lake Hopi then spilled into a "trough" west of the Kaibab Plateau forming "Lake Toroweap" that backwashed north onto the Kanab Plateau, west of the Kaibab Plateau, and south into the southwest Coconino Plateau (Austin et al., 2020, Figure 4, p. 156). Subsequently, Lake Toroweap breached west with the draining of the north and south plateaus carving the deep Kanab and Havasu Creek valleys, respectively, at the same time the western Grand Canyon was carved.

Conclusion

Uniformitarian scientists have made little progress in 150 years in attempting to explain the origin of the Grand Canyon. Hill and Polyak (2020) promote another hypothesis, while holding to some recent research on paleocanyons, an "Arizona river," etc. Their unlikely solution is piping underneath the Kaibab Plateau. The failure of uniformitarian scientists indicates that they are operating under the wrong paradigm; a catastrophic solution is more likely.

Any catastrophic solution requires immense volumes of moving water. Austin et al. (2020) think such water can be found in two post-Flood lakes and an abrupt dam breach. First, I answered several claims by Austin et al. (2020). The dam-breach hypothesis has numerous problems, four I consider major: (1) the lack of bottom sediments; (2) the origin of the long, deep tributary valleys; (3) the lack of wave-cut shorelines; and (4) the lack of a cobble and boulder delta at the mouth of the Grand Canyon. Austin et al. (2020) claim the lake bottom sediments are found in the Bidahochi Formation, but these are well above the top of the lake. Features found at other paleolakes, such as glacial Lake Missoula, and pluvial lakes of the Great Basin, are not present here. Bottom sediments that should have collected in the deepest part of the lake, such as from Cameron to Holbrook in association with Lake Hopi, and therefore preserved, are missing. It does not matter what the claims are for the Bidahochi Formation.

The challenging features of the Grand Canyon appear to be better explained by late channelized Flood runoff, especially since it easily accounts for the thousands of other water gaps across the Earth (Oard, 2020, 2016a).

Acknowledgements

I thank two anonymous reviewers for significantly improving the manuscript. I also appreciate my wife, Beverly, for editing the English.

References

Aslan, A., K.E. Karlstrom, E. Kirby, M.T. Heizler, D.E. Granger, J.K. Feathers, P.R. Hanson, and S.A. Mahan. 2019. Resolving time-space histories of Late Cenozoic bedrock incision along the Upper Colorado River, USA. *Geomorphology* 347: 106855) [26 pages].

Austermann, J., C.Y. Chen, H.C.P. Lau, A.C. Maloff, and K. Latychev. 2020. Constraints on mantle viscosity and Laurentide ice sheet evolution from pluvial paleolake shorelines in the western United States. *Earth and Planetary Science Letters* 532: 116006 [14 pages].

Austin, S.A. 1994. How was Grand Canyon eroded? In: Austin, S.A. (editor). *Grand Canyon—Monument to Catastrophism*, Institute for Creation Research, Santee, CA.

Austin, S.A., E.W. Holroyd III, and D.R. McQueen. 2020. Remembering spillover erosion of Grand Canyon. *Answers Research Journal* 13:153–188.

Bartis, J.T., T. LaTourrette, L. Dixon, D. Peterson, and G. Cecchine. 2005. RAND Corporation oil shale development in the United States prospects and policy issues. MG-414- NETL.

Berardelli, P. 2008. Did dinosaurs gawk at the Grand Canyon? (April 13) News. sciencemag.org.

Blackwelder, E. 1934. Origin of the Colorado River. *Geological Society of America Bulletin* 45(3): 551–566.

Breed, W.J. 1973. New avian fossils from the Bidahochi Formation (Pliocene), Arizona. In: Fassed, J. (editor). *Cretaceous and Tertiary Rocks of the Southern Colorado Plateau: A Memoir*. Four Corners Geological Society, Durango, CO, pp. 144–147.

Brown, W. 2008. *In the Beginning: Compelling Evidence for Creation and the Flood*. Center for Scientific Creation, Phoenix, AZ.

Clarey, T.L. 2017. Local catastrophes or receding Floodwater? Global geologic data that refute a K-Pg (K-T) Flood/post-Flood boundary. *Creation Research Society Quarterly* 54(2): 100–120.

Clarey, T.L. 2020a. Lava flows disqualify lake spillover Canyon theory. *Acts & Facts* 49(10): 10–12.

Clarey, T.L. 2020b. *Carved in Stone: Geological Evidence of the Worldwide Flood*. Institute for Creation Research, Dallas, TX.

Clarey, T.L., and D.J. Werner. 2019. Compelling evidence for an Upper Cenozoic Flood/post-Flood boundary: Paleogene and Neogene marine strata that completely surround Turkey. *Creation Research Society Quarterly* 56(2): 68–75.

Dickinson, W.R. 2013. Rejection of the lake spillover model for initial incision of the Grand Canyon and discussion of alternatives. *Geosphere* 9(1): 1–20.

Douglass J.C., B.F. Gootee, T. Dallagge, A. Jeong, Y.B. Seong, and B.Y. Yu. 2020. Evidence for the overflow origin of the Grand Canyon. *Geomorphology* 369: 107361 [19 pages].

Dreybrodt, W. 1988. *Processes in Karst Systems: Physics, Chemistry, and Geology*, Springer-Verlag, New York, NY.

Emanuel, K.A., K. Speer, R. Rotunno, R. Srivastava, and M. Molina. 1995. Hypercanes: A possible link in global extinction scenarios. *Journal of Geophysical Research* 100(D7): 13755–13765.

Eyles, N., H.T. Mullins, and A.C. Hine.

1991. The seismic stratigraphy of Okanagan Lake, British Columbia: A record of rapid deglaciation in a deep 'fiord-like' basin. *Sedimentary Geology* 73(1–2): 13–41.

Felton, A., P.W. Jewell, M. Chan, and D. Currey. 2006. Controls of tufa development in Pleistocene Lake Bonneville, Utah. *The Journal of Geology* 114(3): 377–389.

Hill, C.A., G. Davidson, T. Helble, W. Ranney, and K. Wolgemuth (editors). 2016. *The Grand Canyon: Monument to an Ancient Earth—Can Noah's Flood Explain the Grand Canyon?* Kregel Publications, Grand Rapids, MI.

Hill, C.A., N. Eberz, and R.H. Buecher. 2008. A karst connection model for Grand Canyon, Arizona, USA. *Geomorphology* 95(3–4): 316–334.

Hill, C.A. and V.J. Polyak. 2020. A karst hydrology model for the geomorphic evolution of Grand Canyon. *Earth-Science Reviews* 208: 103279 [27 pages].

Holroyd, III, E.W. 1994. A remote sensing search for extinct lake shore lines on the Colorado Plateau. In: Walsh, R.E. (editor). *Proceedings of the Third International Conference on Creationism* (technical symposium sessions). Creation Science Fellowship, Pittsburg, PA. pp. 243–254.

Howard, K.A., S.C. Lundstrom, D.V. Malmon, and S.J. Hook. 2008. Age, distribution, and formation of late Cenozoic paleovalleys of the Lower Colorado River and their relation to river aggradation and degradation. In: Reheis, M.C., R. Hershler, and D.M. Miller (editors). *Late Cenozoic Drainage History of the Southwestern Great Basin and Lower Colorado River Region: Geologic and Biotic Perspectives* (GSA Special Paper), Volume 439, Geological Society of America, Boulder, CO, pp. 391–410.

Karlstrom, K.E., R.S. Crow, L. Peters, W. McIntosh, J. Raucci, L.J. Crossey, P. Umhoefer, and N. Dunbar. 2007. $^{40}Ar/^{39}Ar$ and field studies of Quaternary basalts in Grand Canyon and model for carving Grand Canyon: Quantifying the interaction of river incision and normal faulting across the western edge of the Colorado Plateau. *Geological Society of America Bulletin* 119(1): 283–312.

Karlstorm, K.E., R. Crow, L.J. Crossey, D. Coblentz, and J.W. Van Wijk. 2008. Model for tectonically driven incision of the younger than 6 Ma Grand Canyon. *Geology* 36(11): 835–838.

Larson, P.H., N. Meek, J. Douglass, R.I. Dorn, and Y.B. Seong. 2017. How rivers get across mountains: Transverse drainage. *Annals of the American Association of Geographers* 107(2): 274–283.

Longwell, C.R. 1946. How old is the Colorado river? *American Journal of Science* 244(12): 817–835.

Lucchitta, I., and R. Holm. 2019. Reevaluation of exotic gravel and inverted topography at Crooked Ridge, northern Arizona: Relicts of an ancient river of regional extent. *Geosphere* 16(2): 533–545.

Lucchitta, I., R.F. Holm, and B.K. Lucchitta. 2013. Implications of the Miocene (?) Crooked Ridge River of northern Arizona for the evolution of the Colorado River and Grand Canyon. *Geosphere* 9(6): 1417–1433.

Meek, N. 1989. Geomorphic and hydrologic implications of the rapid incision of Afton Canyon, Mojave Desert, California. *Geology* 17(1):7–10.

Neuendorf, K.K., J.P. Mehl, Jr., and J.A. Jackson. 2005. *Glossary of Geology*, Fifth edition. American Geological Institute, Alexandria, VA.

Newberry, J.S. 1861. *Report Upon the Colorado River of the West*, Part III. U.S. Government Printing Office, Washington, D.C.

Newberry, J.S. 1862. Colorado River of the West. *American Journal of Science and Arts* (2nd Series) 33:387–403.

Oard, M.J. 2004. *The Missoula Flood Controversy and the Genesis Flood*. Creation Research Society, Chino Valley, AZ.

Oard, M.J. 2008. *Flood by Design: Receding Water Shapes the Earth's Surface*. Master Books, Green Forest, AR.

Oard, M. J. 2009. How old is Grand Canyon? *Journal of Creation* 23(2): 17–24.

Oard, M.J. 2010a. The origin of Grand Canyon Part I: Uniformitarian fails to explain Grand Canyon. *Creation Research Society Quarterly* 46(3): 185–200.

Oard, M.J. 2010b. The origin of Grand Canyon Part II: Fatal problems with the dam-breach hypothesis. *Creation Research Society Quarterly* 46(4): 290–307.

Oard, M.J. 2010c. The origin of Grand Canyon Part III: A geomorphological problem. *Creation Research Society Quarterly* 47(1): 45–57.

Oard, M.J. 2010d. The origin of Grand Canyon Part IV: The great denudation. *Creation Research Society Quarterly* 47(1): 146–157.

Oard, M.J. 2011. The origin of Grand Canyon Part V: Carved by late-Flood channelized erosion. *Creation Research Society Quarterly* 47(4): 271–282.

Oard, M.J. (ebook). 2013. *Earth's Surface Shaped by Genesis Flood Runoff*; http://Michael.oards.net/GenesisFloodRunoff.htm.

Oard, M.J. 2014a. Controversy over the uniformitarian age of Grand Canyon. *Journal of Creation* 28(2): 17–22.

Oard, M.J. 2014b. Relating the Lava Creek ash to the post-Flood boundary. *Journal of Creation* 28(1): 104–113.

Oard, M.J. 2014c. *The Great Missoula Flood: Modern Day Evidence for the Worldwide Flood*. Awesome Science Media, Richfield, WA.

Oard, M.J. 2016a. *A Grand Origin for Grand Canyon*. Creation Research Society, Chino Valley, AZ.

Oard, M.J. 2016b. Flood processes into the late Cenozoic: part 2—sedimentary rock evidence. *Journal of Creation* 30(2): 67–75.

Oard, M.J. 2017a. Flood processes into the late Cenozoic: part 3—organic evidence. *Journal of Creation* 31(1): 51–57.

Oard, M.J. 2017b. Flood processes into the late Cenozoic: part 4—tectonic evidence. *Journal of Creation* 31(1): 58–65.

Oard, M.J. 2018a. Genesis Flood drainage through Southwest Montana: Part III: Water gaps. *Creation Research Society Quarterly* 55(2): 81–97.

Oard, M.J. 2018b. Flood processes into the late Cenozoic: part 5—geomorphological evidence. *Journal of Creation* 32(2): 70–78.

Oard, M.J. 2019. Flood processes into the late Cenozoic: part 6—climatic and other evidence. *Journal of Creation* 33(1): 63–70.

Oard, M.J. 2020. Land bridges after the Flood. *Journal of Creation* 34(3): 109–117.

Oard, M.J., and P. Klevberg. 2008. The Green River Formation very likely did not form in a postdiluvial lake. *Answers Research Journal* 1: 99–108.

Oard, M.J., and J.K. Reed. 2019. What uniformitarian interpretations should creation scientists accept? *Creation Matters* 24(4): 4–7.

Perron, J.T., P.R. Richardson, K.L. Ferrier, and M. Lapôtre. 2012. The root of branching river networks. *Nature* 492(7427): 100–103.

Pettijohn, F.J. 1975. *Sedimentary Rocks*, Third edition. Harper and Row, New York, NY.

Sabbeth, L., B.P. Wernicke, T.D. Raub, J.A. Grover, E.B. Lander, and J.L. Kirschvink. 2019. Grand Canyon provenance for orthoquartzite clasts in the lower Miocene of coastal southern California. *Geosphere* 15(6): 1973–1998.

Scheele, P. 2010. A receding Flood scenario for the origin of the Grand Canyon. *Journal of Creation* 24(3): 106–116.

Schmidt, K.-H. 1989. The significance of scarp retreat for Cenozoic landform evolution on the Colorado Plateau, U.S.A. *Earth Surface Processes and Landforms* 14(2): 93–105.

Shoemaker, E.M., C.H. Roach, and F.M. Byers, Jr. 1962. Diatremes and uranium deposits in the Hopi Buttes, Arizona. In: Engel, A.E.J., H.L. James, and B.F. Leonard (editors). Petrologic Studies: A volume in honor A.F. Buddington. (*Arizona Geological Survey*) Geological Society of America, pp. 327–355.

Vail, T. (editor). 2003. *Grand Canyon: A Different View*. Master Books, Green Forest, AR.

Walker, T. 1994. A Biblical geological model. In: Walsh, R.E. (editor). *Proceedings of the Third International Conference on Creationism*, technical symposium sessions, Creation Science Fellowship, Pittsburgh, PA, pp. 581–592; biblicalgeology.net/.

Wernicke, B. 2011. The California River and its role in carving Grand Canyon. *Geological Society of America Bulletin* 123(7/8): 1288–1316.

Whitcomb, Jr., J.C. and H.M. Morris. 1961. *The Genesis Flood: The Biblical Record and Its Scientific Implications*. Baker Book House, Grand Rapids, MI.

White, J.D.L. 1990. Depositional architecture of a maar-pitted playa: Sedimentation in the Hopi Buttes volcanic field, northeastern Arizona, U.S.A. *Sedimentary Geology* 67(1–2): 55–84.

Woodmorappe, J. 2016. The Grand Canyon in the thralls of shallow, doctrinaire uniformitarianism. Review of *The Grand Canyon: Monument to an Ancient Earth* by Hill et al, (editors). *Journal of Creation* 30(3): 17–21.

Creation Research Society Quarterly 2021 57:223–233

The *Tôlĕdôt* Structure of Genesis

Michael A. Harbin*

Abstract

For the past couple of centuries, critical scholars have argued that the differences between Genesis 1 and 2 indicate that they are from two different sources which are contradictory. Those who understand that the biblical accounts actually describe God's creation of the cosmos see them as complementary, but still have encountered issues with regard to how they fit together. This study argues that a critical factor is the transition verse of Gen 2:4 hinging on the key Hebrew word ***tôlĕdôt***, a term which has been difficult to translate. Drawing on the increasingly accepted understanding that the term is part of a technical phrase which should be understood as "this is what became of" as well as the generally accepted observation that this phrase serves as a structural indicator for the entire book, the study proposes that the initial creation account is a preface to the overall book. It then demonstrates that by showing how the phrase ties together the various sections of the book demonstrate sequentially what became of the creation which God proclaimed as very good (Gen 1:21). As such it provided a critical foundation for the embryo nation of Israel at Mt. Sinai where Moses shared God's revelation that the people had been called for a purpose, which would ultimately lead to redemption of the entire world. Seeing the book as a carefully crafted unit built on the ***tôlĕdôt*** phrase highlights the importance of the creation account preface not only to explain origins to us as well as the nation of Israel, but the nature of the world in which we live.

In the past few decades, OT scholars have increasingly agreed with John Skinner's observation that Genesis seems to be organized around the Hebrew phrase *'ēlle tôlĕdôt*. This combination is used eleven times at key transition points through the entire book (Skinner, 1930, lxvi). While this structure is gaining wide acceptance, what the phrase means and its significance is debated (DeRouchie, 2013; Mathews, 1996; Ross, 1988). The phrase consists of the noun *tôlĕdôt* combined with the particle *'ēlle* which means "these are." The crux of the discussion is the meaning of *tôlĕdôt*.

The Meaning of *Tôlĕdôt*

The noun *tôlĕdôt* is understood to be derived from the Hebrew verb *yālad* which means "to give birth, to beget, to bear, to bring forth, or to beget" (*BDB*, 1977; Clines, 2011; Hoogendyk, 2017; Koehler and Baumgartner, 1958; Schreiner, 2006). Unsurprisingly then the traditional English translation has been "generations," which in the phrase *'ēlle tôlĕdôt* might be translated literally as "these are the generations," the transla-

* Michael A. Harbin, Upland, IN
Accepted for publication March 13, 2021

tion the KJV consistently uses. In some cases this phrase precedes a genealogy so that translation makes excellent sense. For example, Gen 5:1 in the KJV begins: "This *is* the book of the generations of Adam" (italics in original). Although this is not the usual Hebrew term for "generation" (Mathews, 1996) it does begin a genealogy of Adam tracing his lineage down to Noah. Similarly, in the KJV, Gen 11:10 begins "These *are* the generations of Shem" (italics in original). The genealogy which follows traces Shem's descendants to Terah and his three sons, Abram, Nahor, and Haran.

However, in most cases where Genesis uses *'ēlle tôlĕdôt*, this translation is awkward at best. For example, in the KJV, RSV, and ESV, Gen 6:9 reads "These are the generations of Noah," while the NRSV provides "These are the descendants of Noah." The next sentence declares that Noah was righteous, blameless, and walked with God, and then simply declares that "Noah had three sons, Shem, Ham, and Japheth." But rather than continue with subsequent generations, the text switches to note how corrupt the earth had become. The remainder of this *tôlĕdôt* section (chapters 6–9) describes how God brought judgment on the corrupt (a word repeated three times in Gen 6:11–12) earth through an extensive flood judgment. Noah's genealogy is not listed until the next section (Gen 10:1–11:9) where it is not part of his *tôlĕdôt*, but is described as the *tôlĕdôt* of his three sons of Shem, Ham, and Japheth. For this reason, the NASB translates 6:9 as "These are *the records* of the generations of Noah" (italics in original) and the NIV gives "This is the account of Noah."

Drawing from the conclusion that the term seems to indicate transitions in structure, along with the observation that the premise that context determines meaning, in recent years a number of scholars have proposed a different translation of the word *tôlĕdôt* when used in the phrase *'ēlle tôlĕdôt*. Ross explains that: "The *tôlĕdôt* heading announces the historical development from the ancestor (or beginning point)…" (Ross, 1988, 72). As a noun, a good translation of the word *tôlĕdôt* might then be "outcome." The question is, how would the phrase *'ēlle tôlĕdôt* ("literally these are the outcomes") fit in the context of entire book of Genesis where it would appear to be used in a consistent manner?

The Use *Tôlĕdôt* in Genesis

For most English readers the presence of the phrase *'ēlle tôlĕdôt* is not always clear, and even when understood, its role tends to be obscured. First, in several cases chapter divisions mask the apparent structural role of the phrase both in English translations and the original Hebrew. For example, Genesis 1 breaks the opening creation account at the end of day six of the seven day structure. The seventh day of the creation week is placed in verses 1–3 of Genesis 2. Then the first use of *'ēlle tôlĕdôt* in appears in 2:4. Most scholars observe that the use of this term in 2:4 introduces "a new stage of the book." But because the chapter division separates the seventh "day" of God's rest from the rest of the introductory creation account, it is easy to gloss over the significance of that transition.

Second, English translations tend to obscure how consistently this phrase is used. Because "generations" does not fit every context well, modern translators generally use various words in different places. Fields of meaning for analogous words vary from language to language so it is not unusual for individual words to require different translations within different contexts. For example, the Hebrew word *ben* literally means son, but its field of meaning expands to cover not only "son," but "grandson," "children generally," "descendants" or "people or items belonging in a category or group" (Martens, 1999, 254). However, embedding a given word into a specific phrase tends to restrict the field of meaning, especially when the phrase is used as a significant literary indicator (DeRouchie, 2013, 235). In this case, the use of the phrase *'ēlle tôlĕdôt* marks it as a structural indicator and thus suggests a specialized and consistent meaning. As such, following Ross, we would suggest this phrase demands a uniform translation proposing specifically: "this is what became of… ." This study will evaluate the merit of that proposal with respect to the book of Genesis.

Given the Documentary Hypothesis which proposed different sources for Pentateuch rather than Mosaic authorship, critical scholars following Skinner quickly suggested the phrase *'ēlle tôlĕdôt* was used by a redactor to piece Genesis together. Skinner himself understood it to be an introductory formula in P (to which he attributed Gen 2:4a) inserted by a later redactor (Skinner, 1930, 40–41). Von Rad also maintains that the term served as "a kind of chapter division in the Priestly document," added by a later redactor at this location for organizational purposes (von Rad, 1977, 63). This perception largely derived from presumed Mesopotamian background to the initial portions of Genesis. Seeing superficial similarities with the Mesopotamian flood and creation myths, they proposed them as sources (Heidel, 1951, 82–140; Kramer, 1972).

Drawing on the proposed Mesopotamian background, P.J. Wiseman proposed that the *'ēlle tôlĕdôt* statements served to identify documents that the redactor of Genesis used as sources. Wiseman supposes a common understanding of the word *tôlĕdôt* as "history, especially family history" (Wiseman, 1985, 62). He then argues that each section is a specific history of an individual or family and the name reflects either the subject or the owner of the history account. Given Abraham's Mesopotamian background, Wiseman then contends that these histories would have originally been written on clay tablets in cuneiform following cuneiform protocols that included a colophon or a brief description of the tablet written on an edge which allowed a scribe to readily find a tablet lying on a shelf. He concludes that each *tôlĕdôt* phrase in Genesis was originally a colophon which had been transcribed when the tablets were copied other media such as papyrus. Retained when the copies were combined into one document, they become in essence citations of the source of the information (Wiseman, 1985, 67–73).

Wiseman's overall view has not been widely accepted. However, the idea that the *'ēlle tôlĕdôt* sentences were colophons added to the end of an individual Hebrew account as a subscription to identify the material preceding it has been accepted by a number, generally among critical scholars. For example, Westermann divides Gen 2:4 and attaches the first half of the verse to the first creation account as a subscription. As such he sees Gen 1:1–2:4a as the first *tôlĕdôt* section (Westermann, 1984, 81–177). Speiser also views Gen 2:4a as a subscription, and translates it as "Such is the story of heaven and earth as they were created" (Speiser, 1962, 5). While Gunkel sees the term as a subscription he argues that in this case it was really a superscription moved to the present location by a later redactor (Gunkel, 1997, 103). The subscription view has its problems, however, and Friedman bluntly asserts that viewing this verse as the conclusion of the previous section "is wrong" and states that the purpose of the *'ēlle tôlĕdôt* phrase is "to construct the book as continuous narrative through history rather than as a loose collection of stories" (Friedman, 2001, 16), although he does not explain how it works in that regard.

In contrast, conservative scholars generally include the entire verse of Genesis 2:4 as part of the "second creation account" making the phrase a superscription (Ross, 1988, 71). Kidner maintains that it introduces "a new stage of the book" (Kidner, 1967, 59). Keil and Delitzsch state that Gen 2:4a "form[s] the heading to what follows" (Keil and Delitzsch, 1970, I:70). Cassuto notes "there are definite indications that it [Gen 2:4] is a unity, and also that the first half belongs to the story of the garden of Eden" (Cassuto, 1961, 97). Mathews argues that it is a heading which "introduces what was the aftermath of that creation" (Mathews, 1996, 189).

Mathews simply states that the colophon (and thus subscription) argument is not compelling (Mathews, 1996, 32). Ross explores the issue somewhat more and says that the "evidence from cuneiform is unconvincing and the outworking of the arrangement in Scripture is impossible" noting that nowhere in the Bible does the word *tôlĕdôt* "refer *clearly* to what has preceded" (Ross, 1988, 71–72, italics in original). It other words, it cannot be a summary of what occurred before, but must transition into subsequent developments.

Admittedly, each view has its problems. If the phrase is a subscription or summary, the final section (Gen 37:2–50:26) does not have one. Wiseman explains this by arguing that the writer of that section would have been Moses who would not have used a tablet for that material (he would have used papyrus), and thus would not have needed a colophon (Wiseman, 1985, 100). Moreover, there are several places where the idea of a summary would not make sense, such as Gen 25:19 which would have the *'ēlle tôlĕdôt* statement of Isaac summarizing the offspring of Ishamael, his half-brother. However, if the phrase is a superscription, the initial section does not have one. Castellino addresses this tension when he observes that Genesis 1 is a "real creation narrative," while Genesis 2 is "strictly an organizational text." (Castellino, 1994, 94). As a real creation narrative, there would be nothing before, which would explain why there is not one at the beginning.

Similarly, several more recent scholars have suggested that the initial section serves as a preface or introduction to further explain the superscription issue. DeRouchie has done excellent work in terms of the overall structure of the book showing how the *tôlĕdôt* sections provide a tight outline of the entire book and serve to narrow the focus from mankind in general to the line of Abraham. He sees the focal point as "the blessing-commission of Gen 1:28" (DeRouchie, 2013, 226). Hart ties the seven day structure of the initial section which describes God working and then resting with the declaration that man is created in God's image as a prologue to man's working in the rest of the book (Hart, 1995, 315–336). Ross sees the introduction focusing on creation setting the stage for "the destiny of the covenant people" (Ross, 1988, 88). However, there has been little work done in terms of the value of the proposed meaning of this structural indicator the *'ēlle tôlĕdôt* phrase.

'Ēlle Tôlĕdôt in Genesis 2:4

Probably the most significant anomaly both in terms of the subject matter and the way various translations and commentators handle the phrase *'ēlle tôlĕdôt* is its first use in the book. In the KJV, Gen 2:4 reads: "These *are* the generations of the heavens and of the earth when they were created…" (italics in original). Here "generations" seems at best a very figurative expression since the context is the creation of the cosmos, rather than any genealogical sequence (Waltke, 2001, 83). In other words, the material prior to the phrase describes the creation of the heavens and the earth in broad terms. The subsequent material appears to explain specific outsomes of that creation account. However, one must exercise caution here. While Tsumura observes that the two accounts "reflect essentially the same cosmology" (Tsumura, 1994, 28), as has

Table 1. Uses of *'ēlle tôlĕdôt* in Genesis.

	Text Covered	Subject	Topic
1	2:4-4:26	Heavens and Earth	"Second creation account" and the fall of man
2	5:1-6:8	Adam	Genealogy of Adam to Noah (plus introduction of Noah)
3	6:9-9:29	Noah	Flood account
4	10:1-11:9	Shem/Ham/Japheth	Table of nations
5	11:10-11:26	Shem	Genealogy of Shem to Terah
6	11:27-25:11	Terah	Account of Abraham
7	25:12-25:18	Ishmael	Sons of Ishmael
8	25:19-35:29	Isaac	Account of Jacob and Esau
9/10	36:1-37:1	Esau	Double genealogy of Esau (1 in Canaan, 2 in Seir)
11	37:2-50:26	Jacob	Joseph and his brothers

been well noted, the two accounts differ significantly. Consequently, translators struggle here using various terms such as "account" which are rather vague and do not satisfy. A key reason is that this *'ēlle tôlĕdôt* section does not stop with the creation material of chapter 2 which describes the creation of the Adam, Eve, and various animals that Adam named in the garden God planted, but continues on to include the fall of Adam and Eve, their expulsion from the garden, the murder of Abel, the exile of Cain and his genealogy. As such, the phrase is much more than a summary sentence of what occurred before, hence Ross's proposed translation.

If the proposed translation of the *'ēlle tôlĕdôt* phrase as "this is what became of" is valid, then it would seem that the initial portion of the book, the "first creation account" (Gen 1:1–2:3) really serves as a preface or introduction to the book which serves to define the situation (see Table 1). Specifically, it asserts that God is the Creator of the entire cosmos which is demonstrated by a very brief and extremely vague overview of the entire creation process where God *spoke* the universe into existence. Clearly it does not provide enough details to really satisfy us today, but then its purpose is simply to show that God is the Creator, and that the entire cosmos is His handiwork. Further, near the end of this account, we read in Gen 1:31 that when the creation was completed, God pronounced it "very good." Then in Gen 2:2–3 we are told how at this point the creation was complete. Today we look at this completed creation and puzzle because in many respects the world in which we live does not seem all that good. Moreover, although this account maintains that mankind was given responsibility to manage that creation, it seems that every time we turn around mankind is messing it up, making it worse and worse. How do we put this together?

This is where understanding both the *'ēlle tôlĕdôt* structure and its meaning helps. If Gen 1:1–2:3 is intended as a preface, then the weight of the entire book is really on what happened afterwards. In other words, while the author begins with a premise that the good creator God produced a cosmos that was not only good, but very good, his main concern is what happened to it. As such, the intent of the first section introduced by *'ēlle tôlĕdôt* (Gen 2:4–4:26) is not to recapitulate the creation of the cosmos, nor even the creation of mankind in God's image, but rather to explain what happened to them, ultimately providing a coherent background for the existence and purpose of the nation of Israel as given by Moses at Sinai (Harbin, 2005, 44–46). To demonstrate this, we will briefly look at how each section introduced by the phrase *'ēlle tôlĕdôt* (termed a *tôlĕdôt* section) serves to advance the author's purpose and to prepare the reader for the rest of the OT.

The First *Tôlĕdôt* Section: What Happened to the Heavens and the Earth (Gen. 2:4–4:26)

As noted, the six days of creation end with the statement that the creation was "very good" (Gen 1:31). Further the entire creation process is set apart from the rest of the book by the seventh day, when God is described as having "rested," a word which Ross notes "describes the enjoyment of accomplishment, the celebration of completion" (Ross, 1988, 114). Cassuto observes this lays the foundation for the Sabbath day directive given subsequently at Mount Sinai and would seem to indicate a tie-in between this material and the covenant that the nation entered with God there (Cassuto, 1961, 63–70). Sarna expands this correlation noting how the concept of a seven-day week, a seven-day pattern of creation, and the institution of the biblical Sabbath are unique to Israel (Sarna, 1989, 14–15).

Translating the phrase *'ēlle tôlědôt* as "this is what became of," clarifies the entire sequence of Genesis 1–4 showing how the so-called "second creation account" doesn't end with the creation of humans (2:25), nor even with the expulsion of the fallen first couple from the garden (3:24), but the new start of a people of God with the beginning of Seth's line (4:26). As Ross puts it, "This first *tôlědôt* traces what became of the universe God had so marvelously created: it was cursed through disobedience, so that deterioration and decay spread rapidly throughout the human race" (Ross, 1988, 117). From both practical and scientific perspectives, there are significant differences between the creation which God pronounced as very good in the preface, and the consequences of the fall event announced in Gen 3:15ff. Just because God created the cosmos does not mean that everything we experience in it today is itself good, although Paul does note that God works everything together for God for those who love Him, but this is in the long term, i.e., preparation for eternity (Rom 8:28).

The entire first section presents two contrastive strains. The positive strain reflects God's grace and promise of redemption. This is seen first when God allows Adam and Eve to continue to live physically, providing them a covering in the form of animal skins (a foreshadowing of blood sacrifices). It is also seen in their exile from the Garden so that they might not eat from the Tree of Life in their fallen state (Gen 3:22). Another positive factor is God's judgment on the serpent after the first couple has eaten from the Tree of Knowledge of Good and Evil. The declaration known as the *protevangelium* contains the promise that the seed of the woman would eventually destroy the serpent. Christian tradition has understood this to be the first anticipation of a redeemer (Mathews, 1996, 245–248). The term "the seed of woman," while it uniquely addresses Eve's offspring as opposed to Adam's, it embeds the promise of redemption in the initial command to have children and multiply (Gen 1:28), placing the hope in the next generation. It appears that Eve anticipated its fulfillment in the birth of Cain, but that idea was crushed with the murder of Abel. Following that debacle, new hope follows the line of Seth and Enosh when "he began to call on the name of the Lord" (literal translation).

But there is also the negative strain of disobedience and sin. Cain's inappropriate worship culminates in his murdering his brother. Then Cain's expulsion from the community of Edenic exiles is followed by his genealogy which is *not* marked off by the term *tôlědôt*. Rather it merely lists a series of births concluding with Lamech who seems to pride himself in how evil he is (Mathews, 1996, 282), indicating that what happened to the heavens and the earth was the beginning of a downward spiral.

The Second *Tôlědôt* Section: What Happened to Adam (Gen. 5:1–6:8)

The tension between the anticipation of a redeemer and the downward spiral of humankind continues. The world is now fallen—that is what happened to that good creation. The natural question then is, what is God going to do about it? Contrary to the reader's expectations, the answer is not short-term. Following Eve's disappointment in Cain and the lineage of their firstborn, the second *'ēlle tôlědôt* section (Gen 5:1ff) shows the long term nature of the situation by rapidly tracing the next ten generations through Adam's genealogy tracing the line of Seth.

Wilson shows how the genealogy ties into the overall structure of the book when he states "a linear genealogy can have only one function: it can be used only to link the person or group using the genealogy with an earlier ancestor or group" (Wilson, 1975, 180). Here it links Noah (and his three sons) back to Adam, designating one selected individual in each generation as the heir apparent. Clines suggests the genealogy serves a theological function of distinguishing the line that remained true while the rest of the mankind drifted further from God (Clines, 1994, 293–294). This is demonstrated by the contrast within the section between the material on Enoch (the one exception to "and he died") and the very enigmatic appendix to the genealogy regarding the marriages between the sons of God and the daughters of men (Harbin, 1994, 16–17). The key to the latter is the observation that "every intent of the thoughts of [mankind's] heart was only evil continually" (Gen 6:5 NASB). This is followed by the decision on God's part to destroy all life—with the exception of Noah and what he would preserve.

The Third *Tôlědôt* Section: What Happened To Noah (Gen. 6:9–9:29)

God's decision to destroy all life, coupled with the observation that Noah was found righteous, sets the stage for the next *'ēlle tôlědôt* section. This section does not contain a genealogy, but rather describes the flood event which describes what became of the increasingly violent, very corrupt world. As a result, many scholars miss its significance. For example, Anderson identifies the passage of 6:1–9:27 as "a long block of narrative material dealing with Noah's lifetime which has been inserted into the heart of Noah's genealogy as presented in the toledoth document (5:1)" totally ignoring the *'ēlle tôlĕdôt* division at 6:9 (Anderson, 1975, 32–33). The section recounts how God called Noah to prepare a large ark and to gather representative animals from every "kind" to preserve them for replenishing the earth after God's judgment. Scholars agree that the literary purpose is to demonstrate both judgment and salvation on the part of God (Delitzsch, 1978, 235; von Rad, 1977, 127; Ross, 1988, 188–189). Kidner notes that the scope of this event is the background for New Testament allusions which present it as a warning for a yet future global judgment seen in passages such as Luke 17:26ff, and 2 Peter 3:6–7 (Kidner, 1967, 59).

While there are a number of parallels with the introductory chapter of Genesis (Anderson, 1975, 36; Ross, 1988, 189; and Westermann, 1984, 393), its correlation with the fall event is more significant. While the fall event marks the beginning of the decay that spread throughout the human race, the overall physical world apparently did not change significantly with just the Garden of Eden isolated. The flood event marks a massive change in the entire physical world changing the entire globe. Given the physical alterations in the world as a result of the extreme dynamics of a global flood, viewed properly the current geological record seems to provide a monument that demonstrates the reality of God's judgment documented in a number of recent works including (Whitcomb and Morris, 1969; Austin, 1994; Clarey, 2020). The bottom line is that this section which relates what happened to Noah presents this flood as an unparalleled world changing event. As Delitzsch observes "[f]or the accomplishment of these inconceivabilities, recourse must be had to miracles of omnipotence… unprecedented in Scripture history" (Delitzsch, 1978, 248). This seems to be the exact intention of the text.

The Fourth *Tôlĕdôt* Section: What Happened to Shem, Ham, and Japheth (Gen. 10:1–11:9)

The previous *'ēlle tôlĕdôt* section concluded with the death of Noah leaving his three sons and their wives to repopulate the world. The post-flood world is now presented as a second new start for mankind to fulfill God's creation mandate. Thus, the fourth *'ēlle tôlĕdôt* section (beginning at Gen 10:1) shows how the mandate to be fruitful and multiply was fulfilled in the three sons of Noah, somewhat paralleling Genesis 5 with the genealogy of Adam. This is done in the form of what Wilson calls a "segmented genealogy," that is, a genealogy which "expresses more than one line of descent from a common ancestor" (Wilson, 1975, 179). Custance claims that the "Table of Nations" in Genesis 10 is an early, accurate but limited delineation of the tribal groupings of mankind which he would date to approximately 2000 BC or earlier (Custance, 1975, 59–79). For our purposes, the more significant point is that the Table of Nations in Genesis 10 contrasts the separation of Cain's lineage from Seth's and the rest of Adam's descendants in Genesis 5 by showing how all the descendants of Noah are viewed as members of one lineage although distinguished by the three family groupings headed by the three sons of Noah (Waltke, 2001, 174–75; Custance 1975, 12–13). The climax of this *'ēlle tôlĕdôt* section occurs at the beginning of Genesis 11 where we see how the directed dispersion of mankind required that God once more over-ride the efforts of mankind to disobey God's directions. The key statement in the passage is in 11:4 where the descendants of the flood survivors make their plan for the tower because "otherwise we will be scattered abroad over the face of the whole earth." The result presented here is the diversity of languages making communication even more difficult.

The Fifth *Tôlĕdôt* Section: What Happened to Shem (Gen. 11:10–11:26)

The fifth *'ēlle tôlĕdôt* section is short, but it changes the focus of the book. Thus far, each *'ēlle tôlĕdôt* section has demonstrated another failure on the part of the expanding human race, and the reader is still looking for the redeemer promised back in Gen 3:15. Up to this point the book's focus has been on mankind as a whole even it traced a specific family line. Now, after the segmented genealogy in the fourth *'ēlle tôlĕdôt* section, the text returns to give a linear genealogy of just one of Noah's three sons, specifically Shem. Commentators pick up on the linear aspect of the genealogy which links a person to an earlier ancestor and quickly focus on Abraham whose story fills most of the next thirteen chapters, and who seems to be presented as the most important person in the book in terms of theology. As Westermann asserts, "[t]he branch that is continued is to be understood only in the light of its goal, Abraham" (Westermann, 1984, 560). The problem is that this section stops with Terah and the notation that he had three sons (Gen 11:26)—not with Abraham, per se. Abraham actually is part of the *'ēlle tôlĕdôt* section of Terah.

The Sixth *Tôlĕdôt* Section: What Happened to Terah (Gen. 11:27–25:11)

The sixth *'ēlle tôlĕdôt* section catches the reader unprepared. It is a very long narrative section—far longer than any previous section and is actually the longest in the book. It is defined as the *'ēlle tôlĕdôt* of Terah, but covers him in just the initial six verses, after which he is not mentioned again. After abruptly noting that Terah died in Haran, the next 13 chapters focus on his son Abraham (properly speaking, when introduced, his name was Abram, but for clarity we will just use his more familiar name). Given the amount of space devoted to Abraham, one must conclude that he is a very significant character—arguably the most significant person in the book. If that is the case, then why is there no *'ēlle tôlĕdôt* section for Abraham?

Ross seems to point in the right direction when he notes that the little information that is given about Terah really is that which is associated with Abraham "and his future sojourn in the Promised Land" (Ross, 1988, 257). Kidner takes us further when he states, "Terah, lacking the vision, lost the will to persist" (Kidner, 1967, 111–112). Given our understanding of the phrase *'ēlle tôlĕdôt* ("this is what became of") it seems that Terah was the patriarch when God called him and Abraham, as a family, to leave Ur to go to Canaan. While the section is difficult, it appears that on the basis of comparison of this passage and Stephen's testimony in Acts that Terah stopped in Haran and Abraham with him (Polhill, 2001, 189). Terah refused to go into the land and as a result died in Haran. That is what became of Terah, but there is more to the story. God then turned to Abraham, who appears to have been part of the original call in Ur. Abraham obeyed in faith and thus received the promise. Even so, the overall section demonstrates that Abraham also struggled with his faith. As discussed elsewhere, in essence this is a situation similar to what Mordecai expressed to Esther when he told her, "relief and deliverance will arise for the Jews from another place and you and your father's house will perish" (Esth 4:16, NASB), except that unlike Esther, Terah failed. In contrast, Abraham demonstrated the requisite faith and thus through him came the promise—reflecting the very strong tension between God's sovereignty and the "free will" of individuals (Harbin, 2016, 19–34).

However, Terah's decision to stop may have had other consequences which are significant for the overall account. Genesis 12:6 states that when Abraham reached Shechem, "at that time the Canaanites were in the land" (so NRSV, and ESV; NIV has "[t]he Canaanites were *then* in the land," italics added). While often taken as an indication that the text had to have been written long after Moses (Spieser, 1962, 87), Cassuto points out that it has also been taken to suggest that the Canaanites were "*already* in the land" (Cassuto, 1964, 327–328; italics in original), which is a better understanding, suggesting that they had settled there in the time Terah hesitated in Haran. Subsequently at different points, additional tribes are noted as then being in the land indicating that in addition to the movement of Abraham and his family, other tribes were in the process of moving in. If so, then it seems that a consequence of Terah's settling in Haran was that other tribes got to Canaan first.

Regardless, as a result, Abraham is now the descendant of Adam who is going to father the line of the redeemer. While the rest of this *'ēlle tôlĕdôt* section sets the stage for a future possession of the land by the descendants of Abraham, the process is complicated by Abraham's up and down faith. Most of these issues lie outside the scope of this study, but one is important enough that the writer devotes an entire *'ēlle tôlĕdôt* section to reflect its outcome—that is the birth of Ishmael, which preceded the birth of Isaac the designated heir.

The Seventh *Tôlĕdôt* Section: What Happened to Ishmael (Gen. 25:12–18)

Initially, this *'ēlle tôlĕdôt* section seems somewhat of a rabbit trail since Isaac has been designated the heir of the Abrahamic covenant, and the reader would expect the text to follow Isaac. The early readers may also have expected that as the firstborn, Ishmael would be the heir. However, one of the dynamics of the entire book of Genesis is that the first-born is not necessarily the heir. For example, later in the book, Joseph, the next to youngest of Jacob's twelve sons is given the double portion normally associated with the firstborn (Gen 48:18–22). In this case, Isaac was named as the heir before conception, but because of Abraham and Sarah's attempted manipulation to fulfill God's promise for Him, Ishmael was born first. Now the reader might wonder about the son who did not receive the promise. In essence this short section ties up what would otherwise be a loose end. Ishmael was Abraham's oldest son, even though he was born to a concubine rather than to Sarah. This segmented genealogy lists only the first generation whose members are deemed the rulers of twelve tribes. Thus, as Keil and Delitzsch indicate, this section shows that God's promises were fulfilled as the writer now turns back to the chosen line (Keil and Delitzsch, 1970, I:264).

The Eighth *Tôlĕdôt* Section: What Happened to Isaac (Gen. 25:19–35:29)

By now the reader is getting used to the idea that each *'ēlle tôlĕdôt* section explains what happened to a figure introduced in the previous section. Consequently, it is no longer a surprise that while the eighth *'ēlle tôlĕdôt* section tells what happened to Isaac, it focuses on his twin sons. In fact, Isaac seems to be almost a bit player in his own *'ēlle tôlĕdôt* section. Actually, the main character here is the younger twin, Jacob, who manages to receive the birthright, but more importantly the blessing through which he would continue the Abrahamic covenantal line.

While the fact that Jacob manages to get the birthright expected for the firstborn is significant, the fact that Isaac gives him his blessing is more important not only for the story line, but the entire OT. Three points stand out. First, and most obvious, the section relates how Jacob got that position despite what the reader might consider serious character flaws. On one hand, he used cunning and deceit to get both, but on the other hand, the text relates that this result was prophesied before birth, in fact before Rebekah knew that she was bearing twins, demonstrating the tension between God's sovereignty and the choices of individuals (Ross, 1988, 433). In contrast to Abraham who through faith received the promise, however, in Jacob's case the stress seems to be on the disdain his brother had for the promises as opposed to Jacob's own gradually developing faith (Kidner, 1967, 152, Ross, 1988, 447–449).

The second point that should stand out to the reader is that this is the first time that a father blessing his son prior to his own death is noted. Because the concept of blessing permeates both testaments, most modern readers just accept the concept as a cultural given. However, the idea of an OT father blessing his son seems limited just to the three generations in Genesis associated with the Abrahamic covenant. In Gen 26:3–5 God clearly communicates to Isaac that he has received the blessing and covenant which had been given to Abraham, although the father blessing the son is not explicitly stated (Sarna, 1989, 183). Then, Isaac gives the blessing to Jacob (Gen 27:27–29; see also Gen 35:12). Finally, Jacob blesses his sons in Genesis 49. Because there is a significant difference in the blessing and this event seems to terminate the practice, we will look at it under the last *'ēlle tôlĕdôt* section.

The third point is one of confusion between the concept of birthright and blessing. Jacob "bought" the birthright from his brother for a bowl of stew in Genesis 25, and in Gen 27:36 at a later date Esau sees it as a done deal. What then is the issue with the blessing, and how is it separate from the birthright? The key is in the wording of Isaac's blessing on Jacob, where Isaac's words in 27:29 cite wording from the Abrahamic covenant in Gen 12:3. The distinction is that the birthright involves a double share of the physical inheritance while the blessing makes the recipient the next link in the Abrahamic covenant (Harbin, 2005, 105–106).

There are a number of challenging issues within this passage which we are not able to cover in this brief structural overview. Collectively, however, they illustrate the process by which Jacob's character is transformed "from trickster to humbled servant" (Mathews, 1996, 70; Sarna, 1989, 397–98). The main point of the *'ēlle tôlĕdôt* section of Isaac is that it shows how Jacob was renamed Israel and became the father of twelve sons. In other words, what became of Isaac, the heir of Abraham, is that he passed the promises on to his youngest son, and his family. We will address the implications of that in the last *'ēlle tôlĕdôt* section, that of Jacob. This section, however, ends with the death of Isaac, who has been mentioned only incidentally since Jacob left Canaan in Genesis 28. He is then buried by his two sons, Esau and Jacob, who are the subjects of the last three *'ēlle tôlĕdôt* sections.

The Ninth and Tenth *Tôlĕdôt* Sections: What Happened to Esau (Gen. 36:1–37:1)

After the tension between Jacob and Esau which began before birth, the reader would necessarily wonder what became of the other brother. The ninth and tenth *'ēlle tôlĕdôt* sections together explain that, relating what happened to the older twin who sold his birthright and was cheated out of the blessing that he considered his.

This is really a double *tôlĕdôt* with the phrase *'ēlle tôlĕdôt* appearing twice—once in 36:1 and then again in 36:9. While unique, the two sections are related. The first genealogy lists Esau's wives and sons "who were born to him in the land of Canaan" (36:5), while the second genealogy relates what became of him "in the hill country of Seir" (36:9). In contrast, Gen 37:1, which is still part of this *'ēlle tôlĕdôt* section states that Jacob lived in the land of Canaan. Thus, in addition to tying up the loose end of what happened to Esau, very subtly we see how the families of Jacob and Esau in essence switch locations with Esau who had remained with his father when Jacob fled to Haran now outside of the Promised Land. This sets the stage for Israel's conquest and settlement when it comes.

The Eleventh *Tôlĕdôt* Section: What Happened to Jacob (Gen. 32:2–50:26)

The final *'ēlle tôlĕdôt* section addresses what became of Jacob. As the section begins, he is back in the land which was promised. Further, while his name has been changed to Israel (although Jacob and Israel seem to be used interchangeably through this section), the section begins by referring to him by the older name of Jacob, reminding the reader that we are still addressing Isaac's younger son. However, the focus of the section is on the next generation, which is demonstrated at the very beginning as the text begins: "*'ēlle tôlĕdôt* [this is what became of] Jacob. Joseph… ." This primes the reader to expect that Joseph will play a significant role in the next step of the narrative, a practice that the reader is now familiar with.

This familiar text traces the conflict between Joseph and his brothers which heightens when the brothers sell Joseph into slavery and he is transported to Egypt. But the account does not stop there. Rather, the narrative climaxes when the brothers are driven to Egypt by a famine and stand before Joseph who now controls all of the agricultural produce of Egypt and thus controls their fate (Westermann, 1986, 24). But, demonstrating God's grace, he brings them down to Egypt along with their father. In the process they fulfill the prophecy given to Abraham that his descendants would be "strangers in a land that was not theirs" (Gen 15:13).

It is here that the *'ēlle tôlĕdôt* structure proves especially helpful. Commentators note Joseph's dominance and tend to call this section the history of Joseph. They then struggle with two incidents that seem to interrupt the story: the Judah-Tamar incident in chapter 38, and Jacob's blessing of his sons and grandsons in chapters 48–49, (Skinner, 1930, 438; Sarna, 1989, 254; von Rad, 1977, 347–48). And yet both really serve critical roles in explaining what happened to Jacob.

In the case of the Judah-Tamar incident, there are a number of issues which lead commentators to puzzle over not only its location, but its inclusion (von Rad, 1977, 356; Ross, 1988, 611–613; Speiser, 1962, 299; Westermann, 1986, 49). While the chronological issues are problematic, the crux of the issue seems to be that God took the life of Er, Judah's firstborn, "because he was evil." While we are not told what he did, the use of this phrase in Judg 2:11–13 suggests that it would involve going after other gods. If that is the case, then one thing that happened to Jacob was that his grandsons started going into idolatry. If so, this incident serves explains why the family of Jacob needed to be quarantined from the land until the time of the fulfillment of the promises to Abraham in Genesis 15. This move served to isolate the embryonic nation from the corrupting influences of the Canaanites as they devolved into greater depravities.

While the book ends with the death and burial of Jacob/Israel at Machpelah followed by the death of Joseph both events really seem to be epilogues to the blessing Jacob/Israel gives his twelve sons in the last recorded patriarchal blessing.

Commentators tend to focus on the prophetic aspects of the blessing which are indeed significant (Ross, 1988, 698–709; Lange, 1960; I:648–659; and Skinner, 1930, 507–535). However, a comparison with the blessing in Genesis 27 contrasts Isaac who could only bless one son with Jacob who blesses all twelve sons. This suggests a major change in the scope of the Abrahamic covenant. Up to this point the sense of Abraham's "seed" (and given the scale of the promise, this would be in a plural sense) had been passed from the father to one son. It is now expanded to include all the sons, or in reality, recognizing the flexibility of the Hebrew term son, to all the descendants of Jacob/Israel. Thus, the book ends with the promise encompassing what would become the twelve tribes, as explicitly stated in Gen 49:28. In other words, both the blessing and the covenant now encompass all twelve tribes of what will become the nation of Israel.

Conclusions

There are a number of implications that result from recognizing that the book of Genesis is organized in this manner. First, the *'ēlle tôlĕdôt* structure of Genesis would point to a unified work that is well crafted with a strong theological purpose (DeRouchie, 2013, 247). It traces a view that begins with an Almighty God who created a very good world and then demonstrates how this ideal cosmos became not only the world in which the reader lives but one in which God has started a redemption process. As a preface which contrasts the state of the world which God created and what became of it, the creation account then takes on greater significance. It requires us to recognize that while the world that God created was good, it is no longer good in the same sense, which is important for those who study God's creation. Further, this would place a stronger emphasis on the rationale for the seven day structure of the creation process suggesting that God utilized a seven day process to set up a model for his people to follow, not only in terms of work but in order to weekly recalibrate their relationship to him (Hart, 1995, 315–316).

Second, as suggested by Wiseman, Ross and others, while this structure might suggest that the writer of the book used source material, and have actually had written sources, it does not preclude Mosaic authorship (Wiseman, 1985, 57–58; 68–73. Ross, 1988, 62–63). Rather, the *'ēlle tôlĕdôt* structure indicates a carefully crafted unit. As such, this model is far different from that of the documentary hypothesis or JEDP theory which builds on apparent contradictions in the text. As Cassuto points out, that theory proposes not a unified work, but excerpts from separate compositions (on the same subject) "which a later editor arranged consecutively by pure chance" (Cassuto, 1961, 85). Moreover, accepting that the writer used sources in this manner does not rule out Moses, the traditional author, from being the writer, since other portions of the Pentateuch (traditionally understood to be by Moses) cite specific sources by name (such as the "Book of the Wars of the Lord" in Num 21:14).

Third, as the book culminates with the embryonic twelve tribes of Israel incubating in Egypt, the *'ēlle tôlĕdôt* structure of Genesis would suggest that the book was designed to serve as a prologue to the subsequent account of the Exodus event. Specifically, for the audience at Sinai, the Exodus event would still be part of "what became of Jacob." As such, this would be a profound explanation to the crowd at Sinai, the implied audience, regarding why they were there. Not only were they fulfilling God's promise to Abraham that his descendants would come out of the land of their captivity but they were part of what happened to Jacob, who became Israel. But more powerfully, they were part of a program intended to reconcile the entire world to God, which, for those paying attention, would add tremendous importance to the system which was being developed at Sinai to guide their relationship with God and their fellow humans.

Consequently, it is deemed that the *'ēlle tôlĕdôt* structure of Genesis provides a framework for the book that prepares the reader to understand the subsequent narratives of the OT as a coherent whole, providing a much stronger foundation for comprehending the culmination of those narratives in the life, death, resurrection and ascension of Jesus as the world redeemer. In the process, it better accommodates various internal anomalies pointing to careful composition of Genesis with a clear agenda. Perhaps most importantly, with this, the initial creation account becomes much more significant. It is not just the story of creation, but the series of "this is what became of's" show how what happened enhance our understanding of why we are here, and why the world is the way it is. With the open-ended conclusion of the book setting the stage for the ultimate redemption, it also shows why there is hope.

References

Anderson B. 1975. "From Analysis to Synthesis: The Interpretation of Genesis 1–11," *JBL* 94.

Austin, S. 1994. *Grand Canyon: Monument to Catstrophe*. Institute for Creation Research: Santee, CA.

Block, D. 2001. *Judges, Ruth*, NAC, vol. 6. Broadman and Holman: Nashville.

Brown, F.; Samuel Rolles Driver, S. R.; and Briggs, C.A. (*BDB*). 1977. *Enhanced Brown-Driver-Briggs Hebrew and English Lexicon*. Clarendon Press, Oxford, England. 410.

Cassuto, U. 1961. *A Commentary on the Book of Genesis: Part 1, From Adam to Noah, Genesis I-VI* 8. The Magnes Press: Jerusalem.

Cassuto, U. 1964. *A Commentary on the Book of Genesis: Part 2, From Noah, to Abraham, Genesis VI 9-XI* 32. The Magnes Press: Jerusalem.

Castellino, G. 1994. "The Origins of Civilization according to Biblical and Cuneiform Texts." In Hess, R. and Tsumura, D. (editors). *I Studied Inscriptions from Before The Flood: Ancient Near Eastern, Literary, and Linguistic Aproaches to Genesis 1–11* Eisenbrauns: Winona Lake, IN.

Clarey, T. 2020. *Carved in Stone: Geological Evidence of the Worldwide Flood*: Institute for Creation Research: Dallas TX.

Clines, D. (editor). 1993–2011. *The Dictionary of Classical Hebrew*. Sheffield Phoenix Press Sheffield, England.

Clines, D. 1994. "Theme in Genesis 1–11," In Hess, R. and Tsumura, D. (editors). *I Studied Inscriptions from Before The Flood: Ancient Near Eastern, Literary, and Linguistic Aproaches to Genesis 1–11* Eisenbrauns: Winona Lake, IN.

Custance, A. 1975. *Noah's Three Sons*, The Doorway Papers, Vol. 1. Zondervan: Grand Rapids, MI.

Delitzsch, F. 1978. *A New Commentary on Genesis*, translated by Sophia Taylor, vol 1. (T & T Clark: Edinburgh, 1888: reprint edition Minneapolis: Klock and Klock.

DeRouchie, J. 2013. "The Blessing-Commission, The Promised Offspring, and the Toledot Structure of Genesis." JETS 56/2. 219–47.

Friedman, R. 2001. *Commentary on the Torah with a New English Translation*. HarperSanFrancisco: NY/ 16.

Gunkel, H. 1997. *Genesis*. Mercer University Press. Macon GA.

Hamilton, V. 1995. *The Book of Genesis: Chapters 18–50*. Eerdmans: Grand Rapids, MI.

Harbin, M. 1994. *To Serve Other Gods*. University Press of America: Lanham MD.

Harbin, M. 2005. *The Promise and the Blessing*. Zondervan: Grand Rapids, MI.

Harbin, M. 2016. "Sovereignty and Free Will in the Lives of Terah and Abraham," *Scottish Bulletin of Evangelical Theology*, 34:1 (2016). 19–34.

Hart, I. 1995. "Genesis 1:1–2:3 as a Prologue to the Book of Genesis." *TB* 46.2. 315–336.

Heidel, A. 1951. *The Babylonian Genesis*. U. of Chicago Press, Chicago, IL.

Hoogendyk, I, ed. 2017. *The Lexham Analytical Lexicon of the Hebrew Bible*. Lexham Press, Bellingham, WA.

Keil, C. and Delitzsch, F. 1970. *Commentary on the Old Testament, Vol 1, The Pentateuch*. William B. Eerdmans: Grand Rapids.

Kidner, D. 1967. *Genesis: An Introduction and Commentary*. Inter-Varsity Press: Downers Grove, IL.

Koehler, L. and Baumgartner, W. 1958. *Lexicon in Veteris Testamenti Libros*. Brill: Leiden.

Kramer, S. 1972. Sumerian Mythology. U. of Pennsylvania Press: Philadelphia.

Lange, J. 1960. *Commentary on the Holy Scriptures: Critical, Doctrinal and Homiletical*. Zondervan: Grand Rapids, MI.

Martens, E. 1999. "בֵּן." in Harris, R, Archer, G, and Waltke, B. *Theological Wordbook of the Old Testament*. Moody Press: Chicago.

Mathews, K. 1996. *Genesis 1–11:26*. Broadman & Holman: Nashville, TN.

Polhill, P. 2001. *Acts*, NAC, vol. 26. Broadman & Holman: Nashville, TN.

Rad G. von. 1977. *Genesis: A Commentary*. Westminster Press: Philadelphia.

Ross, A. 1988. *Creation and Blessing*. Baker Book House: Grand Rapids, MI.

Sarna, N. 1989. *The JPS Torah Commentary: Genesis*. Jewish Publication Society: Philadelphia, PA.

Schreiner, J. 2006. תּוֹלֵדוֹת. In Botterweck, G., Ringgren, H., and Fabry, H. (editors). *Theological Dictionary of the Old Testament*. Eerdmans: Grand Rapids, MI.

Skinner, J. 1930. *A Critical and Exegetical Commentary on Genesis*. T&T Clark, Edinburgh, Scotland.

Speiser, E. 1962. *Genesis*. Doubleday: New York.

Tsumura, D. 1994. "Genesis and Ancient Near Eastern Stories of Creation and Flood," In Hess, R. and Tsumura, D. (editors). *I Studied Inscriptions from Before The Flood: Ancient Near Eastern, Literary, and Linguistic Aproaches to Genesis 1–11* Eisenbrauns: Winona Lake, IN.

Waltke, B. with Fredricks, C. 2001. *Genesis: A Commentary*. Zondervan: Grand Rapids: Zondervan.

Westermann, W. 1984. *Genesis 1–11: A Commentary*. Augsburg: Minneapolis, MN.

Westermann, W. 1985. *Genesis 12–36: A Commentary*. Augsburg: Minneapolis, MN.

Westermann, W. 1986. *Genesis 37–50: A Commentary*. Augsburg: Minneapolis, MN.

Whitcomb, J. and Morris, H. 1969. *The Genesis Flood*. Presbyterian and Reformed: Phildadelphia, PA.

Wilson, R. 1975. "The Old Testament Genealogies in Recent Research." *JBL* 94 180.

Wiseman, P. 1985. *Ancient Records and the Structure of Genesis*. Thomas Nelson: Nashville, TN.

Minutes of the 2020 Creation Research Society Board of Directors Meeting

The 57th annual CRS Board of Directors meeting was held online from Friday, 29 May, through Monday, 1 June 2020. This was the first time the Board of Directors held their annual meeting online.

The entire Board met on Friday to consider preliminary matters. All standing CRS committees met during the weekend. The entire Board met on Monday to finalize the year's business and planning.

The following board members attended: Jerry Bergman, Rob Carter, Gene Chaffin, Tim Clarey, Danny Faulkner, Don DeYoung, Robert Hill, Mark Horstemeyer, Jean Lightner, Gary Locklair, Michael Oard, John Reed, Ron Samec, and Tichomir Tenev. VACRC director Kevin Anderson and professional staff members Diane Anderson and John Trout were also present.

CRS Board members and the Andersons meeting over Zoom.

Only selected highlights of board activities and actions are presented here.

The 2019 Board minutes were approved as published.

175 ballots were received for the 2020 Board of Directors election. All six candidates (Robert Carter, Tim Clarey, Danny Faulkner, Robert Hill, Michael Oard, and Tichomir Tenev) were elected to a 3-year term on the Board. (Many ballots were sent to the recording secretary, while a number were sent to the VACRC in Arizona.)

Recognition was given to Ticho Tenev as a new board member.

Some work accomplished prior to the board meeting follows: We approved funding for architectural work related to our new facility on the campus of Arizona Christian University. We approved some personal loans to bridge funding between our move and the sale of our current facilities in Chino Valley, Arizona. We hired John Trout as a part-time development person for the Society.

Don DeYoung, VACRC (lab) committee chairman introduced John Trout. John, a recent marketing degree graduate, will focus on brand recall, membership renewal, and our social media presence. John is contacting people whose membership has lapsed. Don reported on the work related to moving the lab from Chino Valley to Phoenix. The move opens up new and exciting possibilities for the Society. Don reported on the iDino and eKinds research projects. Each research project has several papers in process for publication. The lab budget was increased by 13% over the previous year to assist with lab moving expenses.

Danny Faulkner reported on the 2019 annual conference. This was the Society's 8th annual conference and was held at Concordia University in Mequon, WI. It was our best attended conference so far with more than 130 people present. Attendees commented on the very good facilities and excellent presentations. At the meeting, Kevin Anderson was recorded presenting instructions for authors who wish to publish (especially in the *CRSQ*). Don DeYoung provided the Henry Morris memorial lecture which was also recorded. The 2020 conference will not be held. We are planning for a 2021 conference on the campus of Arizona Christian University.

Don assured the board that we have liability insurance. He shared that AiG has retired the CRS kiosk that was in the museum. Don recognized and thanked our donors. We lost some members this past year including Glen Wolfrom, George Howe, Philip Johnson, John Whitcomb, and Bill Overn.

Danny Faulkner led a devotion focusing on Moses' words to Joshua: "It is the Lord who goes before you. He will be with you; he will not leave you or forsake you. Do not fear or be dismayed." (Deuteronomy 31:8)

Danny Faulkner, treasurer, reported on donations, membership renewals, designated funds for research and other income for the year. He indicated that expenses were in line with the Society's income.

Rob Carter, internet committee chairman, reviewed our current online presence (website, Facebook page, CRSnet listserv email reflector). This year we engaged an information technologist, Brandon White, to revamp our website, focusing on back-end processes. Rob shared some suggestions for website improvement. There was discussion regarding processes and documenting our online services.

Tim Clarey, periodicals committee chairman, shared information relating to the *CRSQ* and *Creation Matters* (*CM*). As editor, Tim has located a managing editor along with a new printer. One goal was to get "caught up" on our publication schedule and we have made up some time this year. A major Society expense is printing our periodicals. There was discussion regarding electronic versus printed periodicals. Due to the loss of Glen Wolfrom, *Creation Matters* has been scaled back in page size and number of issues. Jean Lightner was thanked for her work on *Creation Matters*.

Mike Oard, publications committee chairman, provided an update about book sales. The number of books ordered has been slowly declining. There are no plans to publish new books this year. The committee is investigating a number of possible future titles.

Rob Carter, membership committee chairman, provided information on the state of the Society. Membership has declined over the past 3 years. We currently have more than 450 life members in the Society. The CRS currently consists of 1457 members and subscribers with 598 being voting members.

Gene Chaffin, research committee chairman, shared a number of research projects funded by CRS grants. As a Society we provide research grants. This year we funded 6 out of 15 submitted research proposals. With more funds, we could support more research.

Gary Locklair, constitution committee chairman, reported on changes to the CRS Constitution and By-laws. Members were notified of the changes during a 90-day review period prior to our board meeting. The Board approved the changes to the CRS Constitution and By-laws. The committee has an additional list of small changes that have been suggested. These will be reviewed and proposed in an additional change cycle. Some discussion of advanced planning ensued.

Financial Secretary Bob Hill shared the financial status of the Society. While the endowments are down slightly, the interest percentage rate is up.

The Board approved an expense budget of $321,500 for the coming fiscal year. The Board authorized Diane Anderson to withdraw up to $20,000 of funds without executive committee action.

The Board submitted the names of Jerry Bergman, Gene Chaffin, Mark Horstemeyer, Jean Lightner, John Reed, and Jeff Tomkins as candidates for the 2021 Board of Director's election.

Board elections resulted in the following:

President – Don DeYoung
Vice President – Gene Chaffin
Recording Secretary – Gary Locklair
The following officers were confirmed for the third year of their 3-year term:
Financial Secretary – Bob Hill
Treasurer – Danny Faulkner
Membership Secretary – Rob Carter

The following were honored for years of service to the board: Jerry Bergman (5), Danny Faulkner (15), and John Reed (20).

The next annual board meeting will be 20–22 May 2021 in Glendale, AZ, at Arizona Christian University.

Respectfully submitted,

Dr Gary H Locklair

Prof. Gary Locklair, PhD, FCRS
CRS Recording Secretary

Letters to the Editor

The policy of the editorial staff of CRSQ *is to allow letters to the editor to express a variety of views. As such, the content of all letters is solely the opinion of the author, and does not necessarily reflect the opinion of the* CRSQ *editorial staff or the Creation Research Society.*

Biblical Science

On August 20th, 1977, the Voyager 2 space probe lifted off from Kennedy Space Center in Florida. It was followed by the Voyager 1 space probe on September 5th, 1977. These probes were designed to study the outer planets. Voyager 1 visited Jupiter on March 5th, 1979, and Saturn on November 12th, 1980. Voyager 2 visited Jupiter on July 9th, 1979, Saturn on August 25th, 1981, Uranus on January 24th, 1986, and Neptune on August 25th, 1989. One of the sensors on these probes measured the planets electromagnetic field.

In 1984, Dr. D. Russell Humphreys, starting with the Word of God, noted that 2 Peter 3:5 indicated that the originally created material was water. Using this as a starting point, he predicted the existence and magnitude of the magnetic field of all the planets. The abstract of his 1984 article is presented below:

> God could have started magnetic fields in the solar system in a very simple way: by creating the original atoms of the planets with many of their nuclear spins pointing in the same direction. The small magnetic fields of so many atomic nuclei add up to fields large enough to account for the magnetism of the planets. Within seconds after creation, ordinary physical events would convert the alignment of nuclei into a large electric current circulating within each planet, maintaining the magnetic field. The currents and fields would decay steadily over thousands of years, as Barnes has pointed out. The present magnetic field strengths of the Earth, Sun, Moon, and planets agree very well with the values produced by this theory and a 6000-year age for the solar system. The theory is consistent with all the known data and explains many facts which have puzzled evolutionists (Humphreys, 1984, p. 140).

Six years later the space probe Voyager 2 passed by the planets Uranus and Neptune. As it passed by, the probe measured the existence and magnitude of the magnetic fields of these planets.

> In 1984, when no space craft had yet reached Uranus and Neptune, I published a theory predicting the strength of the magnetic fields of these two planets… I made the predictions on the basis of my hypotheses that (A) the raw material of creation was water (based on II Peter 3:5, "the earth was formed out of water and by water"), and (B) at the instant God created the water molecules, the spins of the hydrogen nuclei were all pointing in a particular direction….
>
> The straight line in Figure 1 shows the maximum magnetic dipole moment (a measure of the strength of the magnetic field's source) of each planet at creation, according to my theory. The present-day magnetic moments depend on the size and electrical conductivity of each planet's core and on the age of the solar system. Using accepted models (which are really only guesses) of the cores and an age of 6,000 years, I estimated the present magnetic moments for the Sun, Moon, and all the planets for which we had magnetic data in 1984. The values I got agreed with the measured values … In 1984 we had no magnetic data for Uranus and Neptune. I estimated magnetic moments of roughly 2 to 6 x 10^{24} Ampere-Meters^2 for both planets. Because of the uncertainty about the interiors of those planets, I widened my prediction to "on the order of" 10^{24} A-m^2, by which I meant that the magnetic moments would be between 1 x 10^{23} and 1 x 10^{25} A-m^2. And regardless of assumptions about planetary interiors, if the present field of either planet had exceeded the maximum (the [black] line in Figure 1), my theory would have been falsified…. Two years later, on January 20, 1986, Voyager II passed by Uranus. It showed that Uranus has a magnetic moment of 3.0x10^{24} A-m^2, well within the bounds of my predictions…. On August 25, 1989, Voyager II passed by Neptune and found that it has a magnetic moment of 1.5x10^{24} A-m^2 [the red line in Figure 1] (Humphreys, 1990, pp. i–iii).

In part, because of Dr. Humphreys' approach on magnetic fields, Dr. Richard Overman proposed a Biblically-based scientific method (Overman, 2017). This method has six basic steps for studying a topic scientifically.

The Biblically-based scientific approach starts with what the Bible has to say about the topic then builds upon that. In some respects, the mechanics are the same as the typical scientific method. The major difference is the starting point and the worldview of the scientist. The Biblically-based approach uses the following steps:

1. **What does the Bible specifically say?** Under the Biblically-based approach, the scientist begins by searching the Scriptures to see what specific information, if any, the Scriptures contain about the subject. Dr. Humphreys noticed that the Scriptures indicated that the originally created material was water molecules. While the Scriptures may not specifically say this. There was enough there for Humphreys to form a hypothesis.
2. **What Biblical principles apply?** The next step for the scientist taking a Biblical approach is to search the scriptures for any Biblical principles that should be applied to the subject of the inquiry. Humphreys used the Biblical principle that God created everything about 6,000 years ago to provide a timeframe with which to perform his calculations.
3. **Search existing literature and knowledge.** Once the scientist has as good an understanding as possible of the Biblical considerations, information and studies that have already been performed can be identified and evaluated. Such an evaluation will include determining how well the information and results are consistent with the Biblical information and principles already learned. Any information or results that are not consistent with the Biblical information is immediately rejected. Humphreys applied known physics principles and the best available information on the makeup of the planets and Sun to perform his calculations. These were compared to known data where available.
4. **Create hypotheses to fill in gaps of knowledge.** Once the gaps in the knowledge have been identified, research questions, or hypotheses, can be formulated to close those gaps. Humphreys used the information he developed to hypothesize the magnetic field existence and magnitude of the planets that have yet to be studied.
5. **Perform experiments to test the hypotheses.** The scientist is ready to perform experiments to gather the data. These experiments and information-gathering techniques are the same as used by everyone. The difference is the principles, philosophies and information leading up to the development of the experiment. Humphreys compared data gathered by Voyager 2 to test his hypothesis. The data confirmed both the existence and magnitude of the magnetic fields.
6. **Draw Biblically-based conclusions.** The final step is to draw Biblically sound conclusions that are consistent with the specific statements and principles found in the Bible. Such conclusions must be drawn with humility and prayer understanding that "It is the glory of God to conceal a thing: but the honor of kings is to search out a matter" (Proverbs 25:2, KJV). The data supports Humphreys' hypothesis that God originally created water molecules with the atomic spin going in the same direction.

Humphreys successfully applied all six steps of the Biblically-based scientific

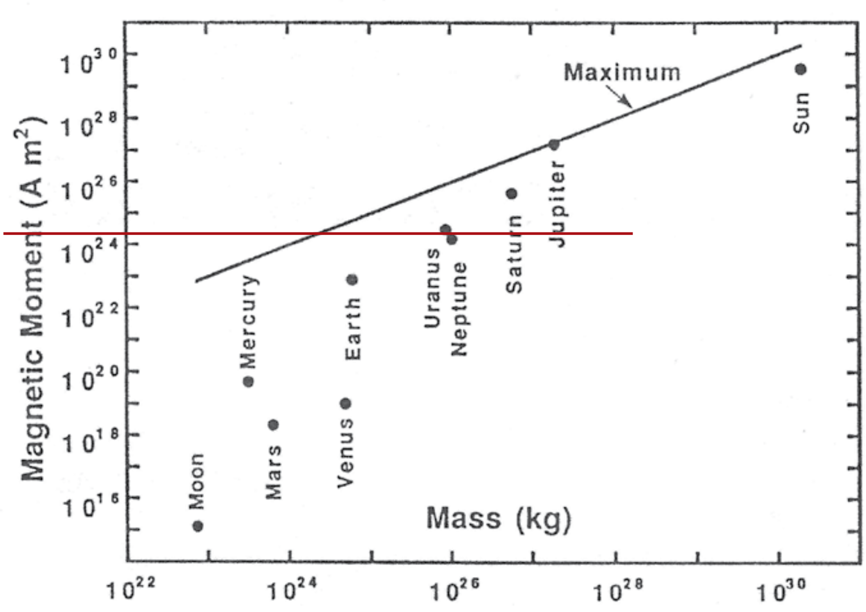

Figure 1. Measured magnetic fields in the solar system.

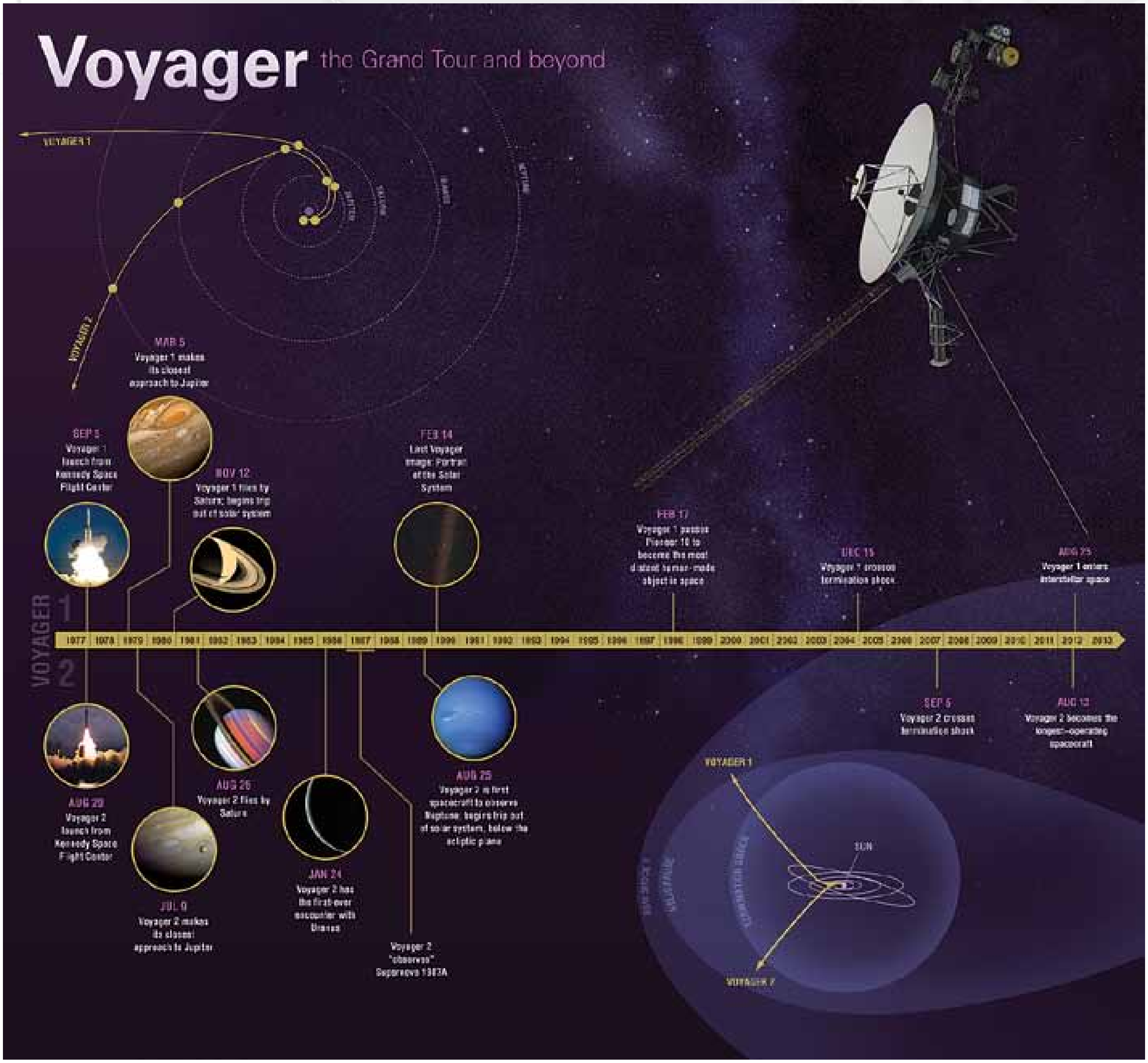

Image credit NASA

method. He searched the Scriptures, applied existing knowledge, identified gaps, formed a hypothesis, made predictions, and tested those predictions. His study supports the veracity of scripture, currently known scientific principles, and provides a basis for future studies of the physical sciences that God created. More widespread use and discussion of a Biblically-based scientific method may be beneficial to the creation science community.

Rich Overman

References

Humphreys, D.R. 1984. The creation of planetary magnetic fields. *Creation Research Society Quarterly* 21(3): 140–149.

Humphreys, D.R. 1990. Beyond Neptune: Voyager II supports creation. *Acts & Facts* 19(5) and ICR *IMPACT*, no. 203.

Overman, R. 2017. The Bible: The foundation for all science. *Creation Research Society Quarterly* 54(2): 154–155. (CRS Conference Presentation Abstracts).

Instructions to Authors

Submission

Electronic submissions of all manuscripts and graphics are preferred and should be sent to the editor of the *Creation Research Society Quarterly* in Word, WordPerfect, or Star-Office/Open Office (see the inside front cover for address). Printed copies also are accepted. If submitting a printed copy, an original plus two copies of each manuscript should be sent to the editor. The manuscript and copies will not be returned to authors unless a stamped, self-addressed envelope accompanies submission. If submitting a manuscript electronically, a printed copy is not necessary unless specifically requested by the *Quarterly* editor. Manuscripts containing more than 35 pages (double-spaced and including references, tables, and figure legends) are discouraged. An author who determines that the topic cannot be adequately covered within this number of pages is encouraged to submit separate papers that can be serialized.

All submitted manuscripts will be reviewed by two or more technical referees. However, each section editor of the *Quarterly* has final authority regarding the acceptance of a manuscript for publication. While some manuscripts may be accepted with little or no modification, typically editors will seek specific revisions of the manuscript before acceptance. Authors will then be asked to submit revisions based upon comments made by the referees. In these instances, authors are encouraged to submit a detailed letter explaining changes made in the revision, and, if necessary, give reasons for not incorporating specific changes suggested by the editor or reviewer. If an author believes the rejection of a manuscript was not justified, an appeal may be made to the *Quarterly* editor (details of appeal process at the Society's web site, www.creationresearch.org).

Authors who are unsure of proper English usage should have their manuscripts checked by someone proficient in the English language. Also, authors should endeavor to make certain the manuscript (particularly the references) conforms to the style and format of the *Quarterly*. Manuscripts may be rejected on the basis of poor English or lack of conformity to the proper format.

The *Quarterly* is a journal of original writings, and only under unusual circumstances will previously published material be reprinted. Questions regarding this should be submitted to the Editor (CRSQeditor@creationresearch.org) prior to submitting any previously published material. In addition, manuscripts submitted to the *Quarterly* should not be concurrently submitted to another journal. Violation of this will result in immediate rejection of the submitted manuscript. Also, if an author uses copyrighted photographs or other material, a release from the copyright holder should be submitted.

Appearance

Manuscripts shall be computer-printed or neatly typed. Lines should be double-spaced, including figure legends, table footnotes, and references. All pages should be sequentially numbered. Upon acceptance of the manuscript for publication, an electronic version is requested (Word, WordPerfect, or Star-Office/Open Office), with the graphics in separate electronic files. However, if submission of an electronic final version is not possible for the author, then a cleanly printed or typed copy is acceptable.

Submitted manuscripts should have the following organizational format:

1. Title page. This page should contain the title of the manuscript, the author's name, and all relevant contact information (including mailing address, telephone number, fax number, and e-mail address). If the manuscript is submitted by multiple authors, one author should serve as the corresponding author, and this should be noted on the title page.

2. Abstract page. This is page 1 of the manuscript, and should contain the article title at the top, followed by the abstract for the article. Abstracts should be between 100 and 250 words in length and present an overview of the material discussed in the article, including all major conclusions. Use of abbreviations and references in the abstract should be avoided. This page should also contain at least five key words appropriate for identifying this article via a computer search.

3. Introduction. The introduction should provide sufficient background information to allow the reader to understand the relevance and significance of the article for creation science.

4. Body of the text. Two types of headings are typically used by the *CRSQ*. A major heading consists of a large font bold print that is centered in column, and is used for each major change of focus or topic. A minor heading consists of a regular font bold print that is flush to the left margin, and is used following a major heading and helps to organize points within each major topic. Do not split words with hyphens, or use all capital letters for any words. Also, do not use bold type, except for headings (italics can be occasionally used to draw distinction to specific words). Italics should not be used for foreign words in common usage, e.g., "et al.", "ibid.", "ca." and "ad infinitum." Previously published literature should be cited using the author's last name(s) and the year of publication (ex. Smith, 2003; Smith and Jones, 2003). If the citation has more than two authors, only the first author's name should appear (ex. Smith et al., 2003). Contributing authors should examine this issue of the *CRSQ* or consult the Society's web site for specific examples as well as a more detailed explanation of manuscript preparation. Frequently-used terms can be abbreviated by placing abbreviations in parentheses following the first usage of the term in the text, for example, polyacrylamide gel electrophoresis (PAGE) or catastrophic plate tectonics (CPT). Only the abbreviation need be used afterward. If numerous abbreviations are used, authors should consider providing a list of abbreviations. Also, because of the variable usage of the terms "microevolution" and "macroevolution," authors should clearly define how they are specifically using these terms. Use of the term "creationism" should be avoided. All figures and tables should be cited in the body of the text, and be numbered in the sequential order that they appear in the text (figures and tables are numbered separately with Arabic and Roman numerals, respectively).

5. Summary. A summary paragraph(s) is often useful for readers. The summary should provide the reader an overview of the material just presented, and often helps the reader to summarize the salient points and conclusions the author has made throughout the text.

6. References. Authors should take extra measures to be certain that all references cited within the text are documented in the reference section. These references should be formatted in the current *CRSQ* style. (When the *Quarterly* appears in the references multiple times, then an abbreviation to *CRSQ* is acceptable.) The examples below cover the most common types of references:

Robinson, D.A., and D.P. Cavanaugh. 1998. A quantitative approach to baraminology with examples from the catarrhine primates. *CRSQ* 34:196–208.

Lipman, E.A., B. Schuler, O. Bakajin, and W.A. Eaton. 2003. Single-molecule measurement of protein folding kinetics. *Science* 301:1233–1235.

Margulis, L. 1971a. The origin of plant and animal cells. *American Scientific* 59:230–235.

Margulis, L. 1971b. *Origin of Eukaryotic Cells*. Yale University Press, New Haven, CT.

Hitchcock, A.S. 1971. *Manual of Grasses of the United States*. Dover Publications, New York, NY.

Walker, T.B. 1994. A biblical geologic model. In Walsh, R.E. (editor), *Proceedings of the Third International Conference on Creationism* (technical symposium sessions), pp. 581–592. Creation Science Fellowship, Pittsburgh, PA.

7. Tables. All tables cited in the text should be individually placed in numerical order following the reference section, and not embedded in the text. Each table should have a header statement that serves as a title for that table (see a current issue of the *Quarterly* for specific examples). Use tabs, rather than multiple spaces, in aligning columns within a table. Tables should be composed with *14-point type* to insure proper appearance in the columns of the *CRSQ*.

8. Figures. All figures cited in the text should be individually placed in numerical order, and placed after the tables. Do not embed figures in the text. Each figure should contain a legend that provides sufficient description to enable the reader to understand the basic concepts of the figure without needing to refer to the text. Legends should be on a separate page from the figure. All figures and drawings should be of high quality (hand-drawn illustrations and lettering should be professionally done). Images are to be a minimum resolution of 300 dpi at 100% size. Patterns, not shading, should be used to distinguish areas within graphs or other figures. Unacceptable illustrations will result in rejection of the manuscript. Authors are also strongly encouraged to submit an electronic version (.cdr, .cpt, .gif, .jpg, and .tif formats) of all figures in individual files that are separate from the electronic file containing the text and tables.

Special Sections

Letters to the Editor:

Submission of letters regarding topics relevant to the Society or creation science is encouraged. Submission of letters commenting upon articles published in the *Quarterly* will be published two issues after the article's original publication date. Authors will be given an opportunity for a concurrent response. No further letters referring to a specific *Quarterly* article will be published. Following this period, individuals who desire to write additional responses/comments (particularly critical comments) regarding a specific *Quarterly* article are encouraged to submit their own articles to the *Quarterly* for review and publication.

Editor's Forum:

Occasionally, the editor will invite individuals to submit differing opinions on specific topics relevant to the *Quarterly*. Each author will have opportunity to present a position paper (2000 words), and one response (1000 words) to the differing position paper. In all matters, the editor will have final and complete editorial control. Topics for these forums will be solely at the editor's discretion, but suggestions of topics are welcome.

Book Reviews:

All book reviews should be submitted to the book review editor, who will determine the acceptability of each submitted review. Book reviews should be limited to 1000 words. Following the style of reviews printed in this issue, all book reviews should contain the following information: book title, author, publisher, publication date, number of pages, and retail cost. Reviews should endeavor to present the salient points of the book that are relevant to the issues of creation/evolution. Typically, such points are accompanied by the reviewer's analysis of the book's content, clarity, and relevance to the creation issue.

Creation Research Society Membership/Subscription Application and Renewal Form

The membership/subscription categories are defined below:

1. **Voting Member** ....Those having at least an earned master's degree in a recognized area of science.
2. **Sustaining Member** ....Those without an advanced degree in science, but who are interested in and support the work of the Society.
3. **Student Member** ....Those who are enrolled full time in high schools, undergraduate colleges, or postgraduate science programs (e.g., MS, PhD, MD, and DVM). Those holding post-doctoral positions are not eligible. A graduate student with a MS degree may request voting member status while enrolled as a student member.
4. **Senior Member** ....Voting or sustaining members who are age 65 or older.
5. **Life Member** ....A special category for voting and sustaining members, entitling them to a lifetime membership in the Society.
6. **Subscriber** ....Libraries, churches, schools, etc., and individuals who do not subscribe to the Statement of Belief.

All members (categories 1–5 above) must subscribe to the Statement of Belief as defined on the next page.

Please complete the lower portion of this form and mail it with payment to CRS Membership Secretary, 1 W. Firestorm Way #145, Glendale, AZ 85306, or fax for credit card payment to (928) 636-1153. Applications may also be completed online at creationresearch.org.

This is a ❏ new ❏ renewal application for the subscription year beginning Summer ❏ 2021 ❏ __________. *(Please type or print legibly.)*

Name ______________________ Address ______________________

City ______________________ State __________ Postal/Zip code ______________ Country ______________

Phone (optional) ______________________ Email ______________________

Degree ______________________ Field ______________________

Year granted ______________________ Institution ______________________

Presently associated with ______________________

I have read and subscribe to the CRS Statement of Belief. Signature ______________________

For foreign orders, including Canadian, payment must be made in U.S. dollars by a check drawn on a U.S. bank, international money order, or credit card. *Please do not send cash.*

Indicate applicable category	*Indicate payment*			
	Paper**			
❏ Voting ❏ Sustaining	USA	Canada Mexico	Other countries	**Paper-less‡**
❏ Regular [per year]	❏ $43	❏ $63	❏ $80	❏ $33
❏ Senior [per year]	❏ $38	❏ $58	❏ $75	❏ $28
❏ Life member	❏ $500	❏ $500	❏ $500	❏ $500
❏ Student* [per year]	❏ $38	❏ $58	❏ $75	❏ $28
❏ Subscriber [per year]	❏ $46	❏ $66	❏ $83	❏ $36

* Student members are required to complete the bottom portion of this form.
NOTE: Student members may qualify for the *Future Leaders Sponsorship* program.
See the CRS website at www.creationresearch.org for details.
** Rates for the paper option include postage for First Class Mail International

‡ **PAPERLESS option:** You may opt out of receiving paper copies of the CRS periodicals (*CRS Quarterly* and *Creation Matters*). By choosing this option you may register for access to the Premium Area of the website, where you may view or download electronic (PDF) versions of these publications. Of course, regular members and subscribers may also have access to the Premium Area. Only members, however, will have access to the Members Exclusive Area of the website.

Member/Subscriber	$______ per year
	x _____ years
SUBTOTAL	$___________
Optional contribution	+ $___________
Life membership	+ $___________
TOTAL	$___________

❏ Visa ❏ MasterCard ❏ Discover
❏ American Express ❏ Check/money order
Card number ______________________
Expiration date (mo/yr) ______________________
Phone number (_______) ______________________
Signature ______________________

***Student Members* are required to complete the following:**

School or institution now attending ______________________
____

Your current student status: ❏ high school; ❏ undergraduate; graduate program ❏ MS ❏ PhD; ❏ other ______________

Year you expect to graduate or complete your degree ______________

Major, if college or graduate student ______________________

Signature ______________________

Order Blank for Past Issues

Cost of complete volumes (per volume): ....members (all categories) – $18.00 + S/H
nonmembers and subscribers (libraries, schools, churches, etc.) – $25.00 + S/H

Cost of single issues (per issue):......................members (all categories) – $5.00 + S/H
nonmembers and subscribers (libraries, schools, churches, etc.) – $7.00 + S/H

	Number					Number					Number			
Volume	1	2	3	4	Volume	1	2	3	4	Volume	1	2	3	4
23	☐	☐	☐	☐	35	☐	☐	☐	☐	47	☐	☐	☐	☐
24	☐	☐	☐	☐	36	☐	☐	☐	☐	48	☐	☐	☐	☐
25	☐	☐	☐	☐	37	☐	☐	☐	☐	49	☐	☐	☐	☐
26	☐	☐	☐	☐	38	☐	☐	☐	☐	50	☐	☐	☐	☐
27	☐	☐	☐	☐	39	☐	☐	☐	☐	51	☐	☐	☐	☐
28	☐	☐	☐	☐	40	☐	☐	☐	☐	52	☐	☐	☐	☐
29	☐	☐	☐	☐	41	☐	☐	☐	☐	53	☐	☐	☐	☐
30	☐	☐	☐	☐	42	☐	☐	☐	☐	54	☐	☐	☐	☐
31	☐	☐	☐	☐	43	☐	☐	☐	☐	55	☐	☐	☐	☐
32	☐	☐	☐	☐	44	☐	☐	☐	☐	56	☐	☐	☐	☐
33	☐	☐	☐	☐	45	☐	☐	☐	☐	57	☐	☐	☐	
34	☐	☐	☐	☐	46	☐	☐	☐	☐					

Add 20% for postage (**for U.S. orders:** min. $6, max. $18; **for Canadian orders:** min. $10, no max.; **for other foreign orders:** min. $15, no max.) **Total enclosed: $______________**

Make check or money order payable to Creation Research Society. Please do not send cash. For foreign orders, including Canadian, please use a check in U.S. funds drawn on a U.S. bank, an international money order, or a credit card.

(Please type or print legibly)

Name ______________________________ Address ____

City ___________________________ State _______ Zip _____________ Country_______________________

❑ Visa ❑ MasterCard ❑ Discover ❑ American Express Card number ________________________________

Expiration date (mo/yr) _____________ Signature____

Mail to: Creation Research Society, 1 W. Firestorm Way #145, Glendale, AZ 85306, USA

Creation Research Society

History—The Creation Research Society was organized in 1963, with Dr. Walter E. Lammerts as first president and editor of a quarterly publication. Initially started as an informal committee of 10 scientists, it has grown rapidly, evidently filling a need for an association devoted to research and publication in the field of scientific creation, with a current membership of over 600 voting members (graduate degrees in science) and about 1000 non-voting members. The *Creation Research Society Quarterly* is a peer-reviewed technical journal. It has been gradually enlarged and modified, and is currently recognized as one of the outstanding publications in the field. In 1996 the *CRSQ* was joined by the newsletter *Creation Matters* as a source of information of interest to creationists.

Activities—The Society is a research and publication society, and also engages in various meetings and promotional activities. There is no affiliation with any other scientific or religious organizations. Its members conduct research on problems related to its purposes, and a research fund and research center are maintained to assist in such projects. Contributions to the research fund for these purposes are tax deductible. As part of its vigorous research and field study programs, the Society operates The Van Andel Creation Research Center in Chino Valley, Arizona.

Membership—Voting membership is limited to scientists who have at least an earned graduate degree in a natural or applied science and subscribe to the Statement of Belief. Sustaining membership is available for those who do not meet the academic criterion for voting membership, but do subscribe to the Statement of Belief.

Statement of Belief—Members of the Creation Research Society, which include research scientists representing various fields of scientific inquiry, are committed to full belief in the biblical record of creation and early history, and thus to a concept of dynamic special creation (as opposed to evolution) both of the universe and the earth with its complexity of living forms. We propose to re-evaluate science from this viewpoint, and since 1964 have published a quarterly of research articles in this field. *All members of the Society subscribe to the following statement of belief:*

1. The Bible is the written Word of God, and because it is inspired throughout, all its assertions are historically and scientifically true in all the original autographs. To the student of nature this means that the account of origins in Genesis is a factual presentation of simple historical truths.
2. All basic types of living things, including humans, were made by direct creative acts of God during the Creation Week described in Genesis. Whatever biological changes have occurred since Creation Week have accomplished only changes within the original created kinds.
3. The Great Flood described in Genesis, commonly referred to as the Noachian Flood, was a historical event worldwide in its extent and effect.
4. We are an organization of Christian men and women of science who accept Jesus Christ as our Lord and Savior. The act of the special creation of Adam and Eve as one man and woman and their subsequent fall into sin is the basis for our belief in the necessity of a Savior for all people. Therefore, salvation can come only through accepting Jesus Christ as our Savior.

iDINO II

Investigation of Dinosaur Intact Natural Osteo-tissue

A fragment of the *Triceratops* brow horn. Fragments, such as this one, still contain tissue and cells.

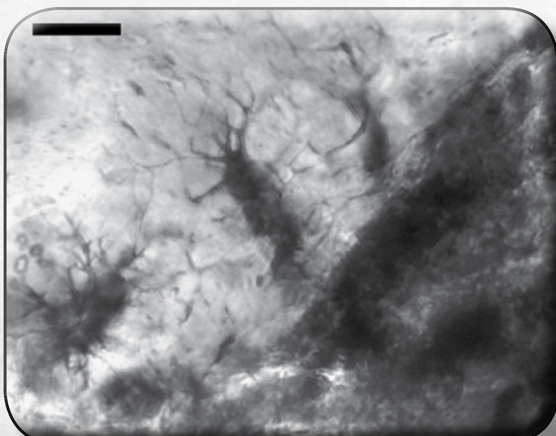

Microscopic examination of tissue extracted from a *Triceratops* horn reveals bone cells still present.

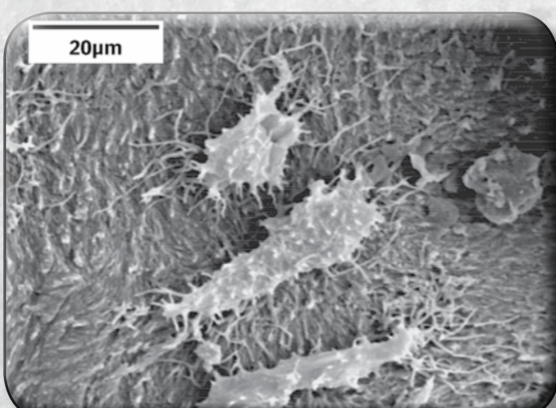

Electron microscope picture of intact bone cells still in tissue extracted from a *Triceratops* horn.

How can pliable, stretchable tissue survive inside dinosaur fossils for over 65 million years?

How can this tissue still contain intact cells and even dinosaur proteins?

How can this fragile biological material survive for so long?

The answer to these questions directly challenges the current, evolutionary-biased, geologic timescale.

The Creation Research Society began its iDINO research initiative for the purpose of studying soft tissue in dinosaur fossils. The first phase of the project detected pliable, unfossilized tissue in a brow horn of a *Triceratops*. Within this tissue were intact osteocytes (bone cells). Some results from the iDINO project have been published in a technical microscopy journal and presented at an international microscopy conference. The Spring 2015 issue of the *Creation Research Society Quarterly* also features a special report of the iDINO project. Plus, to further spread the important information about soft tissue, the Society is developing a video (Echoes of the Jurassic).

The **second phase** of the project (iDINO II) will look more extensively at the process of tissue preservation. Evolutionists have offered various theories of how this tissue could survive for millions of years. iDINO II will methodically investigate these preservation claims, assessing their plausibility.

The iDINO results have already provided a strong challenge to the evolutionary worldview. More extensive and detailed examination may provide even stronger evidence that the age of dinosaur fossils is far less than 65 million years. To this end, the Society continues to seek those willing to fund this project with either one-time gifts or monthly donations.

For more information contact us at (928) 636-1153 or crsvarc@crsvarc.com.

Also visit http://tinyurl.com/nphm2c4 for project updates and details.


V57N3